

## Technische Universität München

Wissenschaftszentrum Weihenstephan für Ernährung Landnutzung und Umwelt

Lehrstuhl für Lebensmittel- und Bioprozesstechnik

**Structure formation in Casein-based food systems**

**Analysis of aggregation phenomena in model processed cheese systems**

**Stefanie Sedlmeier**

**Vollständiger Abdruck der von der Fakultät Wissenschaftszentrum Weihenstephan für  
Ernährung Landnutzung und Umwelt der Technischen Universität München zur  
Erlangung des akademischen Grades eines**

**Doktors der Naturwissenschaften (Dr. rer. nat.)**

**genehmigten Dissertation.**

*Für Claus, der den roten Faden wiedorfand*

*Man muss Chaos in sich tragen, um einen tanzenden Stern gebären zu können. F. Nietzsche*

## Acknowledgments

First of all I would like to thank Prof. Dr. Ulrich Kulozik for his advise and supervision for this project as well as for his patience and giving me the possibility to perform this work. In addition, I would like to thank the whole ZIEL<sup>1</sup> Institute for Food and Health as well as the Institute for Food- and Bio-process Engineering for their support and scientific insight during the experimental part of this work. A special thanks goes to Mrs. Heidi Wohlschläger who gave much needed insight towards the HPLC measurement methods performed in this study.

Also, I would like to thank my office colleagues, Dr. Martin Hartinger, Dr. Christian Kleemann, Franz Fraunhofer and Michael Reitmeier for the good communication and collaboration. A special thanks goes to Mrs. Franziska Kurz, who was always available as a sometimes needed friend during this work, as well as a discussion partner in scientific terms. I will miss the hours in E.25 dearly.

A special honoration goes to my students, Christina Baumeister, Alexander Schmieder and Viktoria Heitler for their tireless work during method development and their fierce interest in the science that is processed cheese. The liberating discussions as well as their considerations towards the experimental results helped a lot to shape this work.

Also, I want to thank my family and friends, who are always true believers in me and never doubt me to achieve my goals. Without them, this thesis would not have been possible.

Last but not least, I want to thank my partner, best friend and soon to be husband Claus Peter Pfeilschifter, on the one hand for giving me the impulse to learn to code for this work as well as for loving and supporting me all the way.

---

<sup>1</sup>Zentralinstitut für Ernährungs- und Lebensmittelforschung

## Summary

In a highly concentrated protein systems, such as processed or cream cheese, wherein large protein aggregates are present next to a dispersed phase, the inner structure is usually very complex and influenced by numerous factors. In order to elucidate these inner structure in compositional terms and in the micro and nano scale of protein interaction, a model processed cheese matrix was reiterated and further developed from previous work (Lenze et al. (2019)). This matrix consisted of store-type plant oil as dispersed phase and different casein powders with protein concentrations ~90%, from which < 1% was from whey proteins. The casein displayed the continuous phase, which is suspected to form the gelled matrix. As it is typical in processed cheese, emulsifying salts were used in the mixture, resulting in a dry matter of the non-processed matrix of ~40%. To formulate a homogenous matrix, the samples were homogenized before processing, using a laboratory mixing device. This process was further referred to herein as premixing, since the processing of processed cheese, of course involves mixing, kneading, stirring or however an applied shear force during heating.

Various model process-cheese matrices using Sodium, Rennet and Native Casein as starting material were investigated in their structuring-behaviour using a Rheometer as a monitoring and processing device for the structure-build up. In sum ten different stages for structure formation were defined and the products obtained were analyzed. In general a two-step increase in viscosity, as it is typical also for the industrial processing of such cheeses, could be observed. For determination of the protein concentrations at the O/W interface, the soluble phase and the insoluble phase, a centrifugational washing procedure for separating the diluted model processed cheese matrix was developed. In addition, a procedure for washing the cream phase and subsequent desorption of proteins from the interphase, using a chaotropic salt, was put together. Thereby obtained phases were investigated afterwards with RP-HPLC for protein quantification and qualification, giving compositional and quantitative data for the distribution of caseins in the matrix. It could be shown, that the emulsification of fat primarily happens during the second step of structuring. This step was considered to be *inter alia* the second exponential or second log phase of structure formation, i.e. processing.

In addition to HPLC analysis, particle sizes of the three phases were measured. The particle sizes showed bimodal distributions, therefore an algorithm for modelling normal distributions in equal mixtures of distributions (“normalmixEM” within the R programming language) was used in the programming of a fit function. This was done to better estimate the particle sizes or particle volumes and their respective density distributions in the analyzed samples. By doing so, a close approximation of distribution and development of large components next to small components in the

analyzed samples could be given. The particle sizes in the pellet gave indications for the formation of a more and more hydrophobically aggregated network, especially during the second half of structure formation. In addition, the separation of the dense matrix in compositional terms could be found. The particle size distributions in combination especially with the compositional data from RP-HPLC analysis indicated the formation of two different types of protein networks. The measurement data hinted towards the formation of a hydrophilic network surrounding alphaS2 caseins and its minor interactions with other caseins. The second network was indicated to be a hydrophobic network mainly comprising of kappa, alphaS1 and beta casein. This network was in close contact with the dispersed phase and showed behavior to form a particulated network. This behavior of the casein matrix also showed itself in its morphology at later processing stages, where the model processed cheese became more and more incoherent or even particulate, if processed long enough.

Previous studies showed the accelerating effect of the addition of pre-processed cheese to the freshly matrix, or chemically spoken, a catalytic seed was given to the educt. This auto catalytic effect was described in previous works in phenomenological terms. In this study, it was tried to find the ‘seed’ that could start such an autocatalytic reaction. Therefore, 1% and 3% solutions of rennet casein were produced with an aliquot of the emulsification salts. These solutions were referred to as colloidal solutions. The formation of a flocculated, insoluble aggregate could be documented in samples with a total protein concentration of 3% after 140 minutes of processing. The colloidal solutions were further processed using ultra centrifugation at 70.000g. The supernatants were analyzed compositionally using RP-HPLC and showed a decrease first in kappa and alphaS1 casein subsequented by beta casein before and during the appearence of the flocculated aggregate. The supernatants were also analyzed in their particle volume using dynamic light scattering. Both concentrations, 1% and 3% showed the phenomenon of reaggregation after filtration. In addition in samples made with 3% total casein, at late processing times, the formation of a large proportion of small aggregates was measured with roughly ~14 nm in size.

Low-resolution NMR measurements were performed using the products of a continuous and therefore upscaled process. The multi-exponential decay was analyzed using a discrete, multi-exponential fit in a non-linear-least-squares (NNLS) algorithm using a three component model. The components found could be attributed to a mobile and immobile water fraction. One component could be attributed to the fatty phase of the matrix, that showed a gradual decrease in T2 relaxation time. The mobile phase of the water increased slightly over a process time of 225 minutes. In addition to the NMR measurements, the samples from the upscaled process were centrifuged at 500g and the remaining serum was analyzed with RP-HPLC. Also, particle sizes of the mixture were determined using laser

diffraction. Analogies to the particle development in the pellet could be found.

In summary, the results of this study revealed matrix separation phenomena in a dense, heated and sheared casein matrix on a compositional level and gave mechanistic explanations as to why they occurred. Kappa casein was suggested to be the seed for hydrophobic aggregation, wherein beta and alphaS1 casein participated strongly in hydrophobic network formation. The hydrophobic aggregation was increased by depletion of alphaS2 casein, water and ions from the hydrophobic network. The caseins beta and alphaS1 interacted with the initially aggregated kappa casein to form large aggregates via hydrophobic interaction. The alphaS2 casein is suspected to show a special calcium sensitivity that the other caseins lack which could give important insights for the binding of the casein micelle.

# Contents

## List of Figures

<b>1 Casein and its interaction properties in complex food systems</b>	<b>1</b>
1.1 Casein: structure and functionality . . . . .	3
1.2 Overview of gelation mechanisms . . . . .	6
1.2.1 Emulsion gels: special types of composite materials . . . . .	7
1.3 A complex food system: processed cheese . . . . .	8
1.3.1 Casein interactions at the presence of melting salts . . . . .	10
1.3.2 The Creaming Reaction . . . . .	14
1.4 Investigation of process parameters and composition on the structure formation during manufacture of processed cheese . . . . .	15
1.5 Compositional analysis of model processed cheese systems . . . . .	17
1.5.1 Analysis by reversed phase chromatography . . . . .	18
1.5.2 Investigation of ${}^1\text{H}$ T2 relaxation . . . . .	19
1.6 Studies related to this work . . . . .	21
<b>2 Motivation and Aim</b>	<b>28</b>
<b>3 Rheological Profile of structure formation in model processed cheese</b>	<b>32</b>
3.1 Introduction . . . . .	32
3.2 Material and Methods . . . . .	33
3.3 Comparison of models tested during model development . . . . .	35
3.4 Results and discussion . . . . .	40
3.4.1 Flow curves during processing of model processed cheeses . . . . .	40
3.4.2 pH values post-processing . . . . .	43
3.4.3 Occurrence of a third log phase and the fitting of a model flow curve . . . . .	44
3.5 Summary and outlook . . . . .	47

<b>4 Quantitative matrix distribution of Caseinates during thermal processing of model process cheese</b>	<b>50</b>
4.1 Introduction . . . . .	50
4.2 Material and Methods . . . . .	51
4.3 Results and Discussion . . . . .	54
4.3.1 Development of protein concentration of single caseins in model processed cheeses from batch preparation . . . . .	54
4.3.2 Development of protein distribution in model cheeses made from sodium caseinate	61
4.3.3 Development of pH of model cheeses and dry matter of respective cream phases .	65
4.3.4 Development of protein concentration of single caseins in the cream phase of model processed cheeses from continuous processing . . . . .	67
4.4 Summary and Outlook . . . . .	69
<b>5 Investigation of particle size development in the bulk phase and at the interphase during processing stages of model process cheeses</b>	<b>72</b>
5.1 Introduction . . . . .	72
5.2 Material and Methods . . . . .	73
5.3 Results and Discussion . . . . .	74
5.3.1 Data processing . . . . .	74
5.3.2 Particle size distribution in cream phase . . . . .	74
5.3.3 Particle size distribution in insoluble or pellet phase . . . . .	78
5.3.4 Particle size distribution in the soluble or serum phase . . . . .	81
5.4 Summary and Outlook . . . . .	83
<b>6 Colloidal aggregation of rennet casein under the influence of shear, heat and emulsifying salts</b>	<b>85</b>
6.1 Introduction . . . . .	85
6.2 Material and Methods . . . . .	86
6.3 Results and Discussion . . . . .	87

6.4	Summary and Outlook . . . . .	92
<b>7</b>	<b>Upscaling and NMR relaxometry of model process cheese</b>	<b>96</b>
7.1	Introduction . . . . .	96
7.2	Material and Methods . . . . .	98
7.2.1	Preparation of cheese samples . . . . .	98
7.2.2	NMR measurement . . . . .	98
7.2.3	Curve-fitting . . . . .	98
7.3	Results and Discussion . . . . .	98
7.3.1	T <sub>2</sub> relaxation in model processed cheese . . . . .	98
7.3.2	Protein concentration in the serum phase . . . . .	101
7.3.3	Particle size distribution in the serum phase of the upscaled, continuous process .	102
7.3.4	”Offline” Rheology of continuous process . . . . .	103
7.4	Conclusion and Outlook . . . . .	104
<b>8</b>	<b>Correlation Analysis of Experimental Data using the R programming language</b>	<b>106</b>
8.1	Results . . . . .	106
<b>9</b>	<b>General Discussion and Outlook</b>	<b>112</b>
<b>10</b>	<b>Bibliography</b>	<b>122</b>

## List of Figures

1	Structures found in cheese in the micro-, meso-, and macroscale as cited in the literature	3
2	sub-micellar binding model of the casein micelle . . . . .	5
3	Dual-Binding model of the casein micelle by as cited in the literature: beta and alpha-caseins (orange) are connected to the CCP (grey spheres), blue represents free beta-casein, hydrophobically bound. Micelle is stabilized by kappa-casein (green) wherein the black coil represents the casein Macropptide (CMP)	5
4	Distribution of calcium in milk . . . . .	6
5	Types of gelation in biopolymers . . . . .	7
6	Types of emulsion gels . . . . .	8
7	Hydrophobic Cluster Analysis (HCA plot) of caseins . . . . .	11
8	Example of a calcium chelat complex associated with three phosphate groups. R can be either a proteinogenic residue, a calcium phosphate nanocluster (CCP), an associated or bound phosphate, pyrophosphate or polyphosphate or similar.	13
9	Casein elution in RP-HPLC as cited in the literature, next to whey protein elution . . .	19
10	Overview of T2 relaxation measurements: from signal to data. . . . .	20
11	Parameters influencing the structure formation of model processed cheese . . . . .	22
12	Most recent model for aggregation phenomena during the creaming reaction . . . . .	23
13	Structure formation of a fat-free processed cheese as in Lee et al. (2003) . . . . .	24
14	LM imaging of processed cheese samples . . . . .	28
15	model process cheese structure after shorter processing times of 100 minutes in hot (A) and cold (B) state and after longer processing times of 300 minutes in hot (C) and cold (D) state . . . . .	29
16	Effect of pre-cooked cheese (rework) addition on structure formation of model processed cheese, suggestion of an auto-catalytic effect . . . . .	30
17	Overview of measured apparent viscosities in samples during model testing . . . . .	36
18	Effect of premixing on the rheological profile of tested samples . . . . .	37

19	Rheological Profile of samples made from native (red) or rennet (blue) casein, processed in a steel cup . . . . .	38
20	Overview of viscosity, depending on the protein source . . . . .	39
21	measured apparent viscosity of models with sodium caseinate . . . . .	40
22	Measured apparent viscosity of native and rennet casein . . . . .	42
23	Apparent viscosity of sodium caseinate and native casein controls . . . . .	42
24	Difference in pH value of tested samples after processing . . . . .	43
25	Structure formation in a steel cup . . . . .	45
26	fitted model flow curve . . . . .	47
27	Sampling events for further analysis . . . . .	52
28	Overview of centrifugational separation and washing procedure . . . . .	53
29	Appearance of cream at various points during the washing method . . . . .	55
30	RP-HPLC chromatograms obtained during the washing procedure . . . . .	55
31	Casein concentrations in native cream samples . . . . .	56
32	protein concentrations in the native serum phase . . . . .	57
33	Protein concentrations in the native pellet phase . . . . .	58
34	Total protein concentrations in the native wash phases . . . . .	60
35	Protein concentrations in the sodium cream . . . . .	62
36	from native casein and sodium caseinate . . . . .	63
37	Protein concentrations in the sodium serum phase . . . . .	63
38	Protein concentrations in the sodium pellet phase . . . . .	64
39	pH values measured over processing . . . . .	66
40	Dry matter of the cream phases . . . . .	67
41	Protein concentrations in the cream of upscaled processes . . . . .	68
42	Measured particle size distribution in the cream phase . . . . .	75
43	Development of Particle Volume of small (red) and large (blue) fat particles over processing time . . . . .	75

44	Development of density distribution of small (red) and large (blue) fat particles over processing time . . . . .	77
45	Measured particle size distributions in the pellet phase . . . . .	78
46	Development of Particle Volume of small (red) and large (blue) insoluble particles over processing time . . . . .	79
47	Development of Density Distribution of small (red) and large (blue) insoluble particles over processing time . . . . .	79
48	Swelling properties of pellet at later processing stages . . . . .	80
49	Measured particle sizes in the serum phase after ultracentrifugation . . . . .	81
50	Modeled particle sizes in the serum phase . . . . .	82
51	Measured particle size distribution of solutions from 1 TP casein . . . . .	87
52	Measured particle size distribution in 3 TP casein solutions . . . . .	88
53	modelled particle sizes for 3 TP casein solutions over processing time . . . . .	89
54	Flow curve of a 3 TP casein solution processed with a vane blade geometry . . . . .	91
55	Measured protein concentrations in the supernatant of 3 TP casein solutions after ultracentrifugation . . . . .	92
56	Visible large flocculated aggregate at the stirrer of the vane geometry after 140 minutes of processing . . . . .	93
57	Proposed reaction mechanism . . . . .	94
58	Development of detected fractions over processing time . . . . .	99
59	T2 relaxation of fat and mobile water over process time . . . . .	100
60	Protein concentrations in serum phases separated with different centrifugation speeds .	101
61	Measured particle size for serum phases separated at 500g . . . . .	102
62	Modelled particle sizes for serum phase separated at 500g . . . . .	103
63	Rheological profile of the upscaled process . . . . .	103
64	Correlation plot of the protein concentrations measured in the cream 1:4 and pellet 5:8 phase. Protein concentrations are displayed in the order alphaS1, alphaS2, beta and kappa casein. . . . .	107

65	Most significant correlations of the concentrations of single caseins in the investigated phases during processing: red colour indicates negative, blue colour positive correlations.	108
66	Cross-correlation for the measured kappa casein concentrations in the different phases; blue indicates positive, red negative correlations.	109
67	Correlation plot for the third washing step; proteins are displayed in their measured concentration in the order alphaS1, alphaS2, beta and kappa casein.	110
68	Correlation of the measured apparent viscosity with the data from the compositional analysis. Displayed are the top 10 correlations as indicated by significance level. A positive correlation is indicated by the blue colour, a negative correlation by the colour red.	111
69	Apparent viscosity of model protein cheeses with varying protein sources	115
70	Particulated gel	118
71	TEM images of model processed cheese at late stages of processing	119
72	Structural changes that lead to an increase in viscosity in model processed cheese.	121

# 1 Casein and its interaction properties in complex food systems

In many complex, highly concentrated food systems, characteristic structure-forming processes take place that have so far only been described in phenomenological terms. The structure of food products is created during the process of transforming the raw materials into the final product (McClements (n.d.)). Overall, it shapes the mouthfeel, which is expressed via sensory attributes such as creaminess, etc., but also plays a role in determining the intensity of the taste and aroma sensation.

The dominant structure-forming components are mostly proteins that are ready to aggregate. Protein-rich product systems play an increasingly important role in human nutrition, but also in pharmaceutical biotechnology. Examples are clinical and geriatric nutrition, where swallowing problems require a specific structure or viscosity controllable by protein aggregates, e.g. to circumvent the problem of “dysphagia.” On the other hand, in certain neuro degenerative phenomena, the occurrence of chronic diseases is often associated with the phenomenon of aggregation, albeit under very different milieu conditions than in food, as it was reported in Mezzenga and Fischer (2013).

Elderly people and athletes require protein-rich foods to counteract progressive muscle loss and to support muscle building, respectively. Ignorant of the fundamental interrelationships of the structure-forming potential of proteins in highly concentrated systems, especially in complex multi-phased systems, one is currently not yet sufficiently able to make targeted use of protein-based structure formation in the sense of efficient, quality- and productivity-guided process control. Further, many modern pharmaceuticals today are proteins whose aggregation behavior determines their efficacy as therapeutic agents.

An emerging trend is the need for structure formation by rapid aggregation, generally for intensification of processes or, for example, in the design of food products in 3D printing processes. Here, novel structure formation processes are a prerequisite to achieve spontaneous solidification of the structure built from liquid or pasty base materials. As a recent example for this emerging trend, the work of Kang et al. (2021) describes 3D printing of cultured meat cells derived from stem-cells into structures similar to fresh-cut meat from Waygu beef. The procedure hereby consisted of printing fibers from muscle and adipose tissue into a tendon-gel, which serves as the meat matrix. Accordingly, the formation of the gel in which novel food structures can be incorporated as well as the printing process itself are of interest when it comes to aggregation phenomena in food systems.

In order to target such specific structure formation processes, it is necessary to understand protein aggregation and especially the interaction with dispersed phases on a molecular level (Hubbard (2003), McClements (n.d.)). Many studies have been performed on a microscopic scale on the

aggregation phenomena in colloidal, or rather liquid systems such as emulsions made from caseins (Brunner (1991), Alexander, Corredig, and Dagleish (2006), Mizuno and Lucey (2005), Liang et al. (2013) ,Wong et al. (2012)). On the other side of the spectrum, many studies have been performed on the physical properties of gelled or solidified systems (Matsumura et al. (1993), Brighenti et al. (2018), Berta et al. (2016), Sadlikova et al. (n.d.), Salek et al. (n.d.)).

If one wanted to analyze both effects simultaneously, i.e. the effects coming from a proteinogenic phase interacting with a dispersed phase, as well as the effects of gelation of said proteins, a system must be investigated, that shows both properties. The gain of knowledge coming from the investigation of such systems would be, that further insight could be given as to how a dispersed phase either stabilizes or destabilizes such systems, and if the formation of a continuous network is overall influenced by the presence of a dispersed phase.

A specific food system, which can be generalized in a way that it is generic towards many food systems, is processed or cream cheese. On the one hand, it is a heat-set gel, where aggregation processes occur during the heating phase, that lead to a gelled structure in cold state. On the other hand, it has a dispersed phase embedded in the gel structure, wherein the emulsification of the dispersed phase also occurs during the heating phase. The heating phase is referred to as processing, however the term processed cheese should not lead to the assumption that store-type cream cheese is processed without the use of heat. An intensive study on the structural behavior of commercial cream-cheese products has been performed by Dang, Wolfschoon Pombo, and Kulozik (2019). Structure formation processes in processed, or sometimes also referred to as analogue cheese samples was investigated extensively also in recent years, Table 1 gives a non conclusive overview of studies performed in such systems.

Lamichhane, Kelly, and Sheehan (2018) gave an overview for the scale levels in native cheese and their functional domains (Fig.1). On the molecular scale, milk salts, lactose, water and whey proteins can be found. The nano-scale which presents to be an important scale for the formation of complex structures, casein aggregates and on the higher nano scale casein micelles can be found. The micro scale in processed cheese is manly attributed to emulsified fat-globules or fat-particles. Native fat globules are not to be found in processed cheese models that are not using dairy cream as the fatty or dispersed phase. The macroscale represents the scale visible to the human eye and represents visible crystals or cracks in the structure.

Such systems can be considered as emulsion gels or ‘soft-solids,’ as in Dickinson (2012), where they are either characterized as an emulsion filled or particulate gel. Hence the main difference lies in the

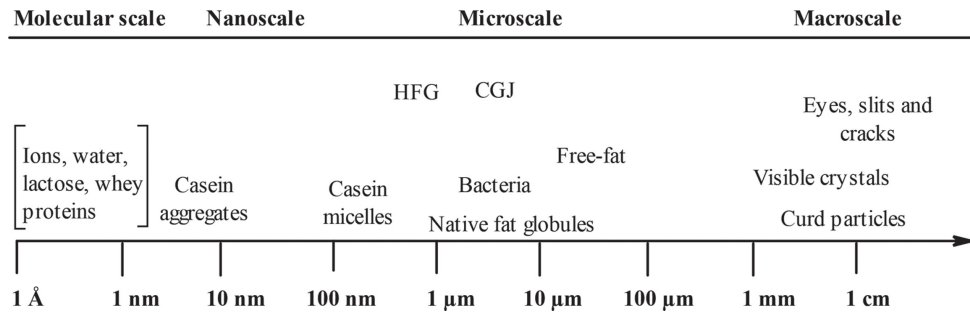


**Fig. 1.** Structures found in cheese in the micro-, meso-, and macroscale as cited in the literature

embedding of the dispersed phase into the structured continuous phase.

The structured continuous phase in processed or cream cheese is built by caseins. As amphoteric proteins, caseins also emulsify the fat or fatty phase. Hence, investigating processed or cream cheese as a representative for a soft, solidified or gelled dispersed food system can provide insight into the structuring mechanisms of such structures. It might also give hints towards the occurrence of aggregation phenomena, or investigations of such, in biogenic systems in general. This concept is explored further down below.

### 1.1 Casein: structure and functionality

Milk contains two main classes of proteins, the mostly globular and heat sensitive whey proteins and the major milk proteins: caseins. Caseins can be isolated from milk, using acid treatment at pH 4.6 and 20°C. Under these circumstances, the caseins will precipitate due to the screening of electrostatic repulsion. This happens as an effect of being close to the IEP, whereas whey (and other) proteins will stay in solution. Calcium precipitation of caseins can be also used in a targeted manner, to isolate specific caseins from the micelle by their differences in calcium sensitivity (Post et al. (2012)). Since milk proteins are thus separated relatively easy, first research on caseins was performed as early as the beginning of the 19th century (T. Huppertz, Fox, and Kelly (2018)).

The casein micelle is a highly aggregated particle, stabilized by hydrophobic interactions and electrostatic interactions internally. Externally, it is stabilized by steric repulsion through the outer “hairy-layer,” mainly consisting of kappa casein. With a surface area of about 4000 m<sup>2</sup>/l at a specific mass of 1.11 g/ml (20°C) and a number of 1014-1016 micelles/ml of raw milk, caseins are the main component of milk proteins. This is also represented by the strong hydration properties of the casein micelle. Caseins are reported to display a mean hydrodynamic radius within a range of 50-500 nm and are able to bind up to 2.5 g of water per gram protein. Thus, caseins make up ~13% of the volume fraction of milk, roughly five times higher than their dehydrated mass proportion in milk

(Dagleish and Corredig (2012), P. F. Fox (2009)).

The average molecular weight of a dehydrated micelle is about 108 daltons. The micelle itself is composed of four different casein fractions, of which different genetic variants exist: alphaS1-, alphaS2-, beta- and kappa-casein. The percentage ratio of the total protein is 30:8:30:10. The dry matter of a micelle comprises 94% protein and 6% colloidal calcium phosphate (CCP). CCP further comprises magnesium, calcium, phosphate, citrate, sodium and potassium ions (Gaucheron (2011)). The exact structure of the casein micelle is not yet fully known and many models have been proposed, most recently by Dagleish and Corredig (2012).

The effect of high pressure (150-300MPa) on the casein micelle structure in milk showed the occurrence of small micelles next to large micelles under the use of cryo-transmission electron microscopy (cryo-TEM). Higher pressurization rates of 400 MPa resulted in the formation of smaller casein assemblies of 30-100 nm in size. It was also found, that free Calcium was taken in by the casein structures and that the substructures induced by high pressure treatment can be also found in untreated milk (Knudsen and Skibsted (2010)). This shows, that the caseins are highly prone to self-assembly and aggregation, especially under the presence of calcium ions.

To this day, the inner structure of the casein micelle is unclear. Elucidation of the inner structure using imaging techniques such as transmission electron microscopy (TEM) is not possible, since the molecular density in the casein micelle is too high. The sub micelle binding model, presented by Walstra (1999) but developed from preceding models considers the casein micelle to be an aggregated particle made out of, again micellar substructures. In the sub-micelles the CCP is incorporated. On the surface of the casein micelle, a so-called “hairy-layer” made out of kappa casein prevents the micelles from *in-situ* aggregation in milk, due to steric and electrostatic repulsion. This model is grounded on experimental evidence. It was, for example, shown that casein monomers self-assemble into sub-micelles, when calcium ions are present.

In later models, the focus of casein micelle stabilization was shifted to the calcium phosphate nano-clusters (CCP). The nano cluster model (Holt et al. (1998)) was followed by the dual binding model. Both models suspected the CCP to stabilize the casein micelle internally, as well as hydrophobic interactions in balance with electrostatic repulsion.

According to investigations of Thom Huppertz et al. (2017), the stabilisation of the micelle in the interior takes place via the CCP nano-clusters. This was found by investigating differently bound water in the casein micelle. It was possible to identify non-spherical particles, which were referred to as primary casein particles (PCP), which form a porous micelle structure through linkages via

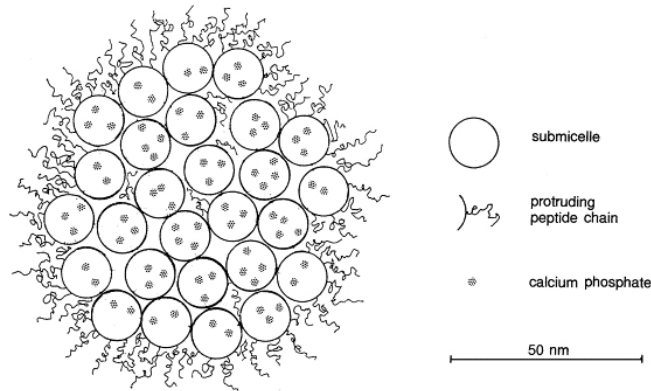


**Fig. 2.** Sub-micelle binding model as presented in the literature: caseins are arranged in spherical sub-micelles, in which CCPs are incorporated

calcium phosphate nanoclusters. What's interesting here is that seemingly rebuilt casein micelles from sodium caseinate displayed similar properties as native and dried casein micelles in terms of radius of gyration, or particle size.

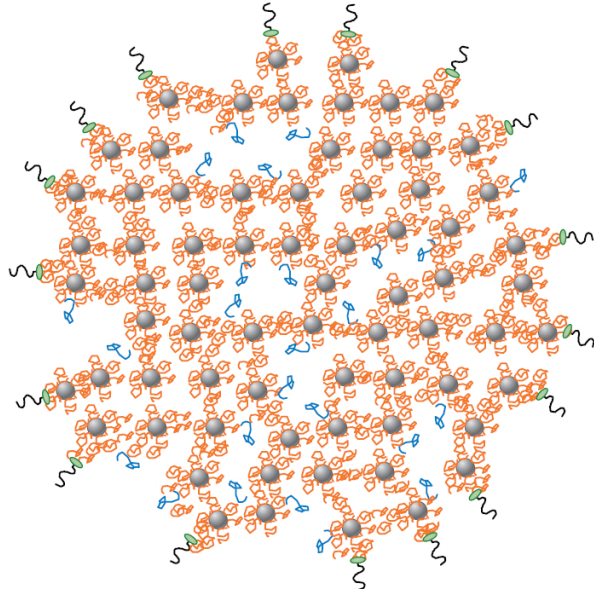


**Fig. 3.** Dual-Binding model of the casein micelle by as cited in the literature: beta and alpha-caseins (orange) are connected to the CCP (grey spheres), blue represents free beta-casein, hydrophobically bound. Micelle is stabilized by kappa-casein (green) wherein the black coil represents the casein Macropetide (CMP)

In the model of the casein micelle from Dalgleish and Corredig (2012) (fig.3), CCPs are connected to the phosphorylated serine side chains of the caseins via a calcium phosphate bridge, as indicated by the grey spheres. Furthermore, hydrophobic interactions and van der Waals forces contribute to the stabilisation. Among the casein fractions homogeneously distributed inside, the kappa casein sits at the surface of the micelle and stabilises the micelle through its outwardly directed, strongly

hydrophilic and negatively charged part, the casein macropeptide (CMP). The negative charge causes steric repulsion of the micelles from each other, which leads to colloidal stability of the micelle. The hydrate shell additionally stabilises the micelle. The kappa casein as “hairy-layer” is also presented in the dual binding model. Also of importance is the fact that a casein micelle is not a static system, but is in a dynamic equilibrium with the milk serum. This equilibrium can be disturbed mainly due to the calcium sensitivity of the individual casein fractions. While kappa-casein reacts quite insensitively to calcium ions, the two alphaS-fractions are strongly calcium-sensitive (Holt et al. (2013)). By binding calcium ions on the surface, the outer kappa-casein protects the calcium-sensitive casein fractions inside the micelle and thus prevents a calcium-induced structural change T. Huppertz, Fox, and Kelly (2018). An overview of the distribution of the calcium in the casein micelle was presented in Dumpler (2018) and can be seen in Fig.4.

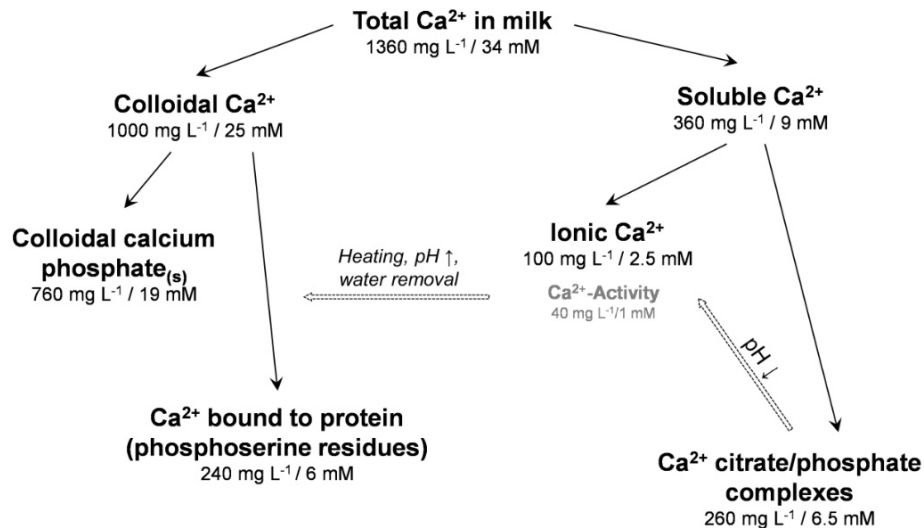


**Fig. 4.** Distribution of calcium in milk

From that it can be seen, that the binding state of calcium in the casein micelle is dependent on milieu conditions (pH, water concentration, Temperature).

## 1.2 Overview of gelation mechanisms

Gelation of biopolymers is a phenomenon generally recognized as the solidification of a matrix by interaction(s) of the biopolymers, here proteins, with the solvent. Gelation can happen due to various reasons, Fig.xx gives an overview of gelation mechanisms in general. Gelation induced by the formation of covalent bonds is used often in organic, non edible gels as in acrylamide gels for gel-electrophoresis. Covalent gelation in casein occurs, when treated enzymatically with

transglutaminase, which connects the glutamine residues in a protein by intramolecular bonds. In general, gels from casein are particle gels, as in (D) of Fig.5.

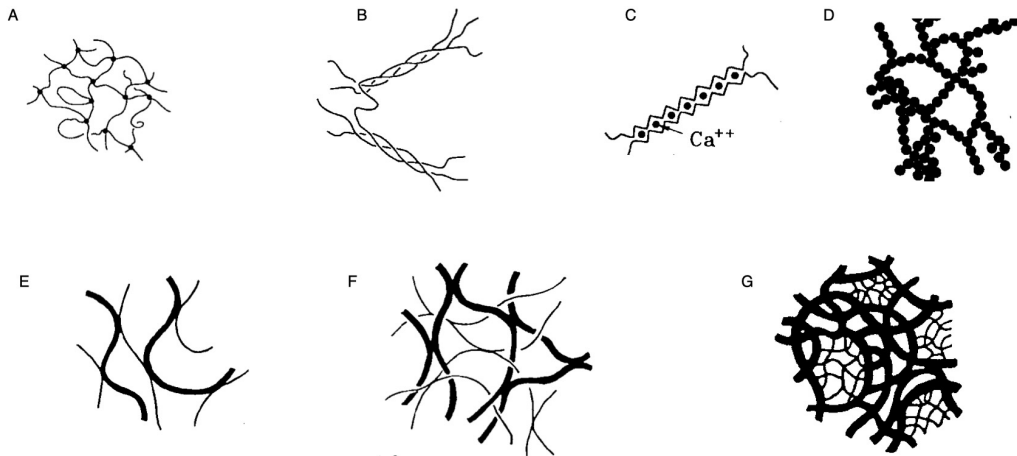


**Fig. 5.** Overview of gelation mechanisms, top row displays single component systems, bottom row shows interaction properties of multi component systems: (A) covalent or chemical gel, (B) thermo-reversible gel, (C) ionic gel, (D) particle gel, (E) coupled networks, (F) inter-penetrating networks, (G) phase separated networks

Casein gels are not monomeric gels but are formed by interaction of the four components: alphaS1, alphaS2, beta and kappa casein. When looking at processed cheese it is evident that it is a composite gel with a dispersed phase embedded in it. Such systems have been described as emulsion gels and will be described in the following section.

### 1.2.1 Emulsion gels: special types of composite materials

Process-cheese based casein gels can be viewed as emulsion gels. Emulsion gels are soft solids with incorporated, emulsified fat droplets or fat particles. Dickinson (2012) made an intensive description of such structures which was also based on his own line of research as in Dickinson and Golding (1998), Dickinson (2006). Emulsion gels can incorporate two basic structures: the emulsion-filled protein gel (A) and the protein-stabilized emulsion gel (Fig.6). It should be taken into consideration, that these two types pose the ideal structure, in real life models mostly a mix of the two gel types is present at the same time.

An emulsion-filled protein gel is characterized as a gelled protein matrix with embedded emulsified fat droplets. The viscoelastic properties of such gels are mostly determined by the continuous phase, i.e. the proteins.

The protein-stabilized emulsion gel is a type of particulate gel whose properties are mostly directed

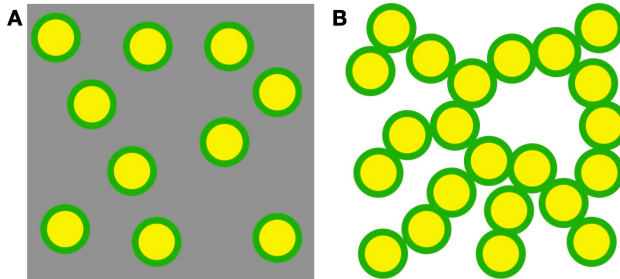


**Fig. 6.** Types of emulsion gels: (A) emulsion filled gel, the proteins (green) emulsify the fat (yellow) and are embedded into the matrix. (B) particle gel, the proteins at the interphase connect the fat particles to a continuous matrix

by the formation of a network of aggregated fat droplets, or rather fat particles. The fat particles are considered filler particles and the properties of the gel are also directed by the properties of the filler (Matsumura et al. (1993)). It was shown, that gels with incorporated filler in form of fat particles had higher shear moduli as their fat free counterparts. Brighenti et al. (2018) described processed cheese as emulsion filled gel. An emulsified fat droplet is considered to be a solid-like material in both systems. Formation of emulsion-filled gels usually takes place, when the bulk phase of a stable emulsion is solidified. Gels of the particulate type are formulated, when the emulsion droplets aggregate. Destabilization phenomena in emulsion gels are, for example, induced by excess amounts of unadsorbed protein that leads to depletion. Another type of destabilization or stabilization, for the respective matter, is bridging flocculation (Semenova et al. (2010), Sapir and Harries (2015)).

### 1.3 A complex food system: processed cheese

In a highly concentrated protein systems, such as processed or cream cheese, wherein large protein aggregates are present, the inner structure is usually very complex and influenced by numerous factors. Furthermore, proteins in biogenic systems generally occur in different molecular structures as well as molecular scales. Such food systems often are multi-phased systems. Thus, proteins arise in combination with other substances, such as fat or carbohydrates. Processed cheese serves as an example of a complex, highly-concentrated, and multi-phased protein system. Milk proteins (caseins), fat, and water form a dense network, triggered by the reaction of caseins with melting salts. The structure-forming reaction takes place in several stages and only under certain process conditions. An overview of the general processing steps and suspected reactions taking place therein is given in Fig.xx. Guinee, Carić, and Kaláb (2004) gives an overview of cheese products that are made under (excessive) heat, meaning they are thermally processed. Such products are also called pasteurized cheeses. Also, a manufacturing protocol for processed cheese products is given.

Patrick F. Fox et al. (2016) gives a summary on processed cheese products, additives in processed cheese and the development of processed cheese throughout the years. It is mentioned, that heating and shearing of a native cheese mass leads to coagulation of casein and the release of fat due to the rupture of the milk fat globule membrane (MFGM) as a result from shear and heat. Emulsifying salts are used to dissociate the caseins from their micellar form, which prevents them from coagulation and leads to hydration of single caseins that can emulsify the fat phase. According to the cited literature, the emulsifying salts fulfill the following functions, or induce them in the caseins:

- upward adjustment buffering of pH
- chelation of calcium after sequestration and de-ionization of the micelle calcium
- casein hydration
- binding or emulsification of free fat
- novel structure formation to the processed cheese matrix.

The steps necessary to form processed cheese are mainly mixing of the educts, i.e. cheese components and subsequent processing of the cheese mass at Temperatures between 70 - 95 C and constant mixing. The educts for processed cheese can be in powdered, liquid or in their native, i.e. gelled form, when natural cheese is used. Hence the type of mixing depends on the grain size or dispersity of the primary components or educts.

Common additives in the production of processed cheeses are whey protein concentrate, starches or hydrocolloids like carageenaan. These can be found especially in cream-cheese products, where the dissociation of the casein micelle is not induced by melting salts, but by acidification. In such systems, stabilizers in the form of hydrocolloids are often used to prevent excessive syneresis of the cheeses. Syneresis, the release of water of gelled dairy systems, is a phenomenon not occurring in processed cheeses. This might be due to high dry matter, however it is likely, that the stronger dissociation of caseins into substructures or monomers (induced by the melting salts) leads to a stronger hydration of the matrix, since more hydrateable protein units are available in total.

The main component in processed cheese is casein. Their primary aggregated structure when derived from rennet or native casein gets disrupted chemically by the melting salts a new structure is build-up due to the constant shearing and heating of the matrix. The type of shear applied to the system is in partial determined by the composition of the educts: when working with fresh cheese curd or (model) cheeses like mozzarella or dried cheese curd, the matrix is more kneaded than stirred, as it is the case in Nessa Noronha, O'Riordan, and O'Sullivan (2008), N. Noronha, Duggan, Ziegler, Stapleton, et al.

(2008), N. Noronha, Duggan, Ziegler, O’Riordan, et al. (2008), Chen and Liu (2012) and El-Bakry et al. (2011). Processing environments, where the emphasis was on the investigation of the structure formation itself at various processing conditions were given, besides others, by Černíková et al. (2018), Lee et al. (2003), Guinee, Carić, and Kaláb (2004), Fu, Watanabe, Satoh, et al. (2018), Fu, Watanabe, Inoue, et al. (2018), Cunha et al. (2013), Lenze et al. (2019) and in the parallel work of Vollmer, Kieferle, Youssef, et al. (2021). In these studies, the samples were of a more homogeneous or even liquid like state in the educt stage and were processed under stirring. A summary of the studies that dealt with similar systems as in this work can be found at the end of this section.

### 1.3.1 Casein interactions at the presence of melting salts

Caseins can be described as amphoteric phosphoproteins with different hydrophobicities (D. Horne and Lucey (2017)). Their amino acid composition is not unlike those of globular proteins, however, the high level of proline hinders caseins to form globular structures. Four different gene products of caseins can be found not only in bovine milk, the alpha-, alpha-, beta-, and kappa-casein. The interactions of caseins that lead to the initial formation of micelles, as well as their interaction properties in general, have recently been debated (D. Horne and Lucey (2017), D. S. Horne (2017), Holt et al. (2013), Thorn et al. (2015)). However there seems to be a common understanding on two major types of casein interactions that lead to micelle formation, hydrophobic interactions and the formation of calcium phosphate nanoclusters (Lucey and Horne (2018)). Accordingly caseins are molecules that can interact with each other via hydrophobic interactions, as well as electrostatic interactions. The casein micelle models presented earlier in this section are both based on the long established theory that hydrophobic interactions are a driving force for micelle assembly as well as casein aggregation (D. S. Horne (2017)). Hydrophobic interactions occur under the exclusion of water. When two opposing surfaces get close, an energy benefit arises from the new conformation of the water molecules that were disrupted by the interacting surfaces or structures.

For estimation of the hydrophobicity of caseins, especially in the special ionic environment present in processed cheese, a hydrophobic cluster analysis (HCA) might give further insight (Fig.xx). This type of computational analysis allows one to take into consideration, that the caseins are not lacking any kind of substructure, since there is evidence by the self-association behavior and the large amounts of hydrophobic areas in the molecule that the caseins are not intrinsically unstructured proteins (IUP) (Thom Huppertz et al. (2017), Lucey and Horne (2018)). Their flexibility is rather derived from the high amounts of proline that allow the protein-string of the casein to remain flexible and to not conform into a globular state. The HCA plots show caseins in a sub-helical structure with

a unit length of ~10. The amino acids in close distance within the plot can form functional areas, such as hydrophobic clusters. The coloring of the HCA plot is designed to highlight hydrophobic interaction sites, or clusters. Other amino acids are highlighted as well. Serin can occur in substituted form (as it is the case in caseins) as well as threonine, glycine poses a potential binding site and proline disrupts helical or higher ordered structures. Therefore, special symbols were chosen, as it is described in Rebehmed et al. (2016). The plots were created with the website:

[http://mobyle.rpbs.univ-paris-diderot.fr/cgi-bin/portal.py?form<sup>1</sup>HCA#forms::HCA](http://mobyle.rpbs.univ-paris-diderot.fr/cgi-bin/portal.py?form%1HCA#forms::HCA).

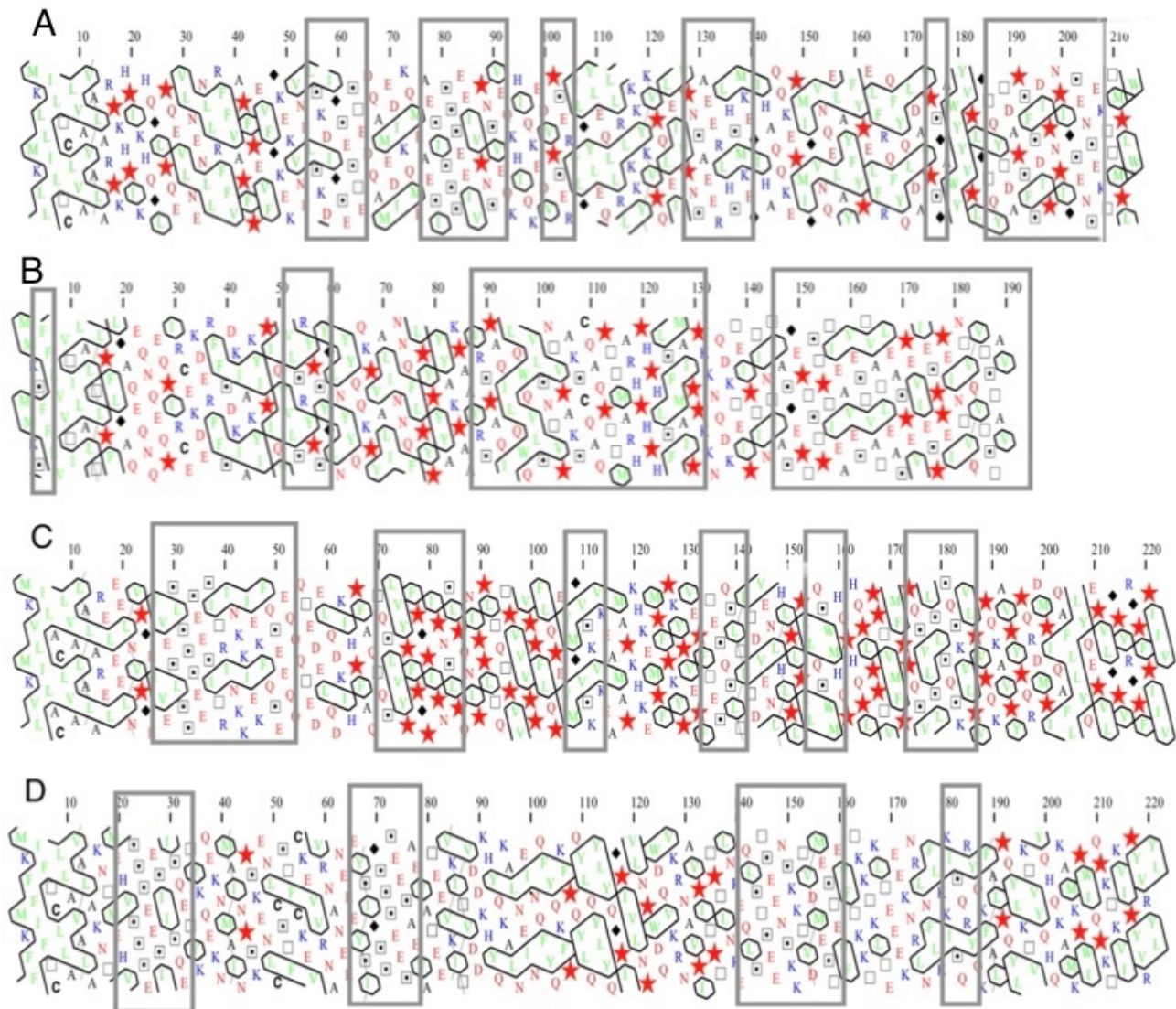


**Fig. 7.** Plots on hydrophobic cluster interactions of caseins: (A) alphaS1 casein, (B) kappa casein, (C) beta casein, (D) alphaS2 casein; legend as in @Rebehmed2016, with addition of grey squares to highlight serin (dotted square) areas. hydrophobic amino acids (green) are grouped and surrounded with a solid black line to form clusters, prolin (red star), glycine (diamond), threonine (square) are also highlighted.

In the HCA plots, caseins comprise of hydrophobic areas that are disrupted by fractions that carry charge by phosphorylation of serin (Fig.7). Serin rich structures were marked (gray boxes), since they are potential candidates for post-translational transformation, and then carrying a substituted phosphate group at the serin residue. The charged areas coming from serine residue display different degrees of phosphorylation. A direct relationship between the degree of phosphorylation and calcium binding by chelation has been shown, which is why the calcium sensitivity of the caseinates is in the order kappa < beta < alphaS1 < alphaS2. The distribution of charged serine residues is not uniform in the caseins (Aoki, Toyooka, and Kako (1985), Clare and Swaisgood (2000)). Looking for example at kappa casein (Fig.7(B)), it can be seen that the serin residues are arranged over larger areas in the so plotted molecule, however in little quantities, when compared to, for example the residues 20-35 in alphaS2 casein (D). Besides the display of charged residues, the HCA plot also reveals planar hydrophobic areas, without charge from phosphoserine, due to high amounts of prolin (indicated by a red star). Such areas can especially be found in beta casein (see for example amino acids 195 - 120), but also in kappa casein (amino-acids 60 - 85) and alphaS1 casein (amino acids 15 - 45). When removing the charge (which means especially removing the CCP in this case), the planar hydrophobic areas of these three caseins become even larger. AlphaS2 casein displays smaller planar hydrophobic areas at amino acids 110 - 120 and 205 - 215. Even more, the planar hydrophobic area is not increased by removal of the CCP, since they are not directly neighboring hydrophobic and proline rich areas in alphaS2 casein. Hydrophobic interaction happens on the surfaces of the interacting molecules. Hence the arrangement of planar and hydrophobic areas in the caseins, with respect to the localization of their serin rich areas in this arrangement, might give insight towards casein-casein interaction in the special environment investigated in this work. The phosphate residues in caseins are relevant in the context of processed cheese formation, since processed cheese is formed into a new or “processed” structure due to the use of melting salts. Melting salts is a commonly used term for the type of salts that are able to chelate a divalent calcium cation. Examples for such salts are Mono-, Di- or Tri-sodiumcitrates, Di- or Tri- Sodium Phosphates, or polyphosphates like Pentaphosphates or medium chain phosphates, to only cite a few existing in the context of food and specifically cheesemaking. An example for a chelated calcium ion by phosphates is given by Fig.8.

The term emulsifying salts is used interchangeably with the term melting salts in this study and elsewhere. However the term emulsifying salt should not lead to the conclusion, that the salts itself have any function as emulsifying agents. Rather, as indicated by the term melting salts, those type of salts lead to a dissociation of CCP in the casein micelle, which leads to free caseins that can then emulsify a dispersed phase. The viscoelastic properties however, have proven to be largely influenced

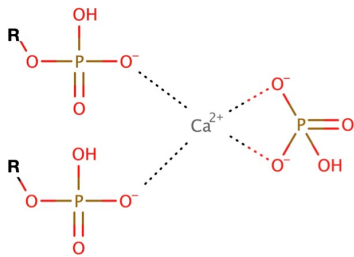


**Fig. 8.** Example of a calcium chelat complex associated with three phosphate groups. R can be either a proteinogenic residue, a calcium phosphate nanocluster (CCP), an associated or bound phosphate, pyrophosphate or polyphosphate or similar.

by the type and concentration of emulsifying salts used (See Table 1 for exemplary studies). It can be suggested, that the chelation properties in the variety of salts used are not affecting the CCP all in the same way, hence the emulsifying salts are mostly used in binary or ternary mixtures of empirically proven salts.

Since the binding structure of the casein micelle is not yet fully understood, a conclusive answer on how the emulsification salts work on the caseins or casein micelles, respectively, cannot be given. The chelating salts enter the casein micelle during hydration through microfluidic channels. To a certain extent, also strongly depending on the type of salt used, the calcium from the CCP gets released, a shrinkage of the micelle and also the release of single caseins was reported at low concentrations, at higher concentrations, complete dissociation of the micelle took place. However, various studies showed the different behavior of a casein matrix, depending on the type of salt used (Sadlikova et al. (n.d.), Salek et al. (n.d.), Awad et al. (2002), Salek et al. (2015), Brickley et al. (2008), Chen and Liu (2012), Nagyova et al. (n.d.) and others). An observation made in the cited works was that ideal ratios of emulsifying salts can target special properties of the final product, such as hardness or spreadability. In general, a higher amount of phosphate salts resulted in higher viscosities or harnesses of cheeses. The best products were given, when not one salt, but a ternary mixture of emulsifying salts was present, ideally combining a polyphosphate, a di- or tri-phosphate and a citrate.

A detailed analysis of the structures of model processed cheeses similar in composition to this matrix were investigated containing different amounts of polyphosphates next to the other emulsifying salts, also used herein (Vollmer, Kieferle, Pusl, et al. (2021)). The samples were analyzed using transmission electron microscopic (TEM) imaging, elucidating the structures on a nano scale. An effective increase in cheese hardness could be found with increasing amounts of polyphosphate. Also a threshold value of 1.5% of polyphosphate was necessary to induce the creaming reaction. A detailed description, what leads to the formation of casein fibrils in other environments can be found in the cited work. Other interactions of caseins in an environment containing melting salts are of

electrostatic or general hydrophilic nature.

### 1.3.2 The Creaming Reaction

The development of processed cheese took place around the beginning of the 20th century. The aim at that time was to develop a method to extend the shelf life of cheese and thus to store it longer and also to be able to export it. In 1911, the Swiss inventors W. Gerber and F. Stettler succeeded in transforming raw cheese into a homogeneous, flowable state through the application of sodium citrate as a melting salt. From this “sol” state, a solid, homogeneous “gel” formed again after cooling. At the same time, a processed cheese based on cheddar cheese was also developed in the USA. Here, citrates and orthophosphates were already used as melting salts. In 1917, the KRAFT company launched the first processed cheddar cheese on the market, which was initially intended for army rations. The company Gebrüder Wiedemann from Wangen in Allgäu did not conquer the European market until 1921.

Initially, the grinded cheese, cheese mass or protein-fat-mixture, is mixed with melting salts and then heated under constant shear. In this melting phase, the calcium is chelated by the melting salts and replaced by sodium. This results in a dispersion of the casein, which increasingly dissociates due to the lack of calcium phosphate bridges and binds the fat into the protein network. Emulsifying salts generally increase the stability of cheese emulsions under thermal treatment (Hougaard et al. (2015)). During the production of processed cheese, first a gel-sol transition and then again a sol-gel transition takes place. The transformation from insoluble gel to sol takes place through the application of heat and mechanical processing. This process works in processed cheese, in contrast to normal cheese, where only a phase separation would occur, through the addition of melting salts. The salts add effective charge carriers to the system, the calcium is removed from the casein by ion exchange, and the polypeptide chains bind water, resulting in swelling of the matrix. The subsequent sol-gel transition, in which the flowable mass becomes a solid cheese again, is achieved by subsequent cooling. Accordingly, the “creaming reaction” is an ion exchange reaction in which the gelatinous cheese structure is converted into an emulsion with a spreadable structure under the action of energy and melting salts. The subsequent structure build-up after melting, during which complex physicochemical reactions take place, is called post-creaming. If the structure loses its spreadability as a result of too long post-creaming, this is referred to as overcreaming of the processed cheese, which results not only in very solid gel formation but also in the escape of fat and water (Lenze et al. (2019)).

Vollmer, Kieferle, Youssef, et al. (2021) suggested to update the term “creaming” or “creaming reaction” to the term “texturizing.” The term creaming can be misinterpreted in this context, since it is also used for the description of emulsion instability: when the fat phase, especially in milk (fat) or cream protrudes to the surface of the emulsion, the emulsion is said to be “creamed.” The term texturization would fit the process in a better way, since texturizing, i.e. the aggregation of caseins in some kind, leads to the formation of the desired structure. The properties of the final product are seemingly effected more by the composition of the matrix than the processing conditions. Hence a more spreadable product will be rather obtained by the use of more water and or fat, than shorter processing times or lower processing temperatures or speeds.

#### **1.4 Investigation of process parameters and composition on the structure formation during manufacture of processed cheese**

The final structure of the processed cheese depends on the starting material as well as the processing conditions. Various studies have been performed analyzing the effects of matrix composition and processing conditions on the final texture of the cheese matrix. Fu, Watanabe, Satoh, et al. (2018) investigated different emulsification conditions for their influence on the microstructure of a model cheese network. Stirring speeds of 400 rpm and 1500 rpm, and process times of 10 min and 30 min were varied. The microstructure of the resulting protein network was identified by SEM, and the distribution of the fat globules by CLSM. Regardless of the stirring speed, a so-called “fine-stranded-network,” i.e. a network of protein (aggregates) arranged together like fibers, was shown here after 30 min. In addition, a start-up phase, as well as an exponential phase, was recognizable during the processing of the matrix of 30 min. However, longer processing times were not targeted here to identify the full course of protein aggregation.

This work also dealt with the effect of rework, i.e. already pre-processed processed cheese mass added to the raw materials at the beginning of the reaction, and its effects on the structure formation. It was shown that only sufficiently processed mass can ensure acceleration of network formation. The effect of the rework is manifested by smaller fat globules and a finer, more ordered network in the final product. However, no mechanistic explanation of the processes is provided, but only the phenomenon or the effect of rework on the final product is described. Černíková et al. (2018) also studied the effect of rework at different concentrations (0 - 20% of dry matter). Again, smaller fat globules as well as a fine, fibrous network and increasing hardness of the final product were observed up to a rework concentration of 10%. When the rework concentration was increased further, no significant change in the final product was observed. Although this work provides a good overview of

compositional and process-related effects of rework addition, it does not provide a mechanistic explanation. Lenze et al. (2019) investigated a process cheese matrix and the effects of rework addition. Processing time was significantly reduced under rework addition. This effect was explained by an autocatlytic effect. Favourably aggregated proteins act, similar to a seeding effect in crystal systems, as a template which leads to structuring the other proteins in the system in the same way. From this, it could be concluded that proteins or proteinogenic systems structurally similar to caseins aggregate within a certain process environment to form hydrophobic clusters and then eventually to a large network stabilized via hydrophobic interactions. Guinee, Carić, and Kaláb (2004) also dealt with similar systems. Here, structure formation was interpreted as a consequence of hydration of proteins and as a consequence of increasing viscosity during cooling of the hot mass.

A possible cause of the viscosity increase was overall described as exposure to the ionic environment with the effect of complexation of stabilizing calcium ions results in dissolution of the casein micelle, exposing the hydrophilic and hydrophobic sections of the individual caseins. Consequently, hydration of caseins occurred due to hydrophilic interactions with the aqueous phase and interactions of caseins with the fatty phase via hydrophobic interactions. These interactions also led to emulsification of the fatty phase.

Cunha et al. (2013) showed the influence of different fats (soybean oil, partially hydrogenated soybean oil and milk fat in the form of butter) on the rheological, functional and sensory properties of spreadable processed cheese analogs. Smaller fat globules were observed in unhydrogenated fats, which was explained by the greater steric inhibition of unsaturated fatty acids and resulting therfrom, lower hydrophobic interactions among fat molecules. In addition, unhydrogenated, or unsaturated, fats have a lower viscosity, which makes the fat easier to break down during processing. Solowiej et al. (2014) investigated the effect of inulin as a fat-replacement in processed cheese. Ramel and Marangoni (2018) gave a protocol for the replacement of milk fat with canola oil in analogue cheeses and also used oat fiber particles for better stabilization. Other additives, such as starches were investigated in the works of N. Noronha, Duggan, Ziegler, Stapleton, et al. (2008). As already mentioned earlier, excessive studies have been performed on the effect of different amounts and types of emulsifying salts. Concluding this section, it can be stated that processed cheese is a vastly investigated model system. The focus was predominantly on the effects of processing or compositional changes on the final product. Only few studies have performed that followed the structure buil-up in a targeted manner. El-Bakry et al. (2011) and N. Noronha, Duggan, Ziegler, O'Riordan, et al. (2008) investigated multiple samples during the formation of a processed cheese mass. However, since the samples were largely inhomogenous, the different stages of structure

formation could be identified but not followed in an analytical way.

## 1.5 Compositional analysis of model processed cheese systems

Model processed cheese systems have been investigated widely in macroscopic terms, as described previously in this section. A compositional analysis can be defined as an analysis not just in the makrostructure represented as viscosity, gel strength or any of the such. In addition, a compositional analysis cannot be given conclusively by imaging techniques, since the electron density of the casein particles is too similar.

Spectroscopic measurements like Fourier Transform Infrared (FTIR) spectroscopy gives insight towards the intermolecular binding in molecular, giving general conclusions towards the structure of molecules. It is best applied to rather dry or powdery samples and was used for example for the structure determination of processed cheese made with additives like starches, as it was done in N. Noronha, Duggan, Ziegler, Stapleton, et al. (2008). FTIR proved to be useful to elucidate such structures in the matrix, that are of distinctly different composition. For structure elucidation of very similar but differently aggregated casein structures, FTIR is not the proper tool since the differences in aggregation are too small in terms of their possible excitation state by IR.

For a compositional analysis of fat-free protein mixtures, native or reducing SDS page is a commonly used method. An SDS page is a type of polyacrylamid gel-electrophoresis (page), where Sodium Dodecyl Sulfate (SDS) is used to charge the protein residues negatively and then separating them by size using a strong electric field. The term “native” in this context means, that no reducing (as respective for the treatment) agent like Dithiotreitol (DTT) was used in the samples. DTT leads to the disruption of Dithio- or Thiol induced bonds or interactions.

Another method to determine the protein concentration in dense matrices is the method by Dumas, where the sample is burned and the total released nitrogen from this process is measured and calculated to a protein concentration, using an empiric factor. As already indicated when describing the SDS procedure, the determination of protein concentration after the method of Dumas also requires almost fat free samples, since the samples are burned and too much fat would lead to the disruption of the measurement due to the burning of the fat phase. Analysis by SDS page also is not suitable for processed cheese samples, since the SDS will, as a tenside, also bind to the fat-phase and therefore, clear protein bonds are not visible in fatty systems. This effect is known to the person skilled in the art and is due to the overlay or “smearing” of the fat in the runs. To determine the structuring mechanisms in processed cheese however on a molecular level, a compositional analysis

seems urgently necessary. Therefore a compositional analysis herein is a description of either the distribution (%) or concentration of certain molecular components within the matrix.

### 1.5.1 Analysis by reversed phase chromatography

Reversed phase high-pressure liquid chromatography (RP-HPLC) is a technique widely used in compositional analysis, especially in food systems. In food analysis, quick and easy measures for Quality Assurance can be implemented, as well as detailed compositional analysis of food matrices up to Liquid Chromatography in general uses a stationary phase and a mobile phase with respective opposite polarities. Besides polar or apolar columns, a multitude of other columns are available, ranging from columns with a special pore size for size exclusion chromatography or ionic columns for respective ion analysis in terms of ion-exchange-chromatography. The detector unit when investigating proteinogenic materials is usually a diode array detector (DAD), with detection in the UV-Vis. For proteins, a detection is usually made around a wavelength of 280 nm, since the aromatic amino acids get excited in the UV. This requires, of course, the use of pure standards for calibration, since the excitation of individual proteins in the UV is specific and different for every species.

The basic principle of a reversed-phase chromatography experiment is the use of a hydrophobically substituted, i.e. a non-polar or reversed-phase, silica gel as the chromatographic column. As already mentioned, the column represents the stationary phase, whereas the solvent or eluent represents the mobile phase, which transports the analytes to and through the column. For RP\_HPLC this means, that the mobile phase is of rather polar nature. In RP-HPLC experiments, specifically designed to target dairy proteins, the mobile phase used is usually used as gradient elution. Gradient elution means, that the polarity of the mobile phase is adjusted (either gradually or step-wise) during the measurement, to better elute the sample components from the column. Bonfatti et al. (2008) first showed a measurement for the simultaneous measurement of caseins next to whey proteins. The buffer system most suitable for this type of measurement was presented by Bonizzi, Buffoni, and Feligini (2009) and is described in chapter 4 of this work. Dumpler et al. (2017) was able to reduce the experiment length significantly by improving the elution of whey proteins next to caseins from the column. The chromatogram which is obtained by that process as well as the identification of the elutes is shown in Fig.9.

It has been shown, that RP-HPLC is a powerful tool for protein quantification. However, as already discussed in the beginning of this section, fat-rich samples pose to be a problem as well. The isolation of caseins from the fat phase seems crucial in order to determine the functional properties of the

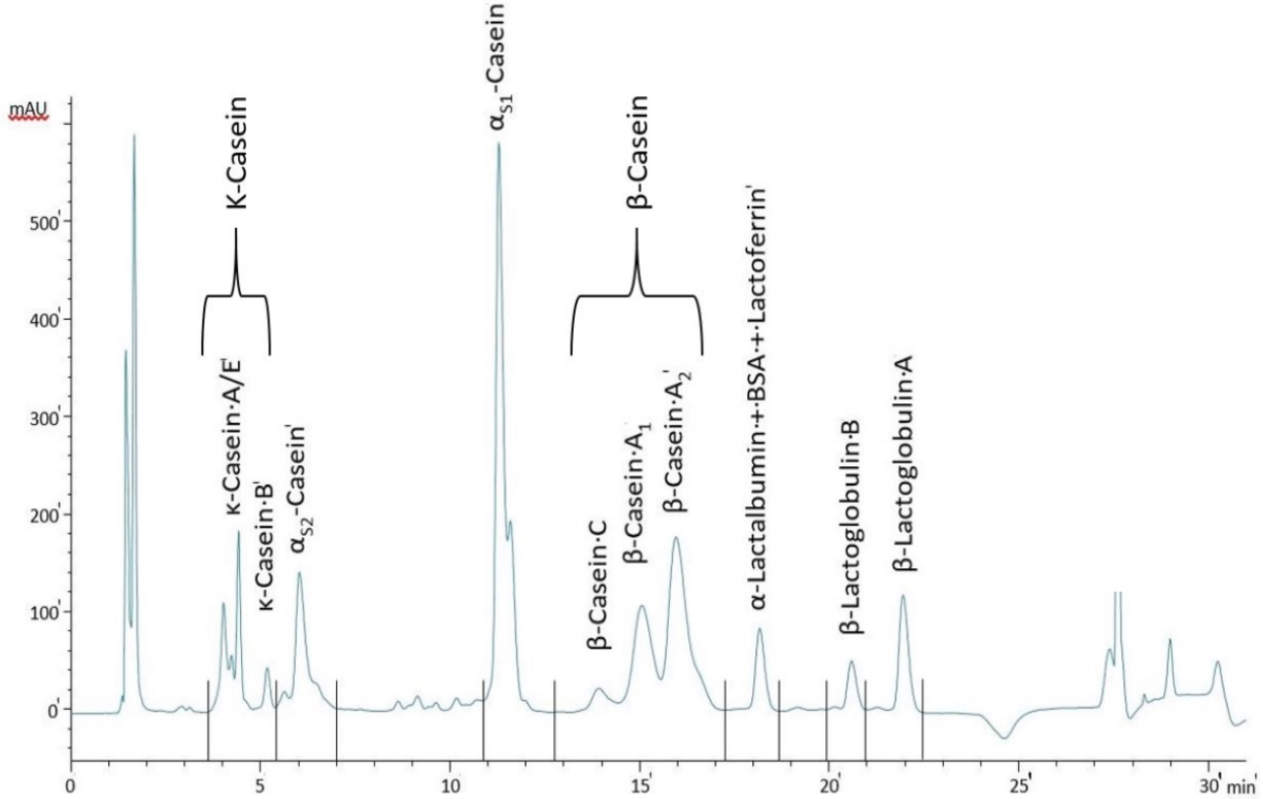


**Fig. 9.** Casein elution in RP-HPLC as cited in the literature, next to whey protein elution

dispersed phase in the system.

### 1.5.2 Investigation of $^1\text{H}$ T2 relaxation

The measurement of longitudinal relaxation of protons after being excited by a magnetic spin is a readily used technique for compositional analysis. The principle of those type of measurements lies in the fact that positive nucleii have a magnetic spin. This spin can be exited using a polarized magnetic field, which is the first 90 degree pulse. By the use of a spin-echo-train, better known as CPMG sequence, a pulsed magnetic field puts the spins back into the direction of the magnetization vector, but with a decaying intensity due to the interaction of the spins with the surrounding matrix. The CPMG sequence is especially useful when applied in dense systems ((Schmidt 2004?)), as in Hinrichs, Bulca, and Kulozik (2007)). An overview, from CPMG pulse to data for NMR T2 relaxation measurement is given by Fig.10.

Some of the composite model systems already described herein were also investigated using T2 relaxation times. In the following section, the systems most similar in their experimental approach or composition are described below in more detail.

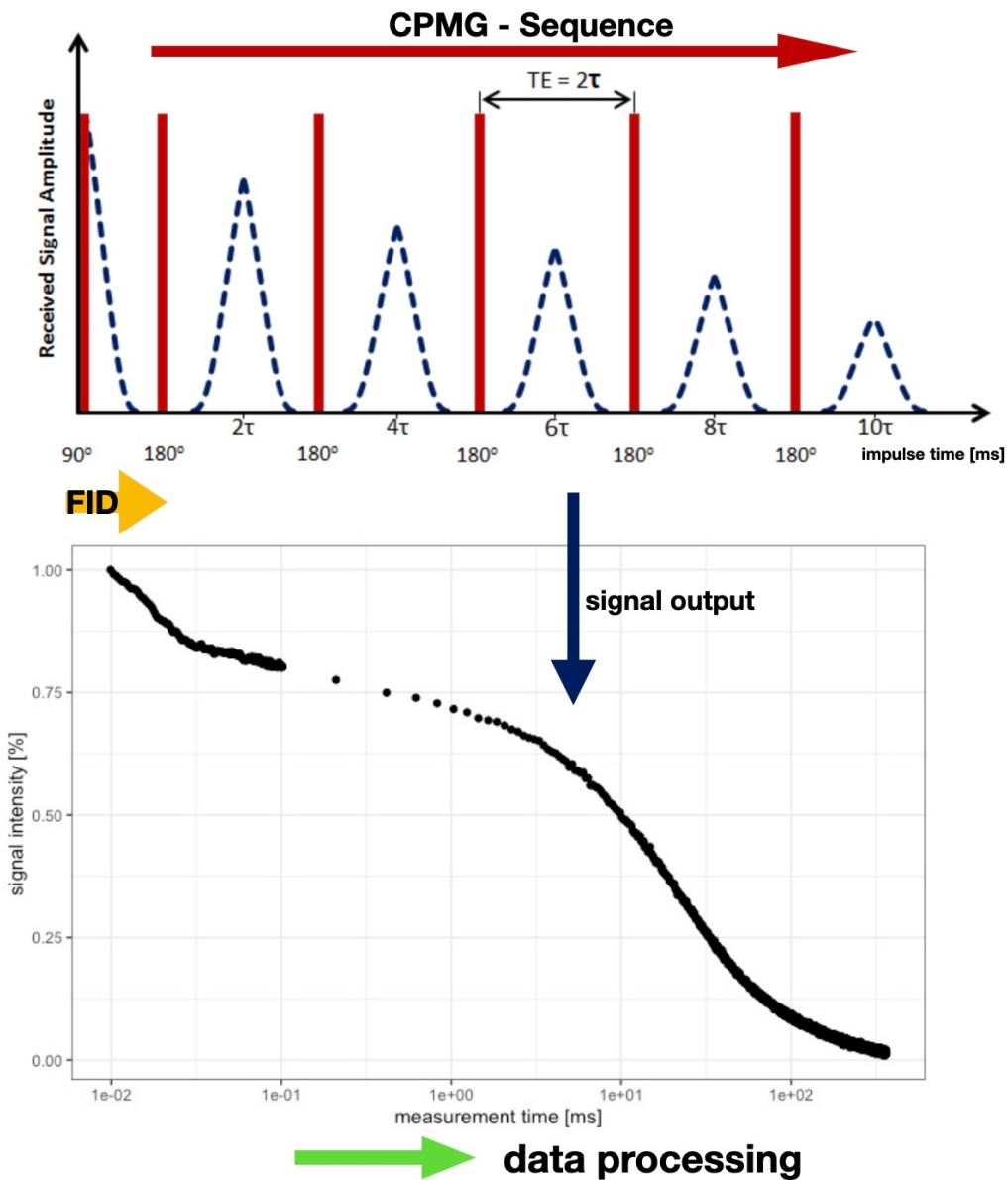


**Fig. 10.** Obtaining the T2 relaxation time: Free Induction decay (FID) after first magnetic pulse (90 degrees at impulse time), subsequent CPMG pulse (red) leads to rephasing of the 1H spins, decaying singal (dashed line) is Fourier transposed to the data output, which represents the envelope curve, or the LaPlace function, depending on the numeric method chosen (data processing).

In Chen and Liu (2012), a matrix consisting of differently ripened mozzarella as the protein source and butter as the fat phase was processed to a coherent cheese matrix and analyzed using T2 relaxometry. The components were fitted using the Laplace inversion computer program, further details of the fitting process were not disclosed. Four components were fitted, however instead of attributing one of the fitted peaks in the distribution to the fat phase as done elsewhere, the two peaks between 1 and 100 ms were attributed to water, with no further explanation as to why. N. Noronha, Duggan, Ziegler, O'Riordan, et al. (2008) investigated an imitation cheese matrix made

from particulate rennet casein, vegetable oil emulsifying salts and 53% water, processed in a Farinograph cooker. The matrix was constantly kneaded and analyzed, *inter alia*, in their T2 relaxation times. The middle component was attributed to the fat fraction. El-Bakry et al. (2011) investigated a model processed cheese system, prepared with a Farinograph-type cooker, in order to follow the structure build-up during processing. Samples with a lowered amount of emulsifying salts were also tested. The T2 relaxation times proved a lesser casein hydration and a longer time for fat emulsification in an environment with reduced amounts of melting salts.

## 1.6 Studies related to this work

The studies performed by Röck (2010), Lenze et al. (2019) and Vollmer, Kieferle, Youssef, et al. (2021), Vollmer, Kieferle, Pusl, et al. (2021) are in direct relation to this work, since an equal model processed cheese composition as it was in this study was investigated. Lenze et al. (2019) (or Röck (2010), respectively) did a vast investigation and characterization of a model processed cheese mass that was processed (constant heating, constant stirring) in a rheometer as a processing device. The rheometer was set-up with a custom made cup and a two blade stirring rod in order to make use of both of its functions; as heating and shearing - in our case stirring - device as well as instrument to detect changes in the Torque of the stirrer, which was interpreted as apparent viscosity during this process. A step-wise structure formation process was reported, and the processed matrix was roughly characterized at distinct processing times, using imaging techniques (LM, TEM). The process parameters influencing the structure formation of the model matrix were investigated. An analysis by comparison was performed, investigating the influence of variances in model composition on the detected structure formation. A summary of the investigated parameters (process and “compositional”) is given in Fig.11. From the obtained data, the step-wise structure formation process could be characterized into the following phases:

- (a) an initial phase (0 - 25 min), where matrix hydration and therefore chemical reactions take place,
- (b) a first exponential phase (25 - 140 min), characterized as an increase in apparent viscosity, dedicated to the formation of a stable emulsion in the system, up to a
- (c) plateau phase (140 - 180 min), characterized as de-emulsification, concluded by
- (d) a second exponential phase (180 - 225 min), characterized as protein network formation.

The formed structures were characterized on a microscopic level by fat globule size and light imaging, on the macroscopic level by oscillatory shear rheology. Values for pH and dry matter of the products

were obtained. Besides sampling for LM imaging, the process was investigated as a whole. No explanations on a molecular, i.e. casein-casein interactions concerning level were made.

Investigated parameter	Key results
Stirring speed	Higher processing speed lead to weaker gels due to a proposed structure corruption from the applied shear
Temperature	$\geq 70^{\circ}\text{C}$ necessary to initiate creaming reaction
Protein composition	Model matrix was derived from natural cheese with addition of 2% (w/w protein) protein powder of varying sources). Presence of whey proteins, native casein and rennet casein promotes the occurrence of a distinct first exponential phase, whereas acid casein and sodium caseinate lead to absence of a first exponential phase but show a pronounced exponential increase in apparent viscosity at late processing times
Protein concentration	Higher concentration in proteins results in stronger gels and stronger display of a step-wise structure build-up
Addition of rework	Highly accelerated structure formation, values of 5% and 10% were investigated, higher rework concentration also leads to even faster structure formation
pH educt	Optimum pH for the creaming reaction to occur in this set-up: 5.83 - 5.96
Fat globule size	Smaller Fat globules accelerated structure formation
Fat composition	Use of surface active ingredient in systems made from oil as the fat phase strongly accelerated structure formation; *Note: model for the present study was chosen from this data set and was the control (oil, no emulsifier, with Lactose as dry matter add-on), but used without Lactose during this trial.*
Fat concentration	Presence of fat is needed to display step-wise structure formation; very low structure formation without presence of fat; Lactose was used as dry-matter add on in samples with reduced fat content

**Fig. 11.** Parameters influencing the structure formation of model processed cheese

Vollmer, Kieferle, Youssef, et al. (2021) investigated the same model processed cheese mass that was investigated in this study, but with adapted process parameters to give a long processing time (total of 415 minutes). The processing of the samples, followed a sampling procedure that is key to this study, and will be presented later on. This allowed, to give six consecutive samples to be investigated by LM imaging and TEM imaging. The obtained images strongly suggested the formation of casein fibrils. In fact, it was suggested, that the casein fibrils were prominent for the structure formation reaction, that is the “creaming”-reaction. An updated model for the proposed structure formation processes that take place in processed cheese is displayed in Fig.12.

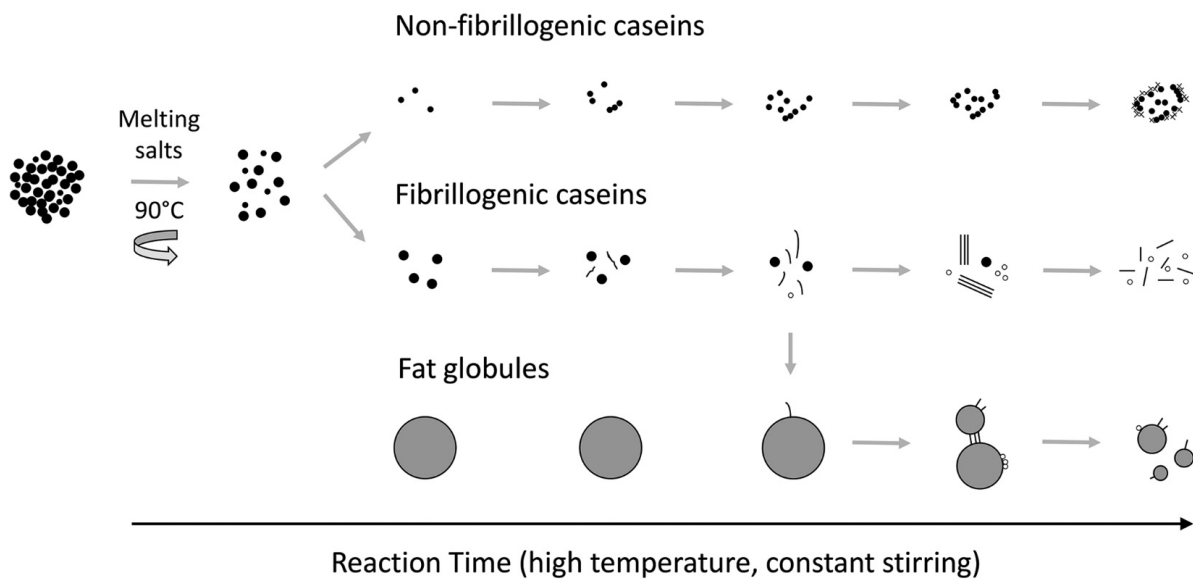


**Fig. 12.** Model presented for structure formation reaction as cited in the literature; formation of fibrillogenic caseins and non-fibrillogenic caseins; fibrillogenic caseins emulsify the dispersed phase and later seem to form a particulate network

The obtained TEM images showed the formation of large entangled or interconnected networks with fibrillar structure. During the plateau phase of the structure formation, elongation of the detected fibrils was apparent. The emulsification of the fat was considered mainly due to specific interactions of the fibrillar structures with the fat phase. Even more, the followed structure build-up revealed the progressive separation of the casein matrix, into protein dense, fibrillary aggregated areas and areas with low protein density. At late stages of processing, degradation of the fibrils becomes evident. Vollmer, Kieferle, Pusl, et al. (2021) investigated a model processed cheese matrix that had varying amounts of a binary mixture of emulsifying salt. The samples were processed in the same manner as above. Casein fibrils were present at later processing times, also the progressive phase separation already beginning at early stages of processing in Vollmer, Kieferle, Youssef, et al. (2021) could be seen at later processing stages. An important threshold value for this study could be given: the

degree of dissociation of the casein micelle in the model system, measured as the amount of insoluble calcium after acid-base titration depends on the concentration of a specific emulsifying salt. A compositional analysis was made to investigate the fibrils, which were detected as a slight increase of kappa casein in the insoluble pellet after ultracentrifugation.

Lee et al. (2003) gave a model description (Fig.13) for the formation of a protein matrix in processed cheese. It was indicated, that the casein monomers form a string like network, not unlike a particle gel, which resulted in a peak in viscosity.

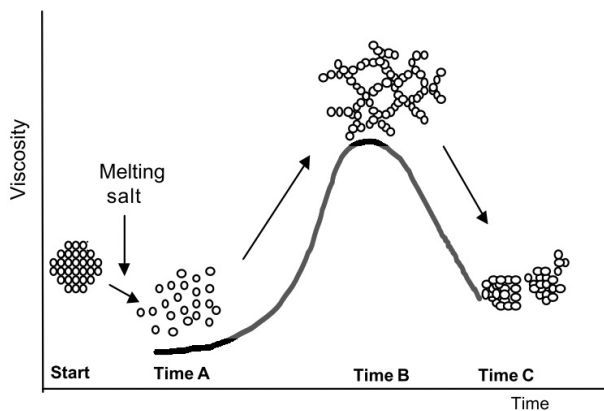


**Fig. 13.** Structure formation and destruction process as indicated by viscosity of a fat-free processed cheese mass as cited in the literature; Protein network formation leads to a peak in viscosity, in a fat free formulation the collapse of the network is visible by decreasing viscosity

From comparison to a fat-free model, it was concluded that the connected protein matrix collapses to form dense units. It was concluded that fat was not prevalent for the creaming reaction to occur and emphasized protein protein interactions. The industrial terms for typical errors in processed cheese, namely “undercreamed,” “creamed” and “overcreamed” were brought into context with the observed structure formation and structure destruction processes. To conclude this section, Table 1 gives a summary of recent works already cited in this section, due to likewise protein matrices.

**Table 1:** Studies on processed cheese relevant for this work

Author(s)	Investigation/Key findings
Brightenti et al. (2018)	Acid induced cream cheese and the effect of low or high pressure (HP) pre-treatment and fermentation temperature (FT) by means of Rheology and numeric analysis
Berta et al. (2016)	Small amplitude oscillatory shear rheology of natural cheese compared imitation (i.e. processed cheese) in conditions relevant for baking

---

Author(s)	Investigation/Key findings
Sadlikova et al. (2010)	Effects of Phosphate salts on the viscoelastic properties of processed cheese, tested with oscillation rheology;
Salek et al. (2015), Salek et al. (2017)	Textural and viscoelastic properties of spreadable model processed cheese (dM = 35%, fat in dM 50%) as effected by mixtures of the following melting salts: disodium hydrogenphosphate (DSP), tetrasodium diphosphate (TSPP), medium chain (n=20) polyphosphate (PP), trisodium citrate (TSC). Hardest cheese was found in 1:1 mixtures of DSP and TSPP. Effects of storage time was also investigated
Awad et al. (2002)	Different ratios of emulsifying salt mixtures and their effect on adhesiveness and hardness during storage.
Brickley et al. (2008)	Effect of emulsifying salts and special ratios on non-fat processed cheese, samples from TSC as emulsifying salt showed higher creaminess and lower pH
Hougaard et al. (2015)	Stability of hot processed cheese mass improved by addition of emulsifying salts during holding
Chen and Liu (2012)	Increase of pH, hardness and casein dissociation with higher amounts of emulsifying salts are reported.
Guinee, Carić, and Kaláb (2004)	Overview of pasteurised or processed cheese products in terms of preparation, composition and properties
Cunha et al. (2013)	Effects of different types of fat (butter, plant oils and hydrated plant fat) in spreadable cheese analogues on mainly viscoelastic properties and consumer acceptance
Sołowiej et al. (2014)	Fat replacement with inulin in model processed cheeses with added whey proteins resulted in higher cheese hardness and lower meltability
Černíková et al. (2018)	Effects of the addition of rework (i.e. pre-processed cheese) from 2.5 -10% on the viscoelastic properties of processed cheeses, increased firmness was reported due to rework addition, amounts exceeding 10% had no further effect

---

---

Author(s)	Investigation/Key findings
El-Bakry et al. (2011)	Casein hydration and fat emulsification investigated during processing, also with the influence of emulsifying salt reduction (resulted in weaker gels)
Noronha et al. (2008(1), 2008(2), 2008(3))	Textural properties, effect of additives monitored parameters were the hydration of the casein matrix and the emulsification of fat as investigated by T2 relaxation NMR, FTIR and texture analysis methods; Samples were taken during processing.
Ramel and Marangoni (2018)	Replacement of milk fat with canola oil to increase nutritional value of analogue cheese; addition of oat fibres for better product stability
Sharma et al. (2016)	Model mozzarella cheeses and the effect of different amounts of shear work input; non-linear increase in apparent viscosity with increasing shear work input (i.e. kneading).
Lee et al. (2003)	Ground work for many subsequent study like this one, step wise structure formation reported as well as its independence from the presence of fat
Gogaev, Kalutskii, and Voropaev (2009)	Analysis of varying amounts of protein and fat concentrations on the microstructure of processed cheeses
Nagyova et al. (2014)	Effect of ternary mixtures of emulsifying salts on viscoelastic properties.
Barth, Tormena, and Viotto (2017)	Effect of pH and polyphosphate on the cheese structure, measured with $^{31}\text{P}$ nuclear magnetic resonance technique

---

Author(s)	Investigation/Key findings
Urgu (2018)	Effect of fat and emulsifying salt reduction on physicochemical properties of white brined cheese emulsions; apparent viscosity with pseudo plastic flow behaviour increased with fat reduction; essentially a degree of emulsifying salt concentration is necessary to form a stable emulsion without effects of creaming or clustering.
Vogt et al. (2015)	Dissfusing wave spectrometry (DWS) and small amplitude oscillation rheology performed on heated cheeses (Mozzarella, medium Cheddar, aged Cheddar), progressive increase of free water in the system as cheese is heated.
Patrick F. Fox et al. (2016)	Fundamental principles on cheese, recent review on processed or imitation cheese matrices

---

## 2 Motivation and Aim

The aim of this project was to elucidate reactions with caseins as the main players in structure formation, with a special focus on the presence of a dispersed phase. A prerequisite of the concept is to use casein in high concentrations to make them the determining factor in structure formation and the only surface active ingredient to emulsify the dispersed phase.

A representative model to elucidate mechanisms and process-structure interactions in structure formation processes in multiphased, highly-concentrated protein systems are observations in product systems such as fresh or processed cheese. A general conclusion from the investigations made on this type of structure formation so far is, that fat is incorporated into the matrix over the course of processing and that a network from protein is formed progressively, that shows different protein densities (Fig.14) within the developed structure. The determination of the composition of these structures is a main aim of this work and should serve additional insight to the parallel investigations of Vollmer, Kieferle, Youssef, et al. (2021), where the structures were characterized morphologically at a molecular scale, using TEM. At best, a reaction mechanism for the creaming reaction, with respect to casein-casein interactions might be given by combining the morphological and compositional analysis, to a reaction pathway that explains conformational changes of the casein monomers that would lead to such a type of aggregation.

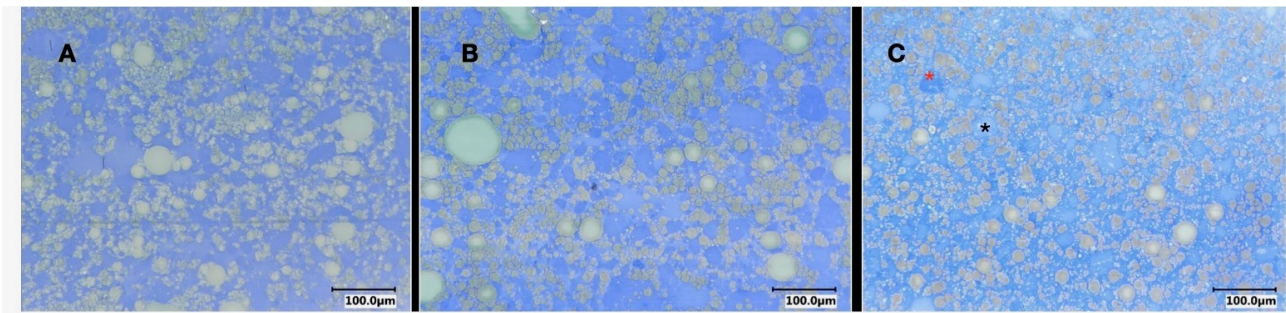


**Fig. 14.** Microscopic images of the model processed cheese investigated herein. Protein has been stained using Coomassie blue, (A) (B) and (C) show the matrix at early, medium and late processing stages. Shrinkage of the fatglobules (grey areas) can be seen as well as areas with higher (darker blue, red asterix) and lower (lighter blue, black asterix) protein density, especially in (C)

The model system by Lenze et al. (2019) is built to follow the structure formation processes during the “creaming” reaction in a Rheometer as simultaneous processing and measurement device. The set-up is used to process the model processed cheese matrix, that has only caseins as the proteinogenic and also as the surface active agent. The structure formation is suspected to display a step-wise increase in matrix resistance during processing, as it is in the red curve in Fig.16. Recent

findings (Vollmer, Kieferle, Youssef, et al. (2021)) however suggested a gradual matrix development. Thus the matrix is investigated at different processing times in order to clarify, which interactions are responsible for the sudden increase in apparent viscosity.

Many analytical methods are available for obtaining compositional data. The matrix is a solidified gel at room temperature. Thus, dilution of the matrix is a requirement. Since RP-HPLC analysis is a readily used tool, it was chosen for compositional analysis of the diluted matrix. Analyzing the solely diluted matrix would give, of course, little mechanistic insight towards the targeted specific casein-casein interactions. Dispersed systems are easily separable by means of centrifugation. It is expected that after centrifugation, the matrix should present itself at least two-phased, due to the presence of the dispersed phase.

The compositional analysis consists also of the characterization of the separated matrix in terms of particle size analysis. On the one hand, fat globule size is to be investigated, but also the diluted matrix separated into probable functional compartments. It is primarily to be determined, if an insolubly aggregated network is formed, that can be followed during its build-up. Additionally, a colloidal analysis of low concentrated casein solutions in the presence of the emulsifying salts might show a behaviour that is also found in the dense matrix. The aim of this investigation was also, to explore the theory of reactive building blocks, or seeds, that are suspected to be formed during this process, and promote an autocatalytic reaction (Fig.15).

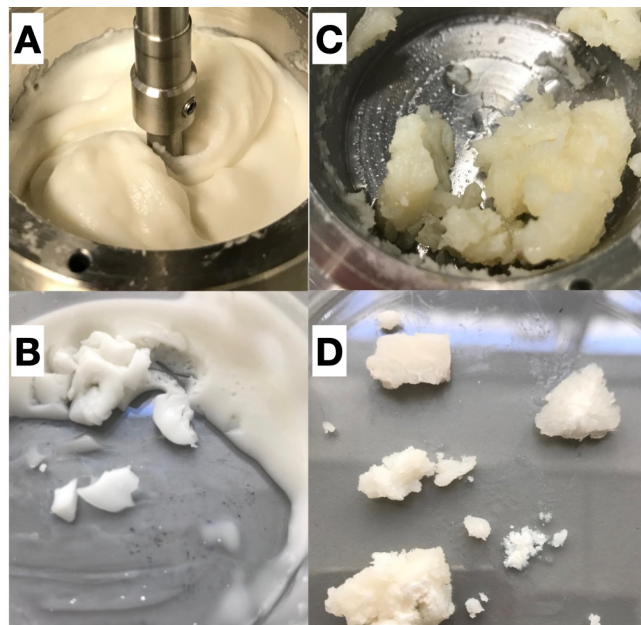


**Fig. 15.** model process cheese structure after shorter processing times of 100 minutes in hot (A) and cold (B) state and after longer processing times of 300 minutes in hot (C) and cold (D) state

In addition, a compositional analysis is performed on the non-diluted matrix by T2 relaxation

measurements to best support the overall compositional findings in this study. In order to give a more detailed overview of T2 relaxation events during processing of a model processed cheese matrix, an upscaled process is used. In a final step, numeric analysis on the obtained experimental data is performed using the tools of the R programming language. The aim here is to elucidate correlations that seem reasonable in terms of structure formation and would give more mechanistic insight about the complex processes occurring during the structure build-up in model processed cheeses.

So far, there is no compositional mechanistic explanation for such a type of structure formation process or for the causes of the sequence of their individual phases. It has been suggested, that the formation of casein fibrils is a key element of structuring the matrix. Fig.15 displays differently long processed samples of the model processed cheese. It is apparent that the affinity of the matrix to bind or incorporate fat during structuring lessens, since free oil is apparent after long processing times. Also, in cold state, a shorter processed gel still shows elasticity, whereas a longer processed gel has a particulate, almost crystalline structure. Characterization of these two apparently differently aggregated structures is a key element of this work. Further, it is to be clarified how the matrix is developing from the elastic to the particulate structure during processing.

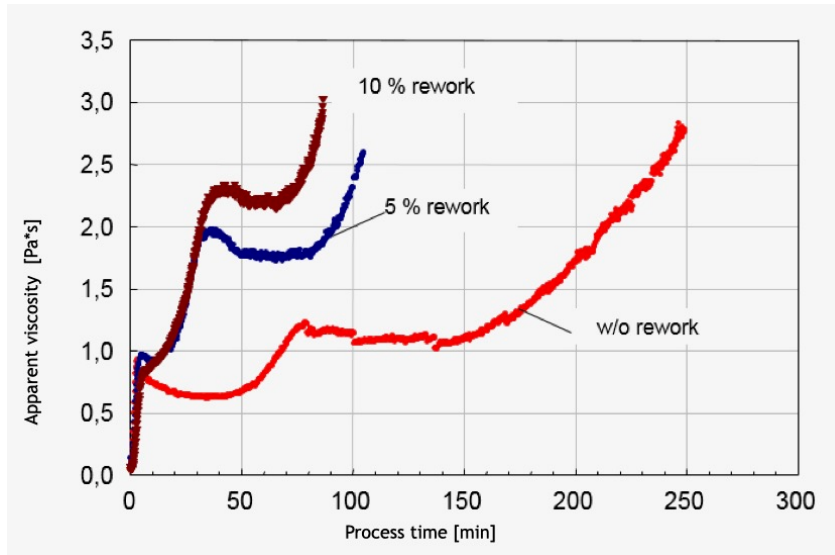


**Fig. 16.** Effect of pre-cooked cheese (rework) addition on structure formation of model processed cheese, suggestion of an auto-catalytic effect

Therefore, the model cheese is processed using a Rheometer with a custom made stirring rod and processing cup up to distinct sampling times during structure formation. The set-up is further equipped with a lid, to diminish water evaporation during processing. The optimum parameters for processing the model cheese mass are chosen from the process and compositional analysis preceding this work in Röck (2010), and were a shear-rate of 200/s of the stirrer, which is  $\sim 16 \text{ min}^{-1}$  stirring

speed. The temperature was chosen to be 90 C, the total protein concentration is set to be 15% and only derived from casein, the pH for the educt was set to 5.88.

The data obtained from this procedure is herein referred to as either measured apparent viscosity, rheological profile or flow curve. However it is important to note, that the measured apparent viscosity in no way represents the dynamic or complex viscosity  $\eta$  or  $\eta^*$  respectively, which is measured with standard geometry, and protocols. The increase in overall cohesiveness of the matrix is displayed as an increase in rotating resistance induced by the sample, or the torque of the stirring rod. Accordingly, the apparent viscosities presented herein were presented as a unitless but integer value.

Investigation of the structure formation and characterization of the interactions between components of such systems should lead in extended approaches to generic knowledge for highly concentrated protein systems.

### **3 Rheological Profile of structure formation in model processed cheese**

#### **3.1 Introduction**

The rheological profile or generally spoken the viscosity of dispersed systems in the food, pharmaceutical or cosmetic industry is an important parameter for the quality assurance of such products. Additionally, the rheological behaviour under certain process conditions can give insight towards the structuring mechanisms occurring on a molecular level. Many studies have been performed on dispersed and highly concentrated food systems such as processed cheese. Most of them were compositional in nature (see also Tablexx in section 1), meaning that effects of certain educt components on the properties of the final product were investigated. Salek et al. (n.d.) investigated the effects of special mixtures of emulsifying salts on the hardness of processed cheeses. Maximum hardness was achieved by a combination of DSP and TSPP. Cunha et al. (2013) studied the effects of different types of fat (hardened and non hardened plant oil in comparison to butter) on the texture of processed cheese. Samples made with both plant oils showed lower fat globule size, higher viscosity and higher hardness than those made with butter.

The step-wise structure build-up has been described in detail by Lenze et al. (2019). The aggregation process was identified as the formation of a continuously aggregated protein matrix wherein the fat is first emulsified and then de-emulsified prior to network formation of the proteins. To the authors knowledge, either other proteinogenic entities than predominantly casein were present during processing, or surface active ingredients or dairy cream was used as the fat phase, hence the structuring and simultaneous emulsifying properties of casein alone has not yet been determined. The TEM images obtained by Vollmer, Kieferle, Youssef, et al. (2021) are from samples that were free of proteins or surfactants other than casein. The samples were prepared by the author, with reduced processing speed in order to get a detailed representation of the structure formation processes occurring. TEM imaging revealed the early presence of fibrillar structures, that hold the fat in the matrix and also form a dense network.

Step-wise structure formations were also detected in the works of Nessa Noronha, O'Riordan, and O'Sullivan (2008) and N. Noronha, Duggan, Ziegler, O'Riordan, et al. (2008). Two peaks were detectable during processing of a model processed cheese in a blade cooker. The first peak or increase was attributed to water uptake and the formation of a hydrated casein matrix, since it was reported that 75% of the added water was absorbed. Subsequently, a fat emulsification took place. After

sufficient emulsification of the dispersed phase, the fat particles were reported to be incorporated into the cheese matrix which lead to the formation of a cohesive matrix as indicated by a second peak.

It has already been shown by others that initially micellar casein sources such as native casein or rennet casein only perform the process known as “creaming reaction” under the presence of emulsifying salts. The micelle must be (at least partially) dissociated to form new structures. When using sodium caseinate as source material, no such dissociation is necessary or even possible, since the caseins are already present in monomeric form. In order to get an overview of the structure formation induced by casein overall, several model cheeses with varying protein sources are produced in this study: rennet casein, native casein and sodium caseinate. Salt composition is varied in samples made from sodium caseinate using HCl and citric acid in order to investigate potential structure formation processes that occur from caseins alone without the addition of melting salts. A further simplified model system was used, which contained 15% total protein for the structure formation and 20% fat (plant oil). The dry matter of the system is around 40%. In order to investigate structural changes during processing, the dairy matrix can be processed in a shear-stress rheometer, in which the structure build-up under controlled shear and heat can be followed as in Lenze et al. (2019).

The aim was to find two distinctly different rheological profiles in order to further investigate (chapter 4) if the changes in rheological behavior can also be seen in distributional and compositional data of the matrix, analyzed at multiple steps of processing.

### 3.2 Material and Methods

#### Production of model process cheese premix

The composition of the processed cheese premix used corresponded to the model processed cheese recipe developed by Lenze et al. (2019) as follows:

**Table 2:** Recipe for the model processed cheese investigated throughout this study

Ingredient	Source	Amount (w/w, %)
Protein	Casein (rennet, native or sodium)	18.42
Fat	Sunflower oil	19.59
Water	Milli-Q water	58.48
Emulsifying salt	Trisodium citrate, dibasic ( $\text{Na}_3\text{C}_6\text{H}_5\text{O}_7 \cdot \text{H}_2\text{O}$ )	0.44
—	Disodium phosphate dihydrate ( $\text{Na}_2\text{HPO}_4 \cdot 2\text{H}_2\text{O}$ )	0.44
—	Pentasodium triphosphate ( $\text{Na}_5\text{P}_3\text{O}_{10}$ )	1.75

Ingredient	Source	Amount (w/w, %)
Acid for target pH=5.88	Citric acid monohydrate (C <sub>6</sub> H <sub>8</sub> O <sub>7</sub> · H <sub>2</sub> O)	0.88

The emulsifying salts displayed in Table 2 stayed the same throughout this trial to ensure an equal dissociation of the caseins and therefore making the single analyses comparable with each other. In the subsequent sections of this work, the single emulsifying salts will be referred to as their abbreviations (i.e. TSC, DSP, PP) shown in Table 2. Also when speaking of “the emulsifying salts” or “the emulsifying salt mixture” or “the melting salts,” the combination of these salts with citric acid as acidulant is meant. In Figures and plots within this work, the term “emS” is used as abbreviation for the emulsifying or melting salt combination.

The recipe displayed in Table 2 is based on the original product; yet, influencing factors such as the type of fat or the age of the cheese can be reduced in order to obtain a system that is as reproducible and comparable as possible. In the course of the present work, native (micellar) casein, rennet casein and sodium caseinate were used as protein sources. Sodium and rennet casein were commercially available products (ICL, Tel Aviv, Israel), the native casein was produced as it was described in detail in Dumpler (2018). Sunflower oil was used as fat. The pH value, which should be ~5.88, was adjusted using powdered citric acid. The melting salts were also weighed out as powder the dry matter.

The individual recipe components were weighed into a beaker on an analytical balance. The protein powder was weighed separately into a weighing dish. The protein-oil-water dispersion was prepared with the aid of the dispersing device “Ultra Turrax T25” at a speed of about 5,000-9,000 min<sup>-1</sup>. First, the salts, oil and water were mixed to form emulsion until the salts were dissolved. Then the protein powder was slowly mixed in to obtain a homogeneous processed cheese premix. The pH value was determined shortly before processing using a solid pH meter.

### **Production of the processed cheese and viscosity measurement**

Thermal processing of the processed cheese premix and the simultaneous online viscosity measurement was carried out using the “AR Rheometer 1000” from TA Instruments. The rheometer is equipped with a Peltier element and an external water bath to control the temperature in the sample cup. A stirrer blade with a length of 6 cm was used as the measuring geometry, which is attached to the drive shaft with a screw connection. This was used both for viscosity measurement and for mixing and shearing the cheese mass. To close off the sample cup and prevent water loss, a suitable lid was made and fitted until the stirring blade could rotate smoothly. The samples were processed at ~15 min<sup>-1</sup> at 90 C. In a later experimental set-up that was also used to produce the

samples in Vollmer, Kieferle, Youssef, et al. (2021) and Vollmer, Kieferle, Pusl, et al. (2021), the aluminum cup was replaced with a V4 stainless steel cup, to reduce friction of product, that adhered to the walls of the aluminum processing cup. The steel-cup was used on an “Anton Paar MCR-700” Rheometer, temperature and speed settings remained the same for samples analyzed during this trial. An image of the experimental set-up can be seen in Vollmer, Kieferle, Youssef, et al. (2021).

Shortly before the measurement, the process temperature was set. The premix was placed in the sample cup and the measurement started as soon as the desired temperature was reached. Flow curves were obtained as a function over time and measurements were performed in triplicate.

### 3.3 Comparison of models tested during model development

The models tested in this section were derived from the model processed cheese samples as they were presented in Lenze et al. (2019). The model was further developed, to include only, or mainly caseins as the proteinogenic phase in order to follow the structuring events happening only from caseins. The three different casein powders were comparable in their composition, with ~90% protein and 1% whey proteins. The manufactured native casein had a lactose content of ~1%, the lactose content in rennet casein was the highest with ~7% (w/w), sodium caseinate had ~5% of lactose. This was resembled by the darker color of the samples made from the latter two after processing, probably due to the formation of early Amadori products. Since lactose was used as a dry matter supplement in samples with reduced fat content in Lenze et al. (2019), the gamma-lactosylation of lysine residues in the casein, which is responsible for the colouring, is not a reaction that hinders the structure formation in any way.

The varying parameters of the tested models are summarized in Table 3, an overview of their flow-curves is displayed in Fig.17.

**Table 3:** Composition and processing conditions of the samples tested during model development

casein	salt	fat	premix	cup-applied shear
native	emulsifying salt mixture (emS)	oil	yes	alu-200
native	emulsifying salt mixture (emS)	oil	yes	steel-200
rennet	emulsifying salt mixture (emS)	oil	yes	alu-200
rennet	emulsifying salt mixture (emS)	oil	yes	alu-100
rennet	emulsifying salt mixture (emS)	oil	yes	steel-200
rennet	emulsifying salt mixture (emS)	milkfat	no	alu-100

casein	salt	fat	premix	cup-applied shear
rennet	emulsifying salt mixture (emS)	milkfat	yes	alu-100
rennet	emulsifying salt mixture (emS)	oil	no	alu-100
sodium	citric acid (CitAc)	oil	yes	alu-200
sodium	emulsifying salt mixture (emS)	oil	yes	alu-200
sodium	Hydrochloric Acid (HCl)	oil	yes	alu-200

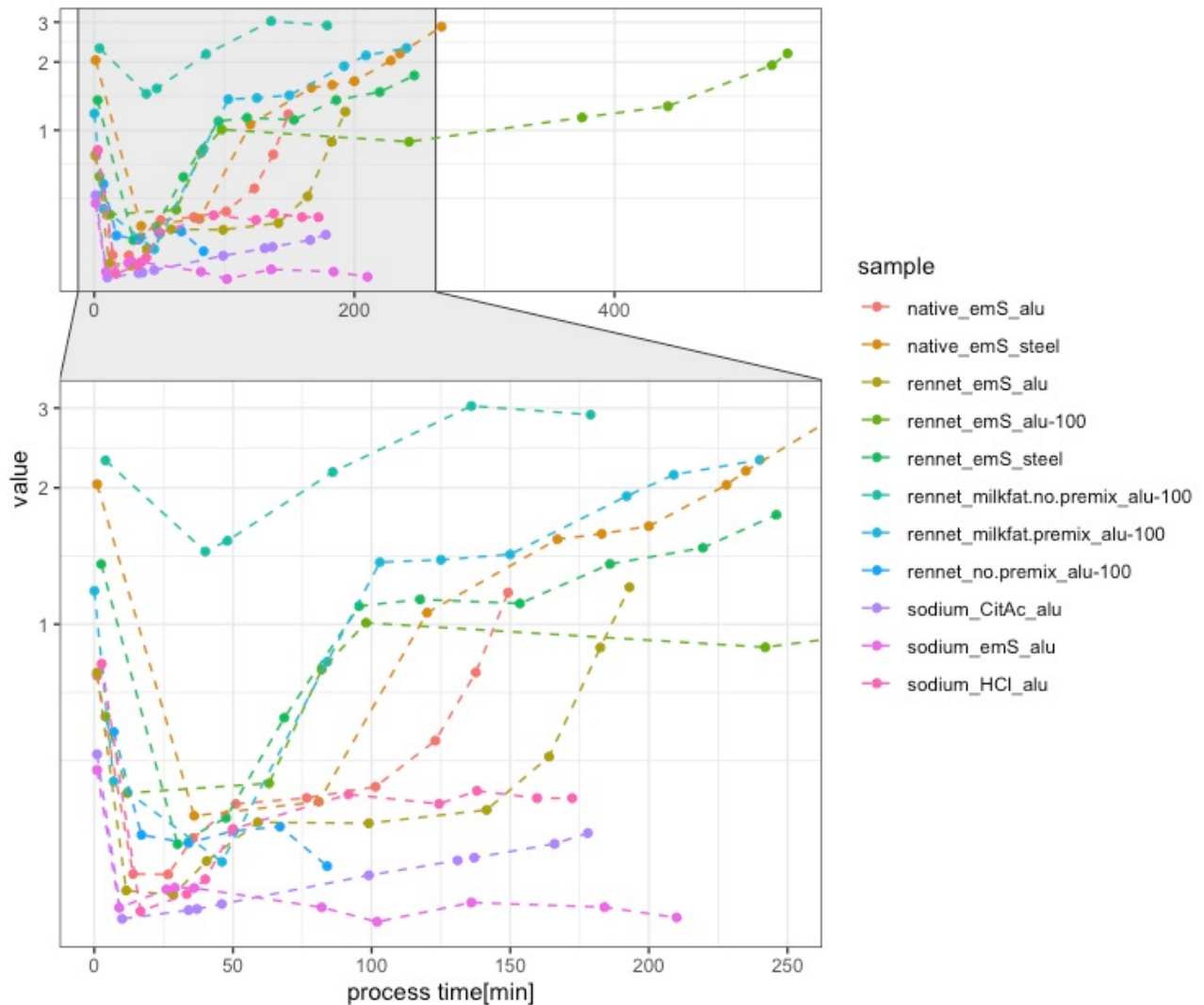


**Fig. 17.** Overview of Viscosity Development during structure-formation reaction in model processed cheeses varying either in composition (native, rennet or sodium casein[ate] with the mixture of emulsifying salts used herin [emS] or sodium caseinate with either [HCl] or citric acid [CitAc] for pH adjustment), preparation (pre-homogenisation [premix, no.premix] and pre-emulsification of fat [milkfat, oil is the default]) or processing conditions (heat-transfer i.e. free Energy [alu, steel], or shear rate i.e. mixing/aggregation rate [alu-100, alu 200/s is the default])

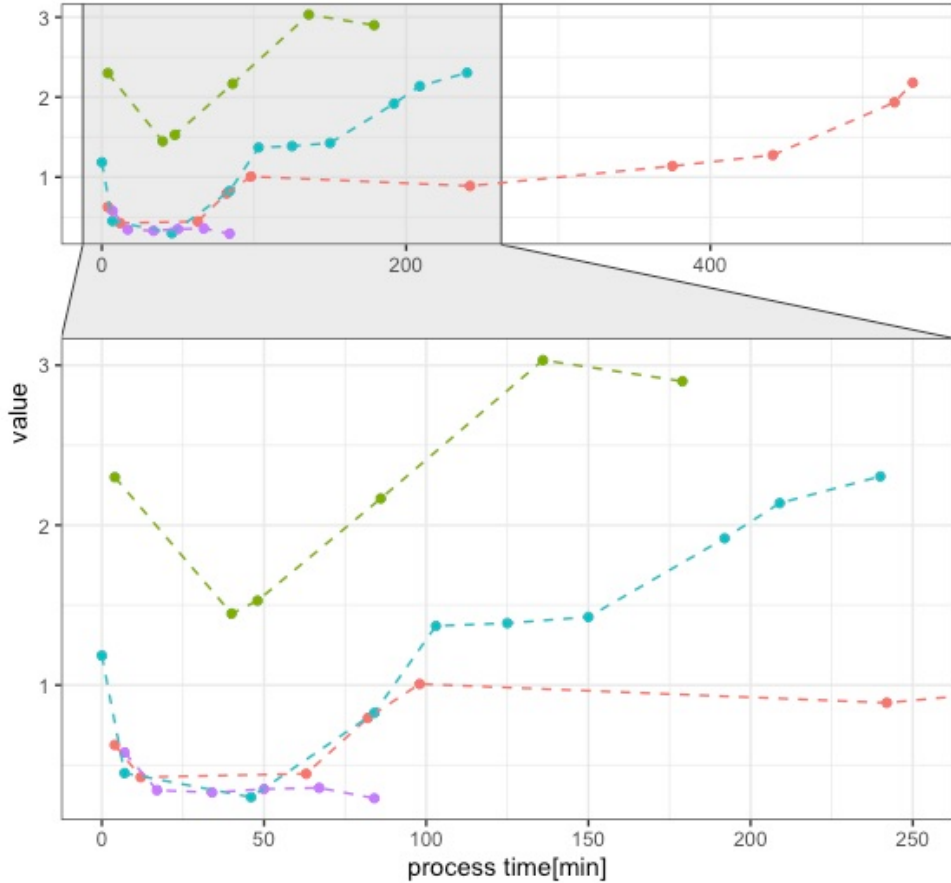


**Fig. 18.** Comparison of Rheological profile during structure formation of pre-homogenised (red, blue) or non-homogenised (violet, green) samples and of pre-emulsified (green, blue) fat (in form of milkfat) or unemulsified (red, violet) fat (in form of oil). Note that the red and violet curves are identical in their composition but vary in terms of pre-homogenisation.

Fig.18 shows the viscosity increase of the tested models that were different in their oil composition. If the fat source was dairy cream, structure formation took place even without an premixing step (green). The aim of this work was, however, to investigate *inter alia* the emulsification properties and further potential aggregation of casein coated fat globules or particles, at later stages of processing. To do so, no pre-emulsified fat other than emulsified with caseins, should be present. Milk fat is pre-emulsified fat, The milk fat globule is stabilized by milkfat globule membrane proteins. Therefore, plant oil in the form of sunflower oil was used as the dispersed phase. However, without a pre emulsifying step which is furthered referred to herein as premixing was included in the sample preparation. The effect of premixing can be found in Fig.18 as well, the violet points show a non-premixed system, the red points are the same sample, processed after premixing at  $\sim 8000$  rpm.

The overall rheological profile of samples made from native or rennet casein, differs only slightly. Native casein samples show a faster structure formation than rennet casein samples, as well as an

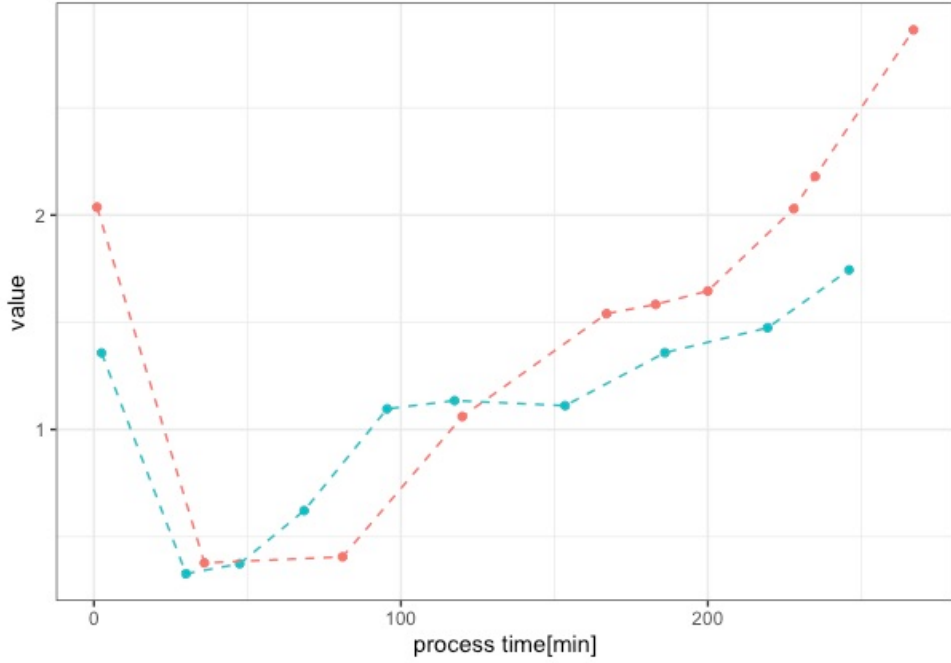


**Fig. 19.** Rheological Profile of samples made from native (red) or rennet (blue) casein, processed in a steel cup

overall higher viscosity. This can be due to the different initial particle sizes of the casein powders, since the rennet casein powder had a more granular consistency, whereas the native casein powder was powdery. Dickinson (2012) described the formation of stronger gels from inhomogenously hydrated or dispersed samples, due to faster bridging-flocculation of the fat particles.

Bridging-flocculation was promoted by vast amounts of unadsorbed and also in parts unhydrated protein or casein particles. This also lead to a preferred formation of particulate fat globules and thus, for an emulsion filled gel to the formation of a particle gel. This is represented in Fig.20 by the faster processing of the native casein model cheeses, since a particle gel has a higher rigidity than an emulsion filled gel.

When comparing Fig.19 and Fig.20 it becomes apparent, that the aluminium cup leads to faster processing, which is due to a better heat transfer of the aluminum and the higher porosity in the aluminium cup, which might provoke an autocatalytic effect. Comparing the shear rates, we see that the process speed is dependent on the shear rate, which is in conclusion with rheological behaviour for non-Newtonian fluids, as well as with the faster structure formation (i.e. higher reaction rate), due to higher probability of collision of the particles. Faster processing by higher shear rates was also reported by Fu, Watanabe, Satoh, et al. (2018).

The model testing led to the model composition of Table 1. For faster sample throughput, a processing speed of 200/s in the aluminum cup was chosen. The premixing step was made standard

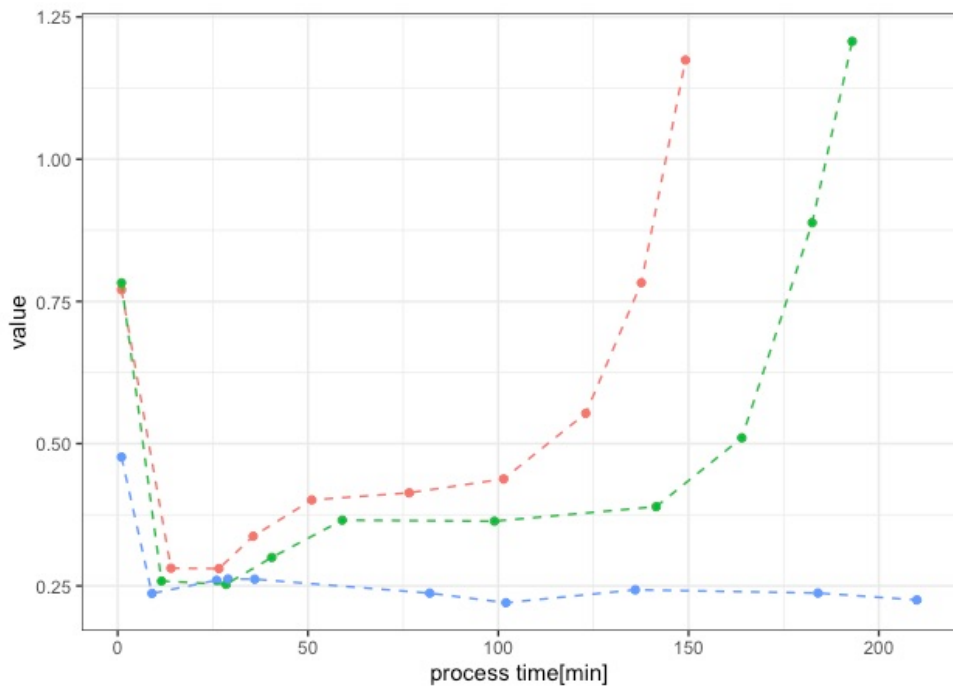


**Fig. 20.** Rheological Profile of samples made from native (red), rennet (green) or sodium (blue) caseinate, processed with the mixture of emulsifying salts used herein in an aluminium cup. The processing conditions for these samples were set to the standard conditions for further analysis.

protocol for sample preparation and was set to not exceed 10.000 rpm.

## 3.4 Results and discussion

### 3.4.1 Flow curves during processing of model processed cheeses

The composition of model process cheese (Table 2) lead to a dry mater of 40 % with protein concentrations from 15-17% TP, depending on the total protein content of the source material. Samples were pre-mixed prior to processing, since it was found that without an initial emulsification step, no stable educt (melt/sol) could be produced in the processing cup. It should be noted that Lenze et al. (2019) used pre-emulsified fat (milk fat or oil + small molecule surfactants) in the process which led to the stable educt.

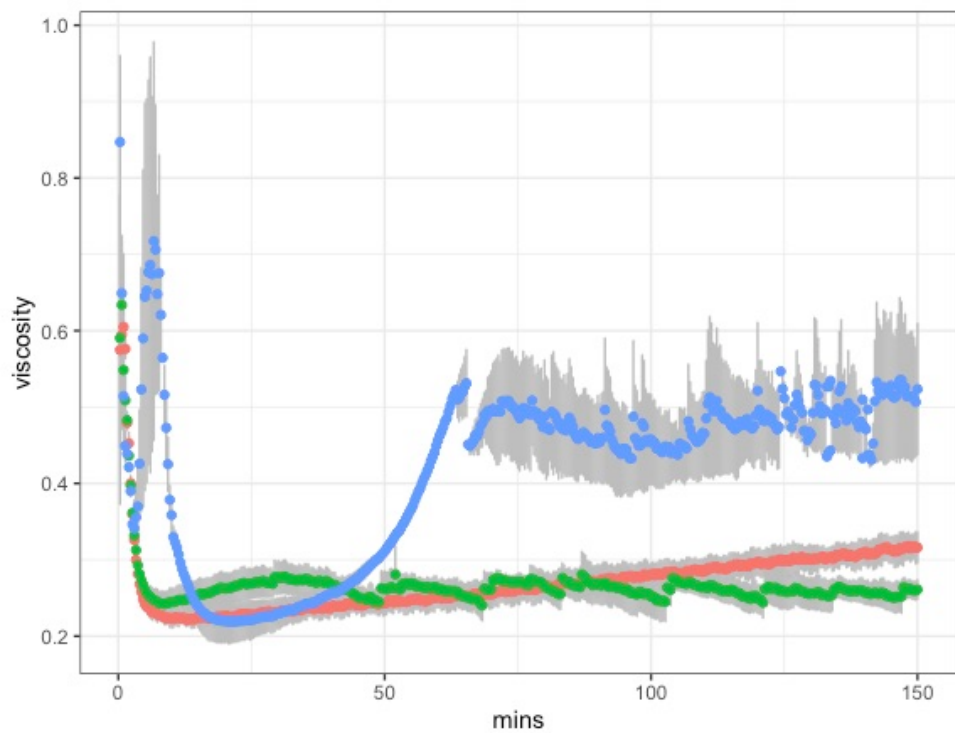


**Fig. 21.** Detailed rheological profile of model processed cheese samples made with sodium caseinate as source material. Variation was in the type of salt used for pH adjustment to a value of 5.88: HCl (blue), Citric Acid (red), emulsifying salts (green). Measurements were performed in triplicate and plotted as mean, variation in viscosity indicated as grey shade.

Fig. 21 shows the flow curves of the processed sodium samples. When processed without melting salts but HCl as pH adjustment, we can see a structure development up to a first plateau (blue). After that, no further structure development could be recorded. This compared to the other samples rather high standard deviations represent a cohesiveness of the matrix at this point, represented by a strong tendency to pull strings, when sampled after 150 minutes. Vollmer, Kieferle, Youssef, et al. (2021) reported that kappa casein fibrils in a similar model processed cheese made from native casein were

the key element for structure formation in model processed cheeses, since their supposed building could be followed as well as their structuring of the matrix. Kappa casein is the only casein that is not affected by calcium, which also means that it is not influenced by the ion exchange process that is used for the production of sodium caseinate, as described in the next paragraph. Therefore kappa casein is present in its more or less native state, at least from the point of view of ionic substitutes. Hence, the detectable increase in apparent viscosity from a level of 0.2 to ~0.5 between 40 and 60 minutes of processing could be assigned to an adsorption of kappa casein fibrils to the interphase, possibly as the only larger aggregate present in the system.

In the green curve which was processed with emulsifying salts, no structure build-up could be detected. This might be due to the little amounts of calcium being available in the sodium caseinate samples, thus a far lesser concentration of Calcium Ions can be released into the serum. Sodium caseinate is generated by acid precipitation of caseins with subsequent alkalization and final neutralization; a process that forms single caseinates, wherein the calcium ions are to some degree replaced with sodium ions, whereby the CCP are completely absent. This means that the remaining calcium ions in sodium caseinate are small in number and directly bound to phosphoserine residues. Chelation of the calcium phosphate nano clusters from the micelle up to a value of 70% is reported to lead to full dissociation of the micellar structure (Patrick F. Fox et al. (2016)). In Vollmer, Kieferle, Pusl, et al. (2021), a critical threshold value of PP of 1.2% is shown, to induce complete dissolution of CCP from the micelle. Hence it can be concluded, that the threshold value for complete micelle dissociation is reached within this study and the caseins are present in monomeric form.

It can be suggested that the initially chelated calcium ions in samples made from rennet or native casein are not immobile, or even inertly bound in their chelated complexes, but could participate in processes that lead to aggregation. This will be discussed in further detail during this work.

Native casein samples build up their structure slightly faster than samples made from rennet casein (Fig.22). Also, native casein had a higher variance in total process duration. The first stages of structure formation up to a processing time of ~100 minutes however, show no difference concerning the source material. The start of the second phase of structure formation is up to 50 minutes earlier than in samples made from native casein. This could be attributed to higher matrix inhomogeneity of the native casein samples, due to smaller particle size of the powder. When pre-mixing the samples, it was observed that the smaller particle size of the Native Casein showed powdered clusters. It has been previously reported, that a higher matrix inhomogeneity, like the appearance of such powdered clusters, leads to higher gel stabilization in emulsion filled gels due to a faster bridging stabilization of the oil droplets (Oliver, Wieck, and Scholten (2016), Dickinson (2012)). Such a bridging stabilization

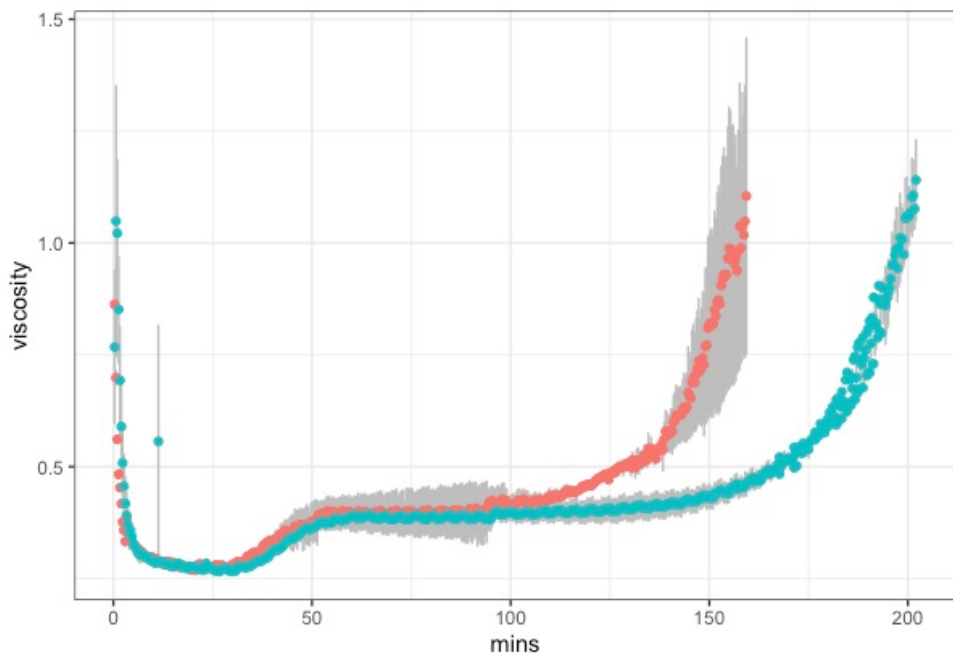


**Fig. 22.** Detailed rheological profile of model processed cheese samples made with native casein (red), or rennet casein (blue) as source material. Measurements were performed in triplicate and plotted as mean; variation in viscosity indicated as grey shade.

was shown to be induced by excess unadsorbed protein (Semenova et al. (2010)). The rennet casein premixes showed a coarser structure, since the grain size was around 0.1 mm. Thus, the matrix hydrates more slowly, as indicated in the slightly later starting time of the first exponential phase.

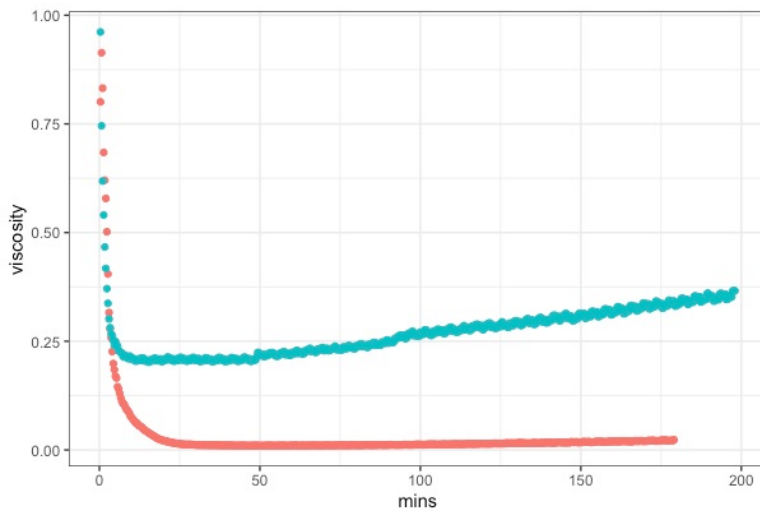


**Fig. 23.** Rheological profile of control samples w/o any addition of salts: native casein (red) and sodium caseinate (blue)

Controls (Fig.23) show that native casein without any addition of emulsifying salts at native pH (6.57) shows a slow, if any, structure formation after about 125 min of processing. This is probably

due to the slight heat induced dissociation of the casein micelle, and/or a possible re-aggregation of released caseins therefrom. Sodium caseinate shows a higher level of viscosity after melting (0.2) than the native control, which was measured at ~.03. The native control did not produce a stable emulsion or gel evenly during heat-processing; a watery opaque liquid with free fat was apparent next to clumped, i.e. amorphously aggregated structure. Samples from sodium caseinate without the addition of salts did form a stable premix and also showed structure formation.

The comparison of the controls shows, that when processed without salt addition at native pH an overall increase of 0.11 a.u. in viscosity takes place, similar to the increase measured in models with sodium caseinate and citric acid. Slight step-wise increases in viscosity can be seen at 50 min and at 100 min. Those were also the process times, where exponential increases in viscosity were detected in the model samples. It can be concluded, that the phosphate and citrate salts, maybe also in combination with their respective sodium cations are responsible for the abundance of a detectable viscosity increase in samples from sodium caseinate made with emulsifying salts.

### 3.4.2 pH values post-processing

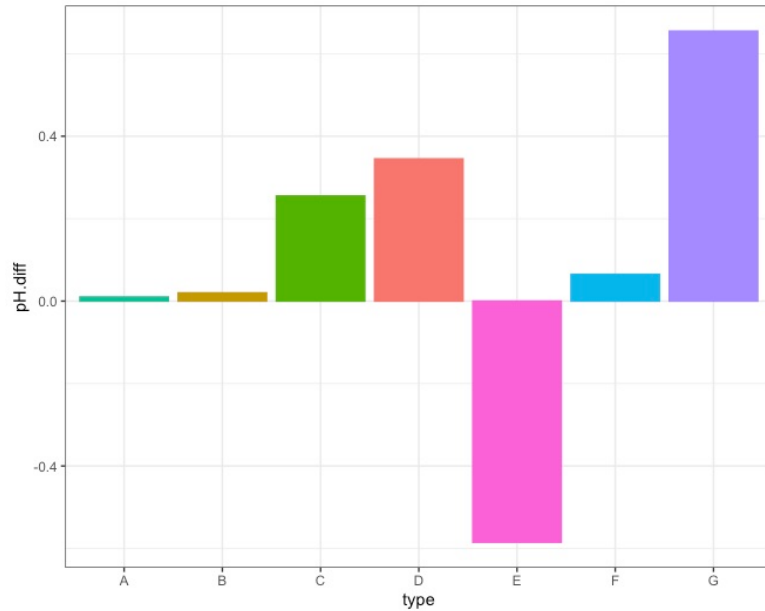


**Fig. 24.** Difference in starting pH of the sample premix and pH of the sample product after processing: (A) sodium caseinate w/o emulsifying salts, (B) native casein w/o emulsifying salts, (C) rennet casein with emulsifying salts, (D) native casein with emulsifying salts, (E) sodium caseinate with HCl, (F) sodium caseinate with citric acid, (G) sodium caseinate with emulsifying salts

The pH for all samples was set to 5.88 +/- 0.02, prior to processing and changed over the course of processing according to Fig.24. Samples from rennet casein and native casein showed an increase in

pH over the course of the reaction (up to 6.17), samples from sodium caseinate showed a slight increase in pH for samples made with citric acid but no additional calcium chelators up to 5.86 +/- 0.01. The strongest increase in pH was apparent for samples made from sodium caseinate with emulsifying salts: pH of the processed sample rose to 6.48 +/- 0.02. Only the samples made of sodium caseinate and HCl (i.e. without any Calcium chelating agents) showed a decrease in pH to 5.22 +/- 0.01. The decrease might be due to over aciding as the matrix was strongly coagulated already during premixing, so the initial pH might have been indeed at a lower level to begin with, and expressed itself only after melting. These samples also showed a structure formation up to the first exponential and second log phase of processing. Due to the low pH, it could be also possible that this is not an effect induced by kappa casein (-fibrils), but due to beta casein being close to its IEP (5.20) and therefore emulsifying the fat phase. We can see that the emulsifying salts otherwise generally increase the pH of the samples and thus change the charge in the casein molecules more negatively. The strong pH increase detected in sodium caseinate samples processed with emulsifying salts could be due to certain degrees of dephosphorylation of the calcium sensitive caseinates (alphaS1, alphaS2 and beta casein). Since the hydroxy group of the corresponding Serin residue is a far weaker acid than the respective phosphate group, the pH of a casein containing matrix will increase with ongoing de-phosphorylation of the caseines.

Buffering the pH at the desired value is crucial for the properties of the final product, a lower processing pH (5.2 - 5.6) resulted in more coarse and particulate gels, whereas a pH value of 5.8 - 6.2 gave creamy products (Barth, Tormena, and Viotto (2017)). It is apparent, that the pH value in the model samples from native and rennet casein was buffered in the desired range, whereas the samples made from sodium caseinate couldn't be buffered at the target level.

### 3.4.3 Occurrence of a third log phase and the fitting of a model flow curve

In another embodiment of the experimental set-up, rennet casein samples were processed in a steel cup, using the same temperature and speed settings. To the authors surprise, longer processing times were needed and the rheological profile appeared to be different than the samples processed in the aluminum cup. In total, the steel cup lead to ~30% longer processing times. However, in relation to the respective full process times, the time needed for the first and second exponential phases to start, displayed the same ratio. In Fig.25 the appearance of another plateau phase during the second exponential phase is visible between 12.000 and 15.000 seconds of processing. This plateau phase was also seen in the flow curves of the samples analyzed by Vollmer, Kieferle, Youssef, et al. (2021). Since the samples in Vollmer, Kieferle, Youssef, et al. (2021) were processed at half the processing speed,

the occurrence of the additional plateau phase seems to display an intermediate halt of structure formation. It is reported that the occurrence of large fibrillar structures are very electron dense, i.e. high in protein, next to areas, where a low electron density is apparent. Before the display of the plateau phase, the casein fibrils appear in bundles, during the plateau phase, these bundles get broken down, which seems a reasonable explanation for this effect. Also, it is to be expected, that this part of the second log phase only displays itself in the set-up with an aluminum cup, due to the different physical properties of steel and aluminum.

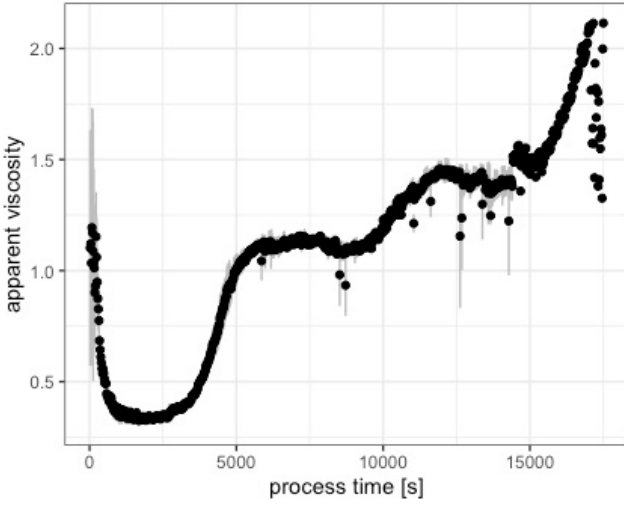


**Fig. 25.** Plotted mean values of the measured apparent viscosity of model processed cheese samples produced from rennet casein prepared in a steel cup: a third lag phase, which represents an intermediate stabilization at an apparent viscosity level during the second exponential phase of structure formation, was observed.

Firstly, aluminum has an ~5 times higher heat transfer capacity than steel. Also, the aluminium cup displayed a higher friction of the samples due to adherence of the matrix to the walls of the cup. This puts a higher amount of shear stress on the sample, induced by the sample itself. Higher shear led to faster processing in general, as it was shown during model development. It is also possible, that an autocatalytic effect took place in the aluminum cup. The addition of pre-processed sample to a new matrix was shown to induce a rapid increase in structure development (Fu, Watanabe, Satoh, et al. (2018), Černíková et al. (2018), Lenze et al. (2019)). It is thinkable, that this effect took also place here to a certain degree, but in-situ by seed formation in pores or cracks of the aluminum cup.

In various other studies, model process cheese matrices similar and comparable to this system were processed by differently shaped means. The unity of all means of processing, either kneading type shearing using a Farinograph as in the works of N. Noronha, Duggan, Ziegler, O'Riordan, et al. (2008), or processing at high speed using a rapid viscometer as in Fu, Watanabe, Satoh, et al. (2018),

a step-wise structure formation is reported. The different structure formation curves that showed a step-wise or two phased process as indicated by exponential increase in apparent viscosity were used to fit a general rheological profile for the model processed cheese, also for the use in later correlation analysis. The flow-curves of native as well as rennet casein were used for the modellation, since it was shown in Röck (2010) and also in this study, that the two protein species displayed no large differences in apparent viscosity.

In order to get the pronounced two step process but also a dynamic lag phase represented in a fitted viscosity model, not the model with the best fit was chosen, but with a good empirical estimation under consideration of the  $R^2$  of the fit. By including the variance of a later or earlier occurring second exponential phase, i.e. the effect of matrix inhomogeneity, either due to different fat globule size or powder particle size, which occurred during the pre-mixing step, could be included in the model. The plotted mean curves with their respective variance can be found in the supplementary material. To also include the intermediate stabilization described earlier, the curves from the steel cup were also included in the fit. The flow curve was fitted using a generalized additive model. Such “gam” models with integrated smoothness estimation are implemented within the R programming language, which was used to prepare this thesis. The ‘gam’ function for basic model fitting takes into account any quadratically penalized general linear model. This means that the regression of every data point or linear sets therefrom are considered within the model. To prevent from over-fitting, the degree of smoothness of model terms is estimated as part of fitting. In more detail, a generalized additive model of the form

$$g(\mu_i) = f2(ix4, ix5) + b0 + ib1x1 + ib2x2 + f(ix3)$$

wherein the response variable, in our example the viscosity, is represented as an expectation  $\mu_i$  within a link function  $g(x)$ . The general additive model (“gam”) of this formula would then be

$$y = x1 + x2 + s(x3) + s(x4, x5)$$

Per definition of “gam” within R, a maximum smoothing term is applied and the fitted

$$y(x) = g(s(x))$$

resulted in an  $R^2 = 0.71$ . As it is the case for many built-in numeric operations in R, the algorithm

for the general additive model has an implemented, nested two-side ANOVA test. The fitted values are displayed in Fig.26.

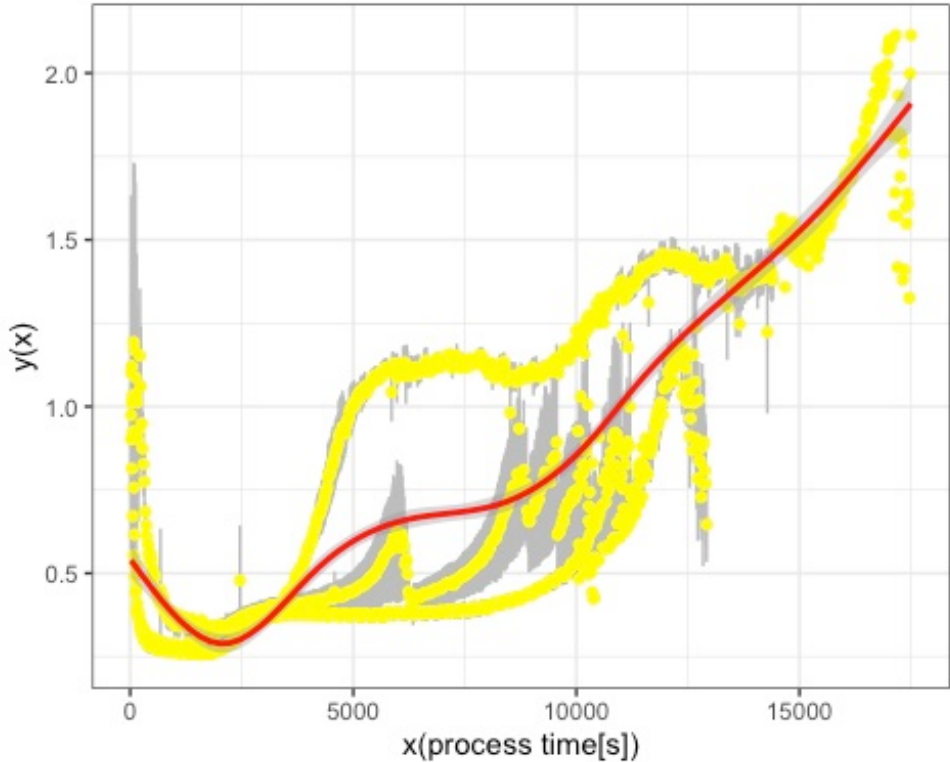


**Fig. 26.** Fitted residuals from the function from the general additive model, applied with internal cubic spline smoothing term; yellow is the data, grey is the standard deviation from the data and the red line represents the fitted values.

### 3.5 Summary and outlook

In this section, a multi-step structure formation for samples made from rennet and native casein could be reported. A “one-step” structure formation was found in samples made from sodium caseinate processed with HCl (to adjust the educt pH to the target value of 5.88) but no further use of buffering salts or agents. This type of structure formation was attributed to soluble beta casein adsorbing to the o/w interphase and thereby decreasing the overall elasticity of the system. The samples made from rennet casein and native casein, displayed similar behaviour, variances were attributed to varying matrix inhomogeneity. The targeted step-wise structure formation as it was displayed in Lenze et al. (2019) could be reproduced with an improved model processed casein system. Furthermore the indifference of native or rennet casein to be used to form the targeted structure could be confirmed.

Interesting here as well was the behaviour of sodium caseinate in relation to the degree of calcium

deprivation. The rest of calcium ions in sodium caseinate is directly bound to phosphoserine residues. When processed without melting salts, we could see a structure development up to the first plateau. After that, no further structure development could be recorded. Combining the models suggests that the initially chelated calcium ions in samples made from native or rennet casein are not immobile or inert in the system within their chelated complex, but can - and will after time- initiate a second structure formation phase, i.e. a second growth phase. Samples made from sodium caseinate, that were still calcium deprived but had no pH buffering (i.e. the sodium caseinate model with HCl) showed an increase in viscosity. Thus the mobility of the caseins to form self-assemblies like in the HCl model as well as the inhibition of structure formation through the lack of Calcium ions could be shown in this section.

For samples made from sodium caseinate, there seems to be no inner force or linking agent to form a secondary structure as seen in samples made from initially micellar (native or rennet) caseins. This is surprising since the levels of PP to induce complete dissociation of the micelle by chelation of CCP were above the reported threshold in similar models (Vollmer, Kieferle, Pusl, et al. (2021)). Therefore, sodium and native models should present caseins in monomeric structure after melting. The caseins even have supposedly the same ionic substitute, since sodium salts were used. It can be suggested that the presence of large amounts of previously colloidal calcium is forcing the proteins to either deplete from the solved calcium ion or readily bind to it.

One aim of this study was to find. models with high similarity in composition (ionic environment and strength) but with very different struture formation properties. Native and Rennet Casein samples showed no significant difference in the overall shape of the structure formation, only the start of second exponential phase showed variance. This effect can be attributed to a differing matrix homogeneity due to differing powder-particle-sizes.

Since calcium is long known to be the factor stabilizing caseinate based emulsions (Dickinson and Golding (1998)), the null model for the creaming process, i.e. the model system that had similar composition but showed no structure formation could be identified. This model was the sodium caseinate system, processed with emulsifying salts. As expected, calcium deprived emulsion gels didn't show structure formation. Therefore the two models that were investigated in their respective composition (see section 4) were chosen to be native casein and sodium caseinate, prepared with oil in a premixing step and processed with emulsifying salts.

The findings herein are in conclusion with findings of other works concerning the creaming reaction, but especially in the context of this work and the connected studies performed by Lenze et al.

(2019), Vollmer, Kieferle, Youssef, et al. (2021) and Vollmer, Kieferle, Pusl, et al. (2021). The modellation of a characteristic flow curve was performed and will be used later within correlation analysis of the experimental data. The modelled flow curve resembled the shape of the flow curve presented in Vollmer, Kieferle, Youssef, et al. (2021).

## 4 Quantitative matrix distribution of Caseinates during thermal processing of model process cheese

### 4.1 Introduction

The stability of many emulsified food, cosmetic or pharmaceutical matrices is defined by the ability to bind a dispersed phase. Many of these matrices are processed under heat and shear. The clarification of the underlying structuring and also emulsification mechanisms would help gain a deeper understanding of structure formation, protein adsorption and protein (re-) distribution during processing. One proteinogenic agent that is known to stabilize emulsions and form gels, also simultaneously, is casein. Casein is highly insensitive to heat degradation, especially when processed below 100°C (Dumpler (2018)). An interesting feature about caseins is their ability to aggregate, i.e. form structures without the help of covalent bonds. Thus, caseinogenic food structures like (processed) cheese are stabilized mostly via physicochemical interactions (Dickinson (2006)). Most gels produced from casein only are expected to be formed via covalent (Disulphide bonds) or electrostatic (crystallisation or dipol-dipol) links. It is known that systems with casein as the structuring agent, such as processed or cream cheese, are not covalently linked (Lenze et al. (2019)). Dickinson (2012) showed mechanisms for non-covalent and non-hydrophilic interactions for structure formation, namely bridging flocculation and depletion flocculation.

There is strong evidence that caseins serve as a model for many other amphoteric unstructured proteins, which undergo structuring under the formation of hydrophobic aggregates. When a dispersed phase is present, proteins adsorb to the fat surface; until now it is unclear how strong these interactions are and how the adsorption towards the interface works. Therefore, a method to investigate, if there is tightly bound protein at the interface which cannot be desorbed using hydrophilic interactions (i.e. washing), was developed. The buffer solution, described by Bonizzi, Buffoni, and Feligini (2009), was used in larger quantities as previously described, to desorb the caseins in the isolated and washed cream phase from the fat in order to put them back into solution and therefore, making them an analyte for RP-HPLC.

Two model systems were investigated, odium caseinate and native Casein, both processed at the same target pH of the educt of 5.88, as adjusted by citric acid and the emulsifying salt mixture as first described in Lenze et al. (2019) and in the parallel works of Vollmer, Kieferle, Youssef, et al. (2021). The systems were chosen according to the findings of section 3 in this work. The aim was to investigate models, which are very similar in composition but show different aggregation behaviour

during structure formation. Both were processed under the same ionic environment. The hypothesis to be tested in this section was if hydrophobic aggregates are formed during processing (aka the creaming reaction) which are inert towards re-solubilization in water. Also, it was to be observed, if the step-wise structure formation in samples made from native casein, or the respective abundance of such a structure formation as seen in samples made from sodium casein in this work, is in any way linked to the obtained compositional data.

## 4.2 Material and Methods

In order to find a linkage between apparent viscosity and intrinsic composition of the matrix, the distribution of caseinates or caseins during structure formation was investigated. Since the model matrix is a dense sol in hot and a soft solid in cold state, the matrix was diluted after cooling and centrifugationally separated. The procedure as well as the sampling of the process times is described below.

### **Preparation of model processed cheese to distinct processing steps as batch**

Cheese samples were premixed and processed as it was presented in section 3.2 of this work. The distinct processing steps that were defined to be further analyzed were chosen roughly at the processing times displayed in Fig.27. To follow the structure formation on a compositional level, the high reproducibility of the flow-curves was used to produce the model cheeses up to the desired processing steps as a batch, which means that for every full follow-up of the structure formation, a total of nine (or five in systems made from sodium caseinate) premixes were produced and processed to the desired time. A triplicate of three full runs was analyzed in its composition, i.e. for native casein, 27 premixes were produced and processed, for sodium caseinate 15, respectively, since no structure formation was detected and thus no strong shifts in particle concentration at later processing stages, thus, a longer sampling range was chosen.

Since the flow curves had variance in the process time that was needed to induce the detected second exponential phase, the samples that should serve as token of the second exponential phase were not processed to the exact same processing times. Instead, the appearance of the second structure formation was monitored, if a first increase in viscosity from the plateau phase was clearly visible processing was stopped to obtain the step G. Steps H, J and K were sampled accordingly. It is also important to note that the end of the process was defined by the matrix not being able to be sheared evenly in the processing set-up anymore, as indicated by the blue dots at the end of the process in Fig.27.

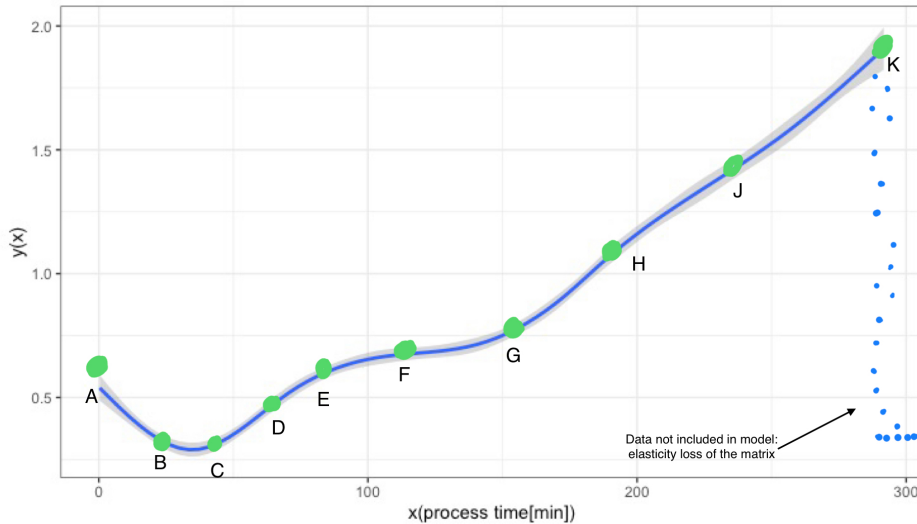


**Fig. 27.** sampling events for further compositional analysis as identified in the flow curves, shown on the modeled flow curve from the previous section: A: premix, B: melting complete, C: beginn 1st log phase, D: intermediate 1st log phase, E: end of 1st log phase, F: plateau phase, G: beginning of 2nd log phase, H: 1st intermediate 2nd log phase, J: 2nd intermediate 2nd log phase, K: end 2nd log phase.

#### Preparation of the upscaled process for the continuous measurement

For upscaling, the the matrix was enlarged ten-fold, with the same respective concentrations of components. In the matrix processed with only 5% fat, the dry matter was replaced using inulin (w/w) as inert dry matter.

#### Sample preparation for phase separation

6 g of the processed processed cheese sample was weighed into 50 ml purifier tubes and diluted 1:3 (w/v) with deionised water. To produce a homogeneous dispersion, a dispersion device was used and the dispersion was prepared at a speed of about 6,000-8,000 rpm. For phase separation, the samples were centrifuged at 6000 g and 10 °C for 30 min on the Multifuge (Heraeus Group, Hanau, Germany). This produces a three-phase system consisting of a fat phase (cream), water phase and pellet. The fat phase was lifted off with the help of a stainless steel spoon and transferred into a prepared 50 ml purifier tube. The water phase was poured into another tube. For better separation of the cream phase the liquid phases were centrifuged a second time. The fat disc was lifted out of the tube and put into a prepared 50 ml purification tube, taking care to lift off as little aqueous phase as possible.

#### Analysis of individual casein fractions by RP-HPLC

The qualitative and quantitative determination of the individual casein fractions alphaS1-, alphaS2-, beta- and kappa-casein was performed by RP-HPLC (reversed-phase - high-performance liquid chromatography) according to a method developed by Bonfatti et al. (2008) and Bonizzi, Buffoni, and Feligini (2009) and further modified and adapted by Dumpler et al. (2017).

## Preparation of the guanidine buffer

The guanidine buffer for use in the HPLC analysis was prepared as follows: first, a 0.1 M Bis-Tris buffer was prepared. The buffer was subsequently used together with weighed guanidine HCl, trisodium citrate and DTT to prepare the final buffer solution. After preparation, the buffer was filled into 50 ml Greiner tubes and frozen at -40 °C until use.

## Processing of the processed cheese samples

The samples were diluted and centrifuged as described. Thus, the starting product was available in three phases, each of which was processed differently for HPLC analysis. An overview of the separation and washing procedure as described further down below is given in Fig.28.

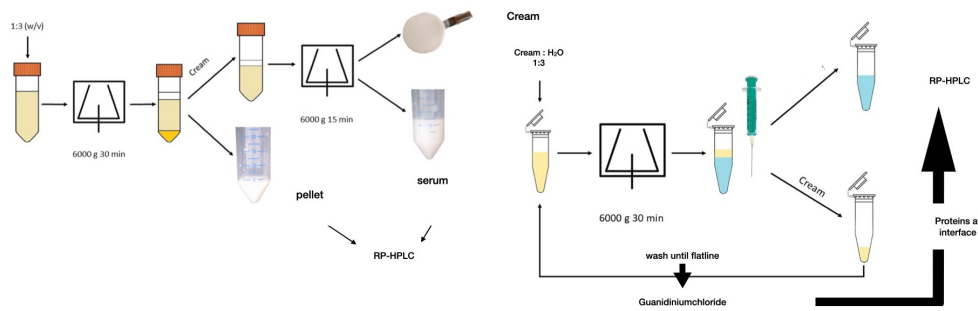


**Fig. 28.** Flowchart of the centrifugational separation method of the three phases further analyzed in this work: Cream, Serum and Pellet Phase. Centrifugation speeds before RP-HPLC analysis varied in later sections of this work, not the overall procedure as displayed here.

## Pellet

The pellet was diluted with 5 ml deionised water to obtain a suitable protein concentration for determination on the HPLC system. The sample was homogenised with a vortex device and 0.2 ml were mixed with 0.8 ml guanidine buffer. After an incubation time of at least 30 minutes, the sample was filtered through a disposable filter (pore size 0.45 um) into the HPLC vials and stored in the refrigerator or freezer (-40 C) until measurement.

## Water phase

To obtain a suitable concentration, the water phase was first diluted 1:1 (v/v) with deionised water. Afterwards, 200 microl of sample was mixed with 800 microl of guanidine buffer, filtered into a vial and stored in a cold place.

## Cream and wash-phases

The cream samples were first washed with deionised water to remove protein from the aqueous phase still in the sample. For this purpose, 0.5 g of the fat phase was weighed into a 2 ml micro tube, mixed with 1 ml deionised water and homogenised on the vortex device. This was followed by

creaming of the fat phase using an Eppendorf centrifuge at 6000 g for 30 min. The base was drawn up into a syringe using a cannula and filled into a prepared micro tube. The wash-out procedure was repeated 4-5 times. The 4-5 wash-phases were mixed 1:5 with the buffer solution, filtered into a vial and stored in the freezer until HPLC measurement. The number of washing steps was determined by the found HPLC concentration in the preceding washing steps. When the protein concentration in the analyzed washing phases dropped below the detection level of the DAD of the HPLC, it was concluded that no further protein can be desorbed from the fat particle using water as a solvent. In Fig.xx, this is indicated by the term "flatline." The washed out cream was then mixed with 500 ul guanidine buffer and homogenized. The buffer causes a strong dissociation and dissolution of the proteins from the fat interface into the aqueous phase. After an incubation time of at least 30 min, the sample was centrifuged again. The now fat-free protein dissolved in the buffer solution was obtained using a syringe and analyzed in the HPLC measurement after filtration through a disposable filter.

### 4.3 Results and Discussion

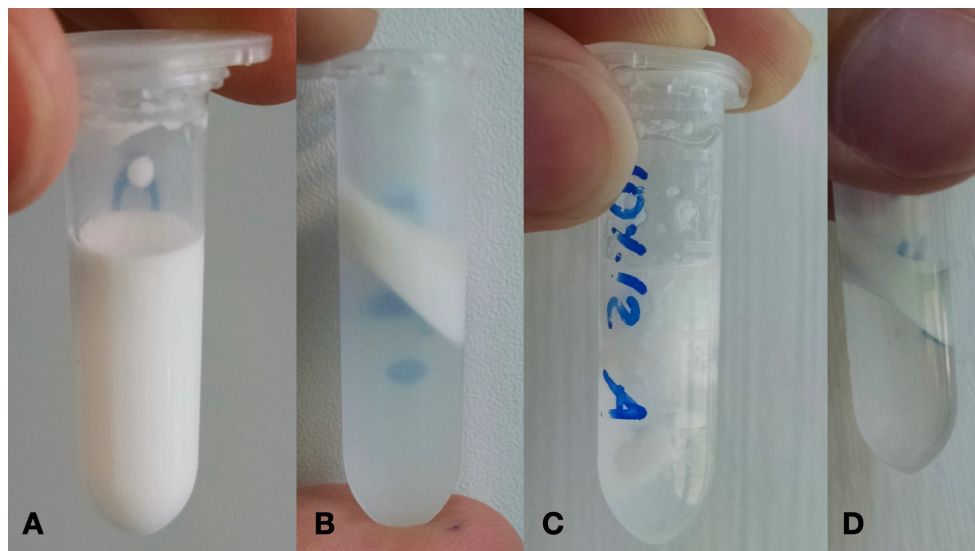
#### 4.3.1 Development of protein concentration of single caseins in model processed cheeses from batch preparation

In this section, the development of the measured protein concentrations and therefore, their distribution within the three centrifugationally separated phases is discussed. After treatment with the guanidinium buffer, the samples showed two clearly separated phases and a pronounced interphase, as can be seen in Fig.29.

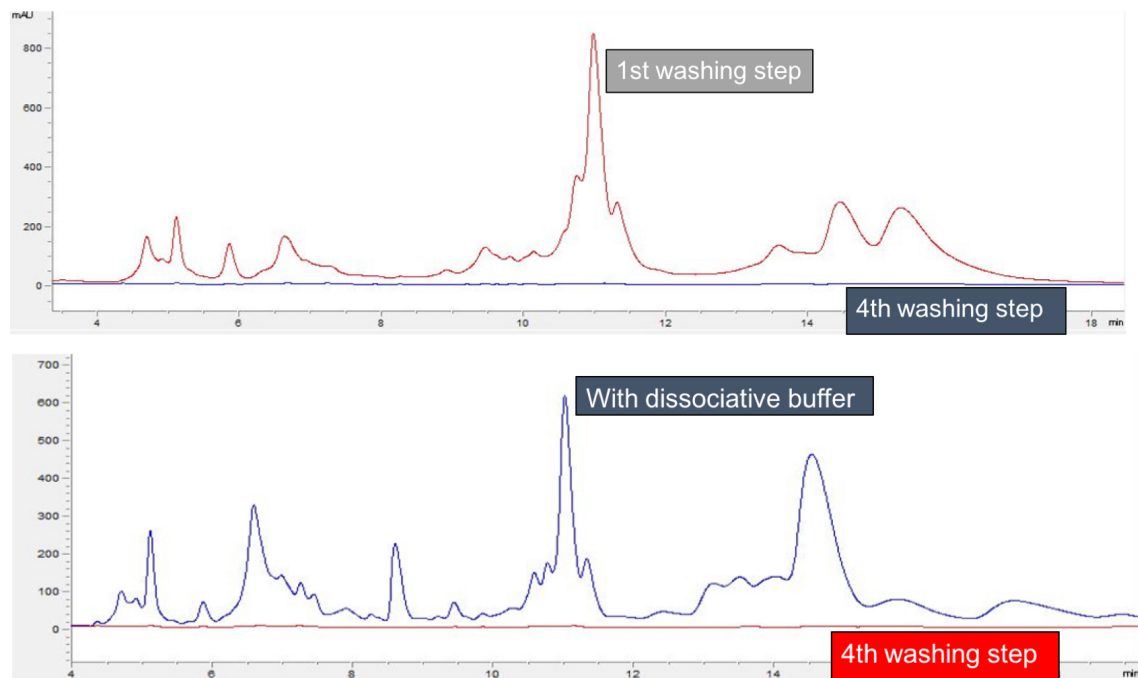
The washing experiment proved to show no measurable protein concentration in the liquid phase after four, in some cases five washing steps. The subsequent treatment of the flocculated cream with the guanidinium buffer resulted in the chromatograms as displayed in Fig.30.

Fig.31 shows the measured concentration of single caseins desorbed from the interphase with the guanidinium buffer, which represents the liquid phase (D) in Fig.29. It is apparent that over the course of processing, especially the concentration of alphaS1 and beta-casein increases in the isolated fat phase. At the investigated times, the proteins in the cream phase were found as follows:

- A: the premix, i.e. the non heated educt that is about to be processed. Especially beta casein can be found in an increased amount of 1.75 mg/ml.



**Fig. 29.** appearance of cream samples over the course of the washing procedure: diluted cream prior (A) to and after (B) 1st centrifugation (i.e. washing step), (C) flocculated state after 4th centrifugation and prior to treatment with buffer solution, (D) after treatment with buffer solution, free fat apparent at the surface



**Fig. 30.** RP-HPLC chromatograms obtained during the washing procedure: effectiveness of cream washing next to effectiveness of the chaotropic salt

- B - C: initiation of the educts, by full dissociation of the micelles and also full hydration of the monomers, represented by the display of a minimum viscosity. Desorption of beta casein from A to B, no increase in protein concentration in cream measureable at this point.

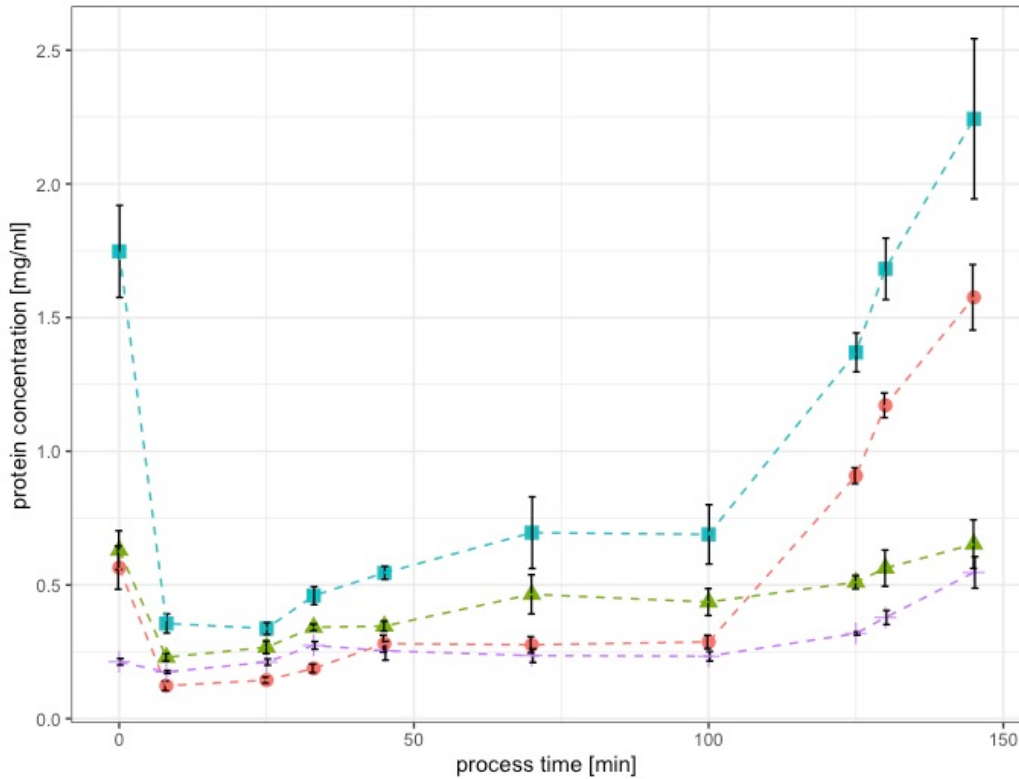


**Fig. 31.** Measured casein concentrations in the cream phase after centrifugational separation and multiple washing steps: beta casein (blue) and alphaS1 casein (red) strongly adsorb to the interphase during the first (25-50 min) and second log phase (100-150 min) of the structure formation (see rheological profiles in chapter 3). kappa casein (violet) and alphaS2 casein adsorb during the second log phase to the interphase, however in smaller amounts

- D: increase of all measured protein concentrations at the interphase.
- E: no increase of kappa casein and alphaS2 at the interphase, increase of beta casein and alphaS1 at the interphase.
- F-G: no significant increase in protein concentration detectable at the interphase.
- H-K: strong increase in protein concentration found at the interphase, especially of kappa casein (from 0.25 to 0.6 mg/ml), alphaS1 (from 0.25 to 1.6 mg/ml), and beta casein (from 0.7 to 2.25 mg/ml). AlphaS2 casein increased as well, however to lesser amounts (0.4 mg/ml to 0.6 mg/ml).

The development of the measured protein concentrations over time suggests the formation of a hydrophobic network that adsorbs to the interphase in order to (further) emulsify it, rather than the formation of the network at the interphase per se. Also, no desorption from the interphase, as suggested in Lenze et al. (2019) could be detected. It can be suggested, that the appearance of free oil in overcreamed samples comes from the particulate structure of the network. It can be

hypothesized, that the network up to points F or G, is an emulsion filled gel (as in Fig.6), whereas the gels at H-K are particulate gels (Dickinson (2012)). This also suggests the formation of an in-situ hydrophobic aggregate (since it is able to emulsify the fat) that requires a conformation or hydration change in the proteins to happen. This will be explored in detail in section 6 of this work, where a colloid model of the processed cheese system is investigated.

The adsorption towards the interphase however, appears to be a two step process. Since we see two log phases during structure formation as in Chapter 3, comparing the time stamps, it becomes apparent that especially the second phase of structure formation is determined by the binding of proteins to the fat globule, or now fat particle. The high concentration of beta casein in the premix (0 minutes) shows the emulsion state of the initial matrix. By the premixing procedure, hydrophobically bound micellar beta casein dissociated from the micelle in order to emulsify the fat during the premixing process.

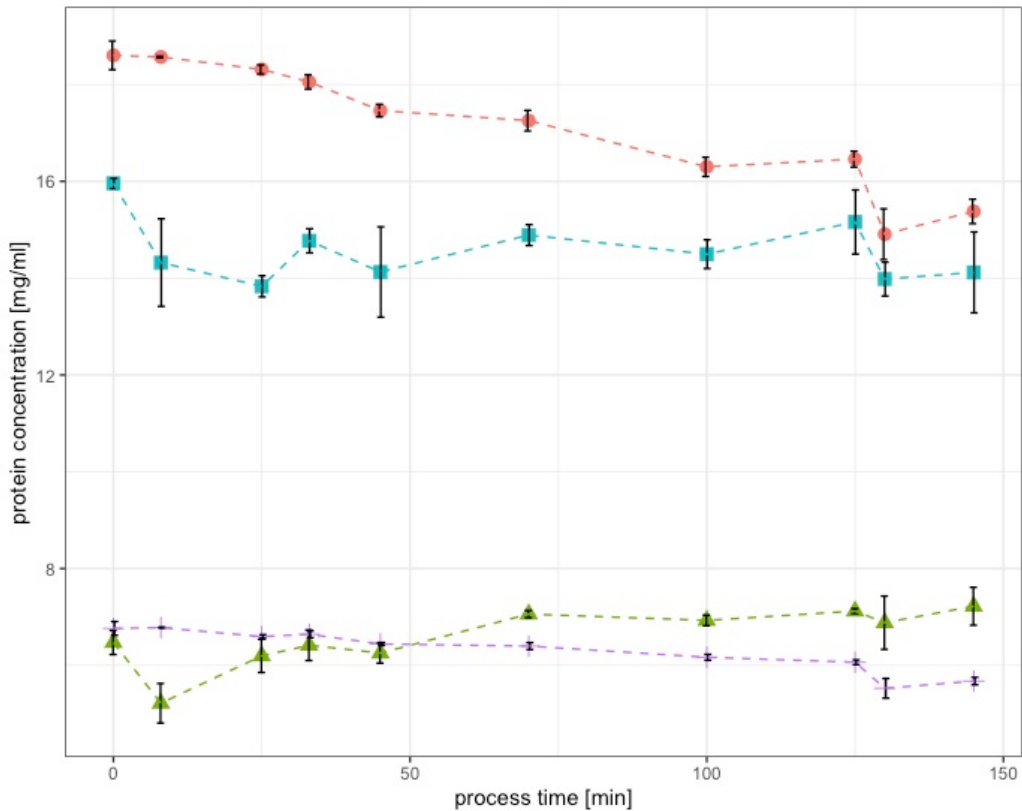


**Fig. 32.** Measured casein concentrations in the soluble or serum phase after centrifugational separation: overall decrease of especially alphaS1 casein (red) and beta casein (blue) during processing; alphaS2 casein (green) showed a slight increase, whereas kappa casein (violet) did not change significantly in its concentration in the serum or soluble phase.

Fig.32 indicates a decrease in more hydrophobic caseins (alphaS1 and beta caseins) in the soluble phase of the model cheese made from native casein. As it will be discussed later in further detail, the

two decreasing casein fractions visible here tend to form aggregates. Since the environment of processed cheese is a ionically charged environment, one can assume that the diluted cheese matrix as represented is ionically charged as well. alphaS2 casein is the only casein fraction to increase in the so obtained serum phase. Since those caseins are the least hydrophobic in terms of hydrophobic amino acid clustering (Lucey and Horne (2018)), it is easy to understand why the alphaS2 caseins gain in concentration in the serum phase over processing. This is especially true, considering the formation of a hydrophobic network, as theorized earlier. The measurement of the protein concentration of single caseinates in the insoluble or pellet phase (Fig.33) should theoretically display the formation of such a network.

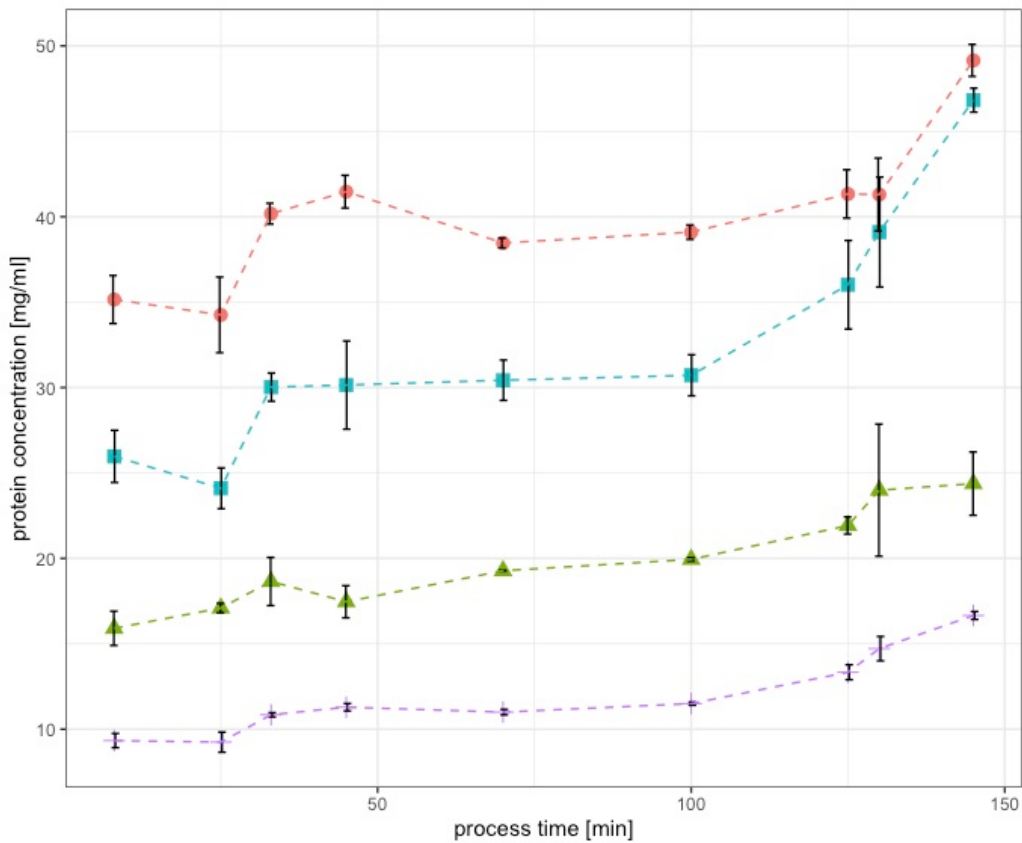


**Fig. 33.** Measured casein concentrations in the insolubly aggregated or pellet phase after centrifugational separation: concentration of all caseins increase in the pellet during structure formation; analogous to the development of protein concentrations in the cream phase; mainly beta casein (blue) and especially alphaS1 casein (red) aggregate in the pellet during the log phases of structure formation. kappa casein (violet) and alphaS2 casein (green) increase in the pellet concentration especially during the second log phase of the structure formation.

The pellet represents (aggregated) protein which is insoluble in the water phase. During the first exponential phase of structure formation (25min - 50 min) and especially during the second phase of structure formation (100min - 150 min), we see an increase of protein in the pellet. Since the same

effect and especially the same proteins show this behaviour as well in the cream phase, it can be suggested that hydrophobic aggregation is also apparent in the pellet phase. Thus, the aggregates we see in the pellet after the first exponential phase might be protein aggregates which are in contact with the cream in the non-diluted matrix. Thus, the washing and the therefore needed dilution separates the model processed cheese from native casein into three fractions. The development of the protein concentration in the pellet showed a step wise increase, as did the development of the protein concentration in the cream phase. Thus, it can be hypothesized, that those two phases are in contact with each other in the non-diluted matrix.

A chemical description can be made for the three phases obtained by centrifugational separation, centrifugational cream washing and respective compositional analysis - cream, pellet and serum - when contrasting the structure formation reaction as a strictly chemical process. The observations on the system made so far here and elsewhere suggest a two step aggregation process. In between these two aggregation processes are two (differently long) lag phases, the first one was already defined by Lenze et al. (2019) and others as the hydration of the casein and simultaneous melting, induced by the melting salts. Since it was shown by Vollmer, Kieferle, Youssef, et al. (2021) that kappa casein fibrils are aligning during the second lag or stationary phase, it can be assumed, that an inner restructuring takes place at this stage of processing. The protein concentrations measured in the respective phases during this stage of processing, did not change significantly, which proposes that this phase is dominated mainly by the reformation of the system into two separated structures later on, i.e. no aggregation that lead to an exponential increase in viscosity took place. This is the holding step or the intermediate step in a two step reaction. Considering this, the investigated phases can be described as follows: (a) protein bound to the surface area/fat particle defines the first fraction; (b1) soluble Protein (i.e. still “reactive” protein that shifts the equilibrium of the reaction to the respective product side, because there is a constant supply of educt, i.e. reaction partners from the soluble phase, and (c) insoluble or insolubly aggregated protein (i.e. protein that has aggregated during processing. The third, i.e. pellet phase is possibly connected by hydrophobic network formation with embedding of the fat particles, that may be surrounded by a hard shell of proteins at later stages of processing. Thus it can be theorized that we see the development from a soft-shell fat particle towards a hard-sphere fat particle.

Fig.34 shows the development of the concentration of proteins in the intermediate spaces between the fat globules or particles over the course of processing of model processed cheese. Washing steps 1 to 4 or 5 in some cases, showed the same general trend. Up to process point D, which represents the middle of the first exponential phase, an increase in the total protein concentration of the wash

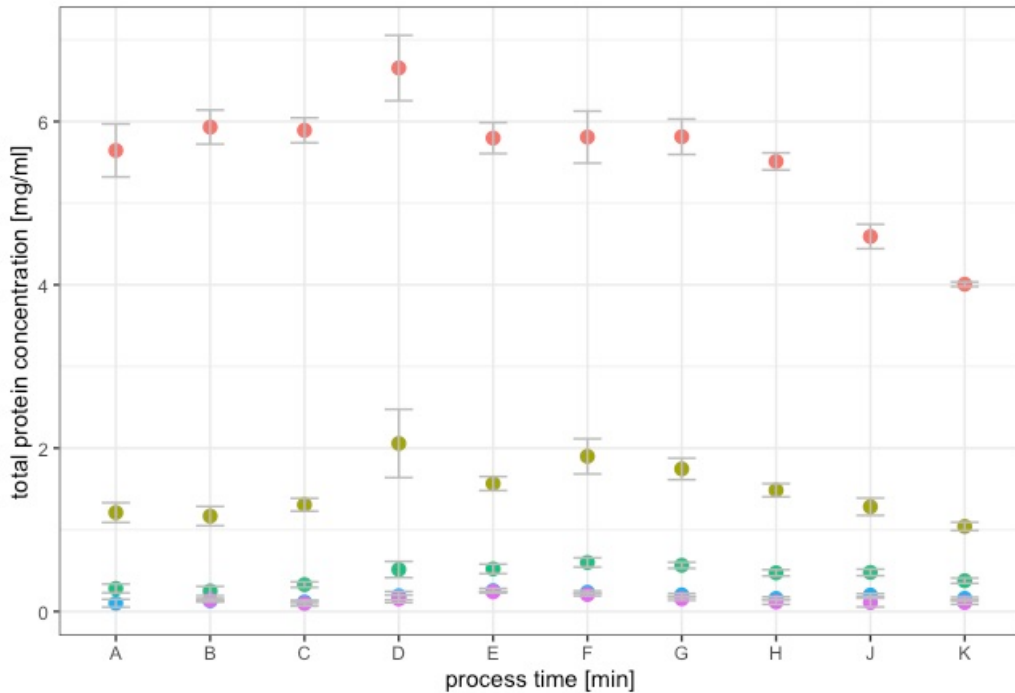


**Fig. 34.** Measured total protein concentration in the wash phases after centrifugational purification of the cream phase: top to bottom is equivalent to washing steps 1 to 5 or 1 to 4 respectively. The measured total protein concentration is the sum of the measured caseins in the wash phase.

phases can be detected. During the second lag phase, represented by process times E to G, the protein detectable from the wash phases stays the same. In the second log phase, represented by process times H to K, a strong decrease of the measured protein concentration in the wash phases is apparent. The protein with the largest amount in the wash phases 1 and 2 was alphaS2 casein.

This leads to the conclusion, that during the first log phase, the proteins actively adsorb to the interface. After that, there is no active adsorption to the interphase, this effect might be due to the growth limiting factor represented by the shear stress applied on the system. There is no change in protein concentration in the cream as well as in the wash phases detectable during the second lag or plateau phase. In the second log phase of the structure development of the model process cheeses made from native casein, there seems to be no active adsorption of protein into the cream phase, hence the decrease in total protein in the wash phases. However, the protein concentration in the washed-out cream phase, i.e. the protein directly bound to the interphase increases.

In order to explain these two somewhat contradicting effects, one has to consider that the now separated phases occur next to each other in the non diluted cheese matrix. We see an increase of protein concentration in the insoluble or pellet phase of the system during the second log phase. Since the insoluble structures in the pellet represent the gelled continuous phase of the model cheese,

the insolubly aggregated structures are also in contact with the proteins that are adsorbed to the fat particle. Hence it can be assumed, that the proteins building up the “shell” of the fat particle in the second log phase, are not fed from reactive or soluble proteins in the serum phase as in the first log phase, but from the already aggregated structures that later (after centrifugational separation) form the pellet. This means also, that during the second phase of structure formation, less unassociated or unbound protein is in between the fat globules, but that the fat globules are interconnected via a fine stranded protein network, which cannot be desorbed from the interface. This leads to the conclusion, that over the course of the structure formation reaction in model process cheese, hydrophobic interactions become the dominating force for aggregation.

#### **4.3.2 Development of protein distribution in model cheeses made from sodium caseinate**

In a comparative study, the protein concentrations in the centrifugationally separated phases of processed cheese samples made from sodium caseinate as a source material were investigated. Section 3 revealed, that model processed cheese systems obtained from sodium caseinate processed with emulsifying salts showed no structure formation, when processed as emulsifying salts. Therefore the hypothesis, that the structure formation can be investigated using the method described here, could be tested. If there are compositional indications for structure formation in the native casein samples, such indications for no structure formation should be present in the samples made from sodium caseinate.

Fig.35 shows the measured protein concentration for the cream samples made from sodium caseinate. Besides the kappa casein up to a process time of 45 minutes, all caseins in the cream phase decrease. kappa casein seems to initially adsorb to the interphase, but later desorbs again over processing, together with the sodium caseinate molecules initially adsorbed to the interphase by the premixing process. The kappa casein however increases at the interphase up to a process time of 35 min. This could again be attributed to the formation of kappa casein fibrils, that can further stabilize the interphase, to a certain extent at least than the other caseins within the system. As it was already discussed, the caseins are the most unsensitive towards calcium ions and therefore also for changes of the calcium environment. The formation of kappa casein fibrils could thus be the initiating step for aggregation, however, in order to form higher structures, other proteins might aggregate at or with the kappa casein fibrils into the large structures seen in Vollmer, Kieferle, Youssef, et al. (2021). To do so, it is thinkable that calcium ions are needed, either to drive the proteins into the possibly

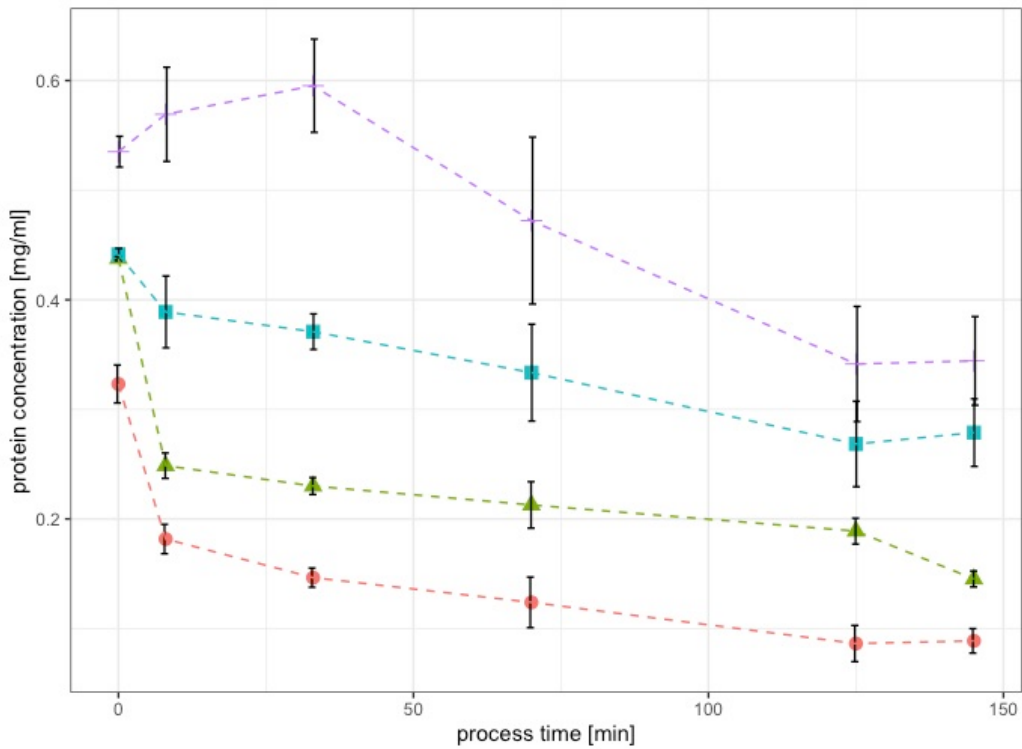


**Fig. 35.** Development of concentrations of beta casein (blue), alphaS1 casein (red), kappa casein (violet) and alphaS2 casein in the cream phase of model process cheeses made from sodium caseinate.

hydrophobic aggregated structures, aka by means of depletion, or to link the hydrophobically aggregated structures via electrostatic bridges.

Fig.35 indicates that the fat particle which is formed in systems with sodium caseinate is of different characteristics than those formed from native casein. This is also represented by the morphology of the cream phases, Fig.36 shows an image of the two separated cream disks. In addition the hypothesis that with this compositional analysis, indications for structure formation can be obtained, cannot be falsified. This leads to the theory, that during structure formation processes in composite gels like processed cheese, either the aggregation phenomena occur at, with or in favour for the interphase. This theory of a hydrophobic network formation will be explored later in this work in further detail, however regarding the cream phases of the two investigated types of model cheeses within this section, they appear different.

Fig.36(B) shows the coarse structure of the cream obtained from samples made with sodium caseinate. Fig.36(A) displays the fine emulsion of a native cream disk. Free oil seems apparent in the sample made from sodium caseinate. The cream phase isolated from samples made from native casein on the other hand shows no free oil and a homogenous texture. The difference in the emulsion stability of the samples could be explained due to the absence of calcium ions in sodium caseinate

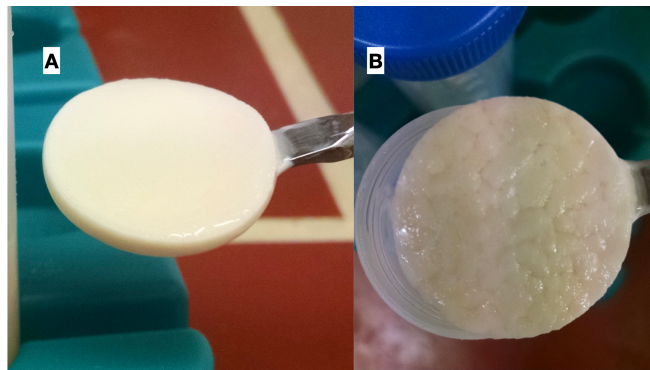


**Fig. 36.** Comparison of centrifugally isolated fat phases in model processed cheese samples made either from native casein (A) or sodium caseinate (B)

cheeses as connecting agent for the proteins to form a particulate shell around the fat globule.

Dickinson and Golding (1998) investigated the gravity creaming of sodium caseinate oil-in-water emulsions under the influence of calcium ions. Calcium deprived systems showed little adsorbance of casein to the interface. It can be concluded, that the primary adsorption of caseinates to the interface in model processed cheese is calcium driven, since the calcium containing native casein systems showed strong adsorbance of caseins to the interphase, whereas sodium caseinate model systems exhibited minor adsorbance to the interface. The same effect seems to occur here.

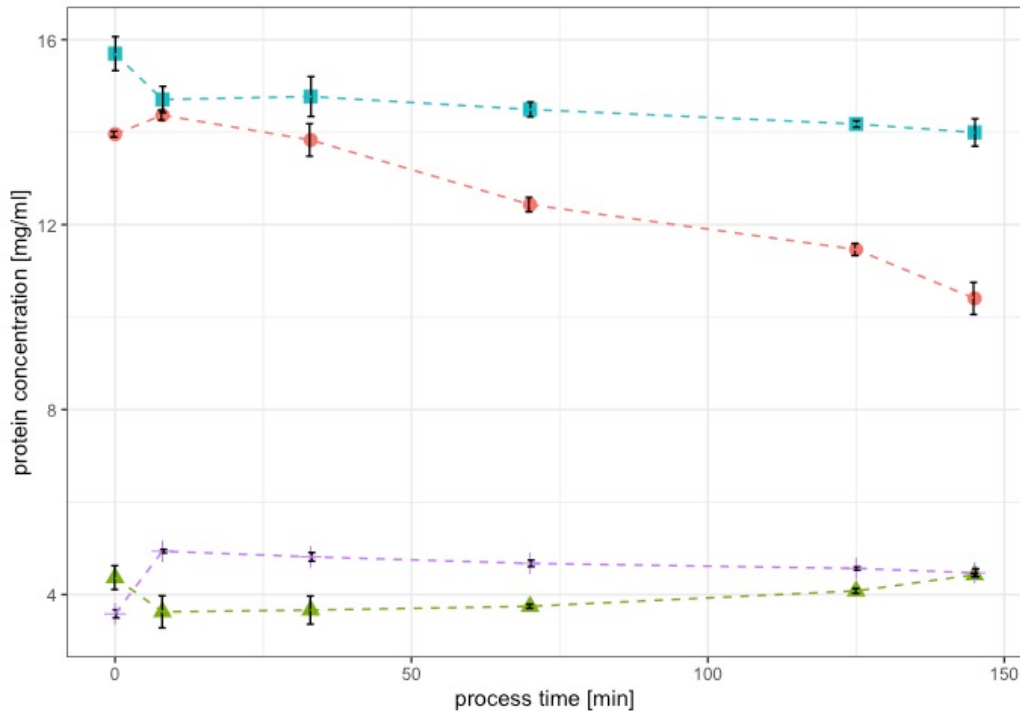


**Fig. 37.** Development of concentrations of beta casein (blue), alphaS1 casein (red), kappa casein (violet) and alphaS2 casein in the serum phase of model process cheeses made from sodium caseinate.

the protein concentrations in the obtained serum and pellet phases of the processed cheese samples

made from sodium caseinate were also measured. In Fig.37, the soluble or serum phases of the cheeses are displayed over the processing time, Fig.38 displays the pellet of such systems in a similar manner.

Protein concentrations in the serum phase in samples made from sodium caseinate didn't change significantly, besides alphaS1 casein, which decreased. The initial concentrations at 0 min in cold state are probably lower in reality, the centrifugational separation and longer incubation of samples probably led to a further solubilization of sodium caseinates into the serum phase from the insoluble phase, which explains the discrepancy in total protein concentration of the samples.

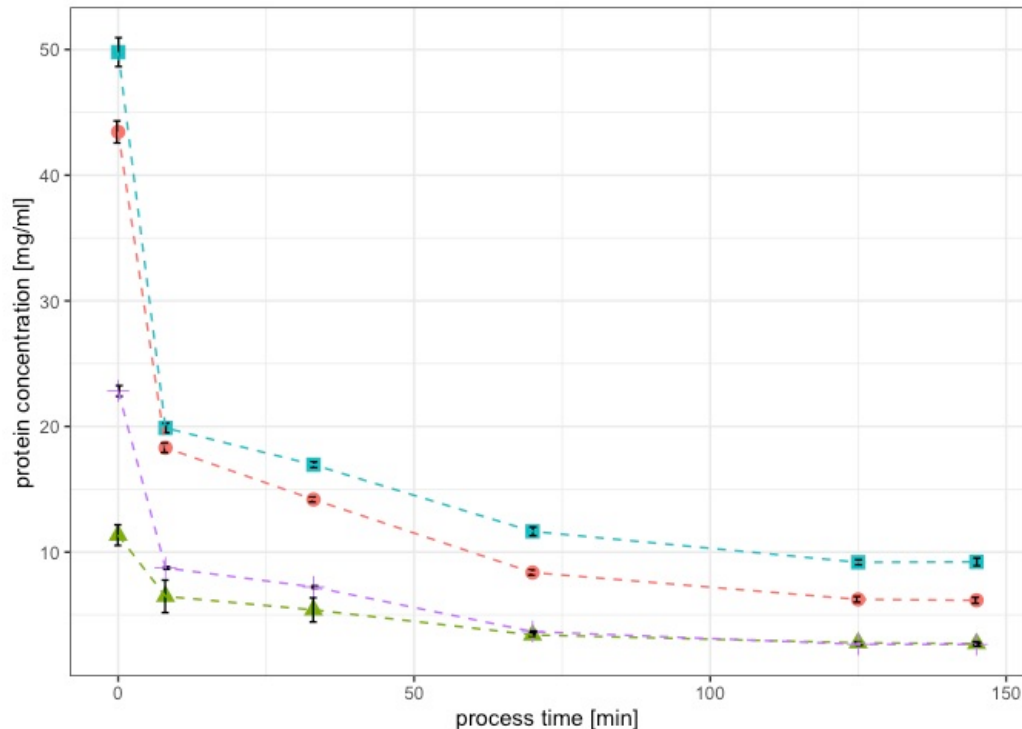


**Fig. 38.** Development of concentrations of beta casein (blue), alphaS1 casein (red), kappa casein (violet) and alphaS2 casein (green) in the pellet phase of model process cheeses made from sodium caseinate.

In comparison to the samples made from native casein, the initially unsoluble proteins during premixing in cold state in samples made from sodium caseinate become more and more soluble during processing. Therefore the protein concentrations in the pellet as displayed in Fig.38 decrease. Analogue to the cream samples, it seems that a certain degree of aggregated insoluble casein particle can be formed, however, a linking agent seems to lack, as no bigger structures can be formed during processing.

The main chemical component lacking in the sodium caseinate systems is the calcium that was chelated from the calcium phosphate nanoclusters (CCP) of the native micelles in their respective model cheese systems. It could be assumed, that especially in the second log phase of the structure

formation, calcium ions are essential. It could connect the caseins by bridging two negative charges from acidic amino acids which is commonly used in cheesemaking under the addition of calcium chloride.

The plateau phase preceding the second log phase is suspected to form homogenously aligned structures, that later form into fibrils. Their secondary connection to clustered aggregates could be connected via electrostatic calcium binding, which would also explain the higher water binding capacity of the investigated pellets, as seen in Fig.??.

The concentration of total protein in the wash phases of the sodium caseinate samples didn't change significantly during processing (data not shown), which is in conclusion with the behaviour of the sodium samples, meaning that no changes in adsorption to the interphase or aggregation to larger structures occurs.

#### **4.3.3 Development of pH of model cheeses and dry matter of respective cream phases**

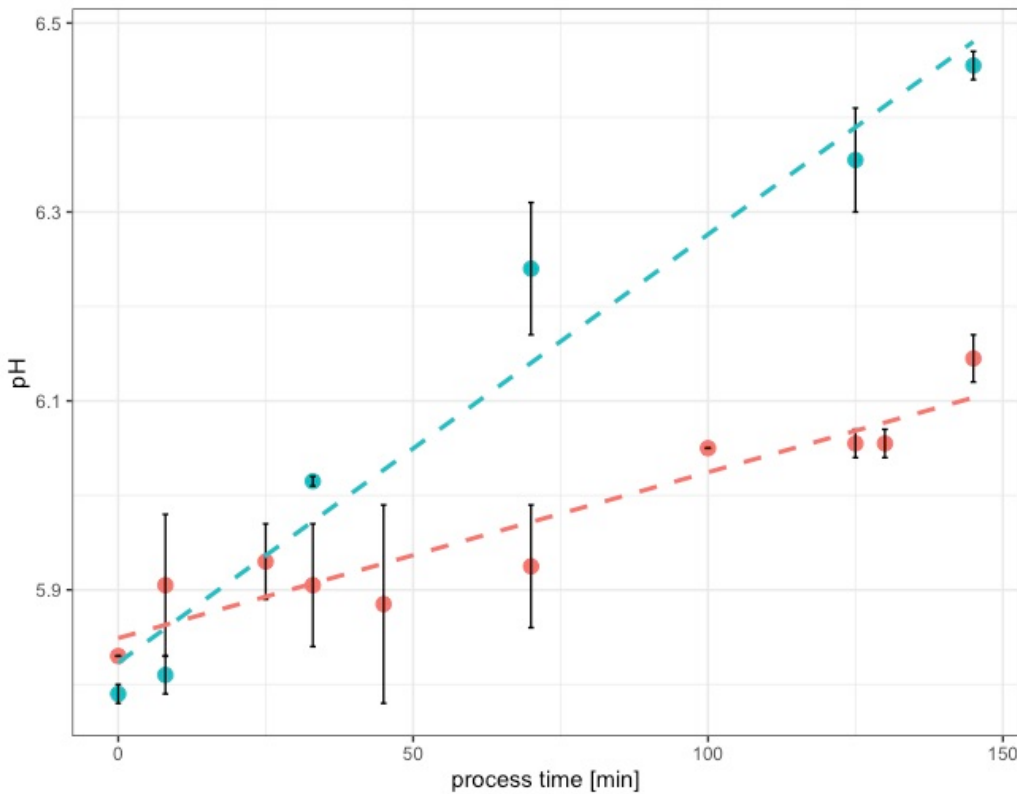
The theory, that free calcium from chelation out of the casein micelle is able to connect the caseins via their centers of phosphorylation to form a tighter structure is also supported by the comparison of the development of the pH of the sodium and native casein models during processing.

Fig.39 shows the development of the pH from samples processed to specific times. The increase in both sets of samples was significant ( $p < 0.05$ ) over the full processing time. The pH increase in samples from sodium caseinate develops to a higher value (6.49) than in the samples made from native casein (6.02) during the same time span. Also, the pH increase in samples made from native casein increased significantly only in a step wise manner, between 70 minutes and 100 minutes of processing time. This time span represents the transition from the plateau to the beginning of the second exponential (second log) phase.

A higher pH indicates a higher negative net-charge of the proteins. Up to the beginning of the second log phase at 100 minutes, the pH in the native samples is buffered around the targeted value (5.88). After that, the pH increases to approx. 6.05, where it stays stable until the end of the investigated process.

A higher negative net charge in the matrix also indicates the potential for possible new electrostatic binding sites, when, at least divalent, cations are present.

It seems however unlikely that structures connected via 'classic' electrostatic binding (or bridging, due to the moist environment) are insoluble in water. Since the insoluble structures were shown to



**Fig. 39.** Development of pH during processing of model processed cheese made from native casein (red) or sodium caseinate (blue), with a linear fit (dashed line)

be formed prior to 100 minutes by an increase in all protein concentrations in the pellet, at least the primary aggregate is connected differently. Hydrophobic interaction presents itself again as a good candidate for such a primary aggregation, since they appears at close range and under the exclusion of water. Calcium, however may play a role in secondary aggregate connection, with a subsequent increase in apparent viscosity.

Comparing the native and the sodium caseinate systems it becomes also possible that the aggregates in the pellet of the native samples form the “soft shell” of the fat particles, which later becomes a hard shell as described in Dickinson (2012). These shell proteins can be detected in the wash phases of the cream after dilution. Before dilution, the gaps between the fat domains were filled with the aggregated “soft shell” protein that we find in the pellet after dilution. This means that hydrophobic aggregates are still able to swell, which is reasonable since they are still colloids, or colloid particles. Interestingly, the aggregates in the pellet as well as in the cream are only prone to swelling, not to resolubilisation in water. This implies that some sort of aggregation is apparent, where hydrophobic clusters form the core with (partially) hydrateable protein at the surface. This theory is supported by the development of the dry matter of the cream (Fig.40) over processing.

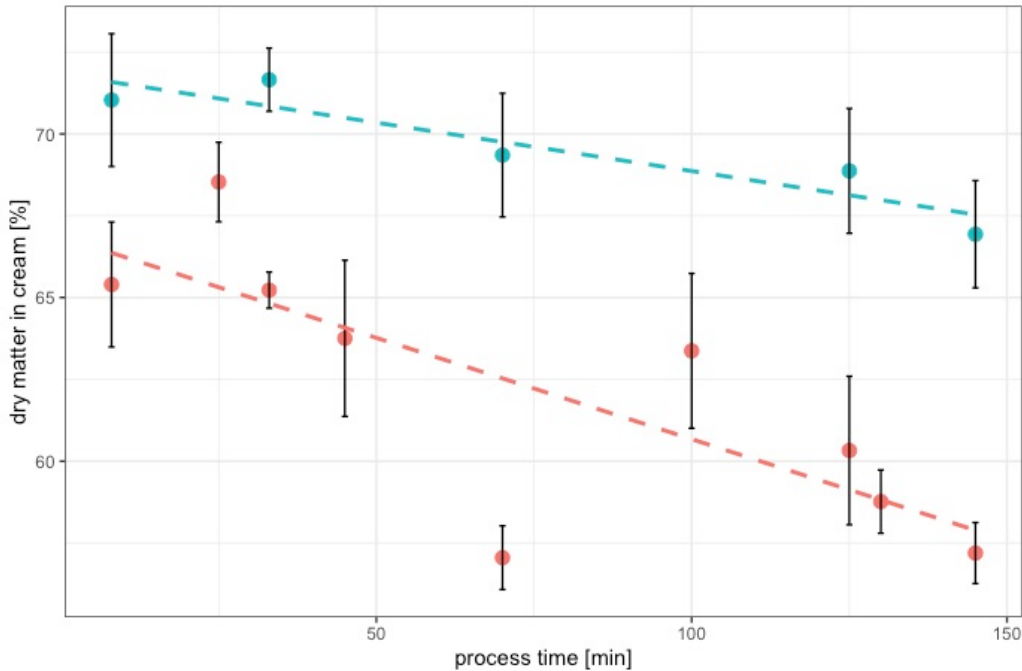


**Fig. 40.** Development of dry matter in centrifugationally separated cream phases of samples made from sodium caseinate (blue) and samples made from native casein (red), with a linear fit (dashed line)

The dry matter of the sodium caseinate cream decreases, if at all, only slightly during processing. The dry matter of the native casein cream first shows a slight increase after melting. Since the protein concentration in the cream decreases between those two processing points, it can be hypothesized, that the more hydrateable proteins leave the interphase, hence the larger dry matter, since less water can be bound to the interphase at this point. Afterwards, a strong decrease in the dry matter of the native cream samples becomes apparent. Before the second log phase of structure formation, which starts at 100 minutes, the dry matter of the native cream increases again, followed by a strong decrease up to the end of processing. The increasing amount of the size of the sphere, which is made up of amphoteric proteins, leads to stronger hydration of the shell after dilution, i.e. a decreasing dry matter. It seems however unlikely that structures connected via ‘classic’ electrostatic binding (or bridging, due to the moist environment) are insoluble in water.

#### 4.3.4 Development of protein concentration of single caseins in the cream phase of model processed cheeses from continuous processing

In order to test the reproducibility of the process as a whole as well as to test the validity of the results of the samples that were treated with the washing method, and upscaled process was investigated in detail. The data showed conclusive results throughout, meaning a strong increase of

protein to the interphase at late processing times. Likewise, the proteins to be dominantly found at the interphase were again kappa casein, alphaS1 casein and beta casein. Fig.41 displays two exemplary results from this trial, the measured protein concentration at the interphase for samples made with 20% and 5% fat, respectively. The viscosity of the samples revealed an increase in viscosity and a pronounced second exponential phase (data not shown).

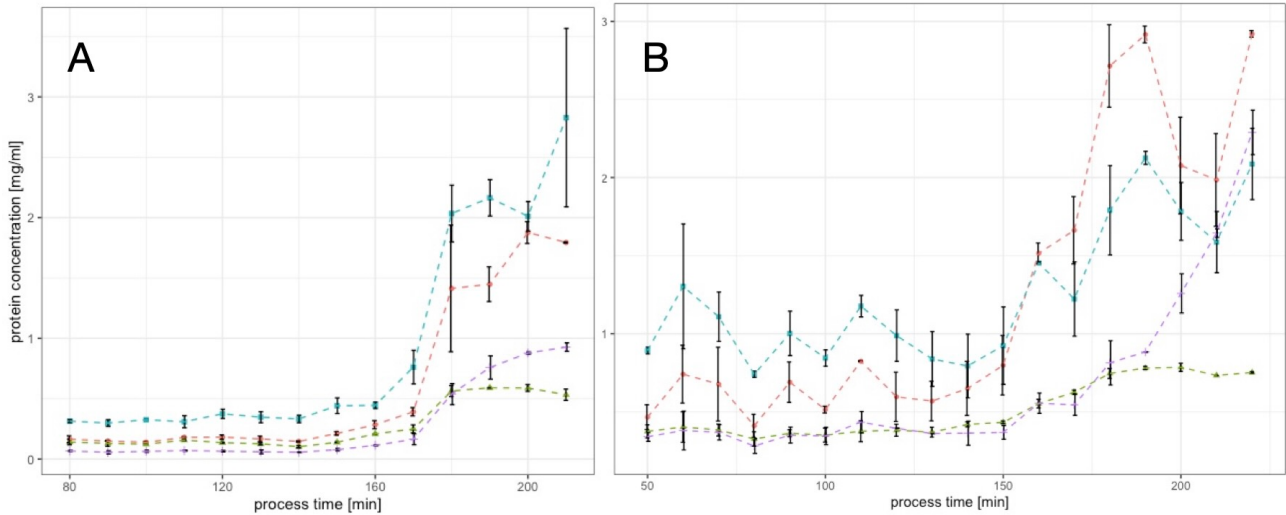


**Fig. 41.** measured protein concentrations in the cream of an upscaled process: (A) 5% total fat concentration, (B) 20% total fat concentration: beta casein (blue), alphaS1 casein (red), kappa casein (violet) and alphaS2 casein (green)

It can be seen, that the lower fat concentration is visible at the interphase up to the beginning of the second exponential phase (after 150 - 160 minutes of processing). This leads to the conclusion, that up to the second exponential phase, the proteins are coated with aggregated protein from the bulk. After that, hydrophobic aggregation occurs at large scale, thus a hydrophobic shell is formed around the fat globule that grows in size during processing.

Also, the adsorption of (potentially aggregated) kappa casein becomes even stronger in an upscaled process, probably due to fact of a higher reactive protein mass to begin with, therefore, more kappa casein primary aggregates can be formed, that later adsorb to the interphase. Liang et al. (2017) investigated the creaming stability of also highly concentrated (10% w/w) sodium caseinate emulsions under the addition of maltodextrin. It could be found, that after an addition of 15% maltodextrin, the fat droplets were effectively hindered to interact, due to the large polysaccharide network. Inulin has been known to bind water as well and was already used as a fat replacement (Sołowiej et al. (2014)) in model acid induced processed cheese. It was found, that inulin didn't alter the water binding properties of the cheese samples but that their hardness increased due to a finer dispersion of fat droplets. Considering the measured protein concentrations at the respective

interphases (Fig. 41, Fig. 35, Fig. 31), it can be seen that the sodium caseinate samples were effectively hindered to form a network of interacting fat droplets, while the calcium containing samples showed large interaction properties, also at low fat concentrations. As it will be discussed also later in this work, this effect can be attributed in part to calcium, however it can be expected, that the constant agitation of the matrix leads to droplet and particle collisions, that show specific interactions that will induce the matrix formation and also separation at later processing stages. The findings of Lenze et al. (2019) that a matrix with reduced fat shows a lesser structure formation could not be seen in the upscaled process. Even more, the viscosity increase as well as the increase in proteins at the interphase were exponential, in samples with 5% and 20% fat content. This is probably due to the different dry matter add-ons used; Lenze used lactose, which is a reducing Di-saccharide, hence it could be possible that the proteins got “blocked” from structure formation due to lactosylation of lysine residues (i.e. formation of early Amadori products as in Dumpler (2018)). Inulin proved itself to be inert towards reactions with protein.

#### 4.4 Summary and Outlook

This data set shows how the proteins in the model processed cheese distribute themselves during processing. Due to the thermal stress, they undergo different aggregation processes, which appear to be distinguishable. Sodium caseinate models show only slight tendencies towards distribution, aggregation or adsorption to the interphase. It seems that something is “hindering” the caseins in the sodium caseinate model to form large aggregates. One could say, the sodium caseinate system is missing some sort of connective force or agent. Respectively it can be said that some driving force in the native casein models is “enabling” the proteins to form aggregates.

A compositional analysis of a centrifugationally obtained pellet was also performed in Vollmer, Kieferle, Pusl, et al. (2021). The protein concentration was treated as % of the total protein concentration in the system, to normalize the natural distribution of casein. No conclusive answers to a detailed distribution of caseins could be given, besides the concentration of kappa casein in the pellet. The centrifugation procedure used in this work had softer conditions, 6.000g compared to ~22.000g. It seems reasonable that higher centrifugation speeds also lead to collective concentration of hydrophobically associated aggregates in the pellet. A different display of the measured concentration was chosen in this work, since it was expected, that the caseins are present as monomers after melting and therefore, their single measured concentration, and not the concentration relative to their concentration in the micelle was chosen for analysis. This was done to see an overall shift of caseins in the matrix, also including their absolute occurrence in the system

(i.e. their single concentrations).

So what are differences between the native and sodium caseinate models? Since the pH and the ionic strength are set the same initial value in both systems, the differences are only two: the size of the initial colloid, and released Calcium. The melting salts lead to the release of micellarly bound or associated Calcium. Calcium Ions are known to form stronger gels when added to a Casein matrix (as it is often done in cheesemaking). Since they are divalent cations, they are able to screen or bridge two negative charges. The pH of the structure formation is  $\sim 5.9$ , the IEP of Caseins (mean) is 4.6, so the Caseins show a negative net charge during the whole course of the reaction. This negative net charge would lead to electrostatic repulsion. Thus, the negative charge is screened by Calcium and therefore, single caseins can interact within very small distances, which then lie in the (distance) range for hydrophobic interactions. Another fact that underlines this theory is that hydrophobic interactions grow stronger at high temperatures, which means that thermodynamically speaking, during processing of the model cheese, this kind of aggregation seems favorable.

From the washing experiment, the underlying reactions for the two lag and log phases can be derived. The first lag and log phase are dominated by the redistribution of calcium and caseins, due to the initial effect of the melting salts. The second lag phase limits the growth of aggregates and shows the effect of the shear stress on the system. The second log phase represents the hydrophobic aggregation of especially alphaS1 and beta caseins. The aggregation occurs in the continuous, as well as at the interphase. It could be shown, that the proteins develop a higher affinity to aggregate than to adsorb to the fat globule, therefore, the fat gets emulsified to a lesser and lesser extent until it is released by the system in form of free oil (see also Fig.xx in Chapter 2).

The advantage of the washing method (in contrast to other methods of investigation like native page, dumas method, IR, etc.) is the possibility to isolate and investigate a hydrophobic surface, in the form of a colloidal fat particle, with proteins forming a soft-shell - represented by the adsorption during the first log phase. This soft shell then develops into a hard sphere during the second log phase. Through the isolation of the proteins from the fat phase using a chaotropic buffer as described in Bonizzi, Buffoni, and Feligini (2009), fat is not disrupting the measurement, in contrast to PAGE and IR, where fatty samples lead to overlayered data response. Dumas gives us total Nitrogen, which can be calculated into protein concentration, using an empiric factor. The big disadvantage is though, that we don't see the concentrations of single Caseinates. Additionally, Dumas works only for concentrations  $> 1 \text{ mg/ml}$  and it's not advisable to measure fat rich samples, due to the flammability of fat. Qualification and Quantification with HPLC (especially the Guanidinium Step) brings robust, reliable, conclusive and easy-to-compare data. By investigation of the proteins in the

fat phase of an upscaled, continuous process it could be shown that the measurement data was not specific to the processing conditions (like mass flow, shear speed, area of heat transfer) in a rheometer. Since the data from the batch processing and continuous processes also displayed a strong increase of protein detectable in or at the interphase during the end of processing, it can be concluded, that the data represents the compositional changes at the interphase in a well suited manner. Also, the variance in fat concentration gave conclusive results, since the amount of protein found at the interphase before entering the second exponential phase, i.e. that amount of not highly aggregated protein at the interphase increased with the total amount of fat used. The occurrence of a second exponential phase of structure formation was found at all fat concentrations, further proving that fat serves not as a structuring agent but mainly has a secondary role as reactive surface, where protein aggregation can occur. Protein aggregation into large networks, that are insoluble by water, however, seems to occur also without the large amount of an interphase present, leading to the conclusion that the fat is emulsified as a by product of the protein aggregation. This also leads to the conclusion that the dominating network formation steering this process is hydrophobic interaction.

The findings presented in this chapter are also in conclusion with the findings of Vollmer, Kieferle, Youssef, et al. (2021). The composition of the samples in the cited work were similar to the native casein samples investigated in this work. The processing conditions in this work were slightly different - only the shear rate (see discussion in Chapter 3) was accelerated, in order to gain a higher sample throughput by the reduction of processing time due to a higher collision rate. The TEM images displayed in the reference study showed the formation of fibrillogenic casein structures in the second log phase, or second phase of structure formation. These structures represent the here described hard-shell of caseins forming the fat particle. By the present study, the composition of the fibrillar structures can be suspected as to mainly being alphaS1 kappa and beta caseins, since they are the dominating proteins at the interphase during the second phase of processing, as well as in the pellet.

## **5 Investigation of particle size development in the bulk phase and at the interphase during processing stages of model process cheeses**

### **5.1 Introduction**

In composite materials, that can be described as emulsion gels or soft-solids, the binding state of the filler particle, which is represented by the fat particle is crucial for the viscoelastic properties and overall appearance of the gels. Fat droplets can be either incorporated into the matrix as an ‘active filler’ that will strengthen the gel, or as an ‘inactive filler’ that weakens the gel towards shear stress (Dickinson (2012)). Composite materials like processed cheese can be viewed as a composite material that is a very concentrated or dense emulsion in hot state, also referred to as sol, but solidifies into a gel structure upon cooling, due to the binding of the water molecules into the protein structure (Patrick F. Fox et al. (2016)). It has been shown that the cheese in hot and cold state is related directly in terms of hot-state viscosity and gel strength (Röck (2010)). Furthermore it has been shown in concentrated sodium caseinate emulsions (10% w/w protein, 30% oil), that high zero shear viscosity was the main reason for preventing phase separation in depletion flocculated emulsions (Liang et al. (2017)).

Therefore, the investigation of the fat particle size over the course of processing a model processed cheese matrix can give insight towards the growth behaviour of the fatglobules in sheared emulsions. Particle size measurements of fat-droplets in processed cheese samples have been done before, see for example Chen and Liu (2012). Particle size or particle volume measurements are commonly used, when the aggregation behaviour of single monomers or mixtures of proteins is to be investigated. Two different set-ups can be found for different ranges of expected particle size. Dynamic light scattering measures the Brownian motion of macromolecules in solution and puts into relation to their hydrodynamic radius (i.e. the measured particle size or also called particle volume in this work) using the Mie-Theory. Larger particles will diffuse more slowly through the solvent than small particles, and therefore, the beam of light that is used as “instrument” in this set-up gets scattered differently according to particle size (Sandhu et al. (2018)). It is commonly used for sizes  $< 1 \mu\text{m}$ . Laser diffraction uses a different approach and puts the diffraction of a laser beam into relation with the particle size using the Fraunhofer estimation (especially in the analysis of fat particles) and is used for expected particle sizes of  $> 1 \mu\text{m}$ .

In order to gain even further insight into the processed cheese matrix, particle size analysis are not

only to be performed in the cream phases of the cheeses, but also in their separated other phases, pellet and serum. It should be investigated, if the particle sizes in the insoluble aggregate follow any trend that can be interpreted toward the recorded aggregation phenomena in the model system so far. Besides the determination of the particle sizes in general, the reproducibility of the centrifugational separation method should be monitored during this part of the study. If the obtained particle sizes, especially in the pellet, since this is the most “reliable” phase appearing due to simple G-Force, show low standard deviations, one can assume that the separated structures by means of centrifugation are not at random, but by underlying aggregation phenomena. Thus, this analysis serves the purpose of giving further insight towards the aggregation mechanisms happening during the processing of model processed cheese on a micro scale, as well as further validating the isolation method prior to analysis.

## 5.2 Material and Methods

6 g of the processed processed cheese sample as manufactured in chapter 3 was weighed into 50 ml purifier tubes and diluted 1:3 (w/v) with deionised water. To produce a homogeneous dispersion, a dispersion device was used and the dispersion was prepared at a speed of about 6,000-8,000 rpm. For phase separation, the samples were centrifuged at 6000 g and 10 °C for 30 min on the Multifuge (Heraeus Group, Hanau, Germany). This produces a three-phase system consisting of a fat phase (cream), water phase and pellet. The fat phase was lifted off with the help of a stainless steel spoon and transferred into a prepared 50 ml purifier tube. The water phase was poured into another tube. The differently obtained phases were further prepared for particle size measurements. To obtain only “truely” soluble proteinogenic structures in the soluble, or serum phase, this phase was prepared with ultracentrifugation (70.000g) and subsequent filtration (cutoff 2500 nm) prior to measurement in a Malvern Zetasizer.

The cream phase was further diluted 1:10 (w/v) using a solution containing 1% sodiumdodecylsulfate (SDS). SDS is a strong tenside and prevents the fat globules or particles in the cream from aggregation during the measurement. In addition, it disrupts (loosely) aggregated fat particles.

The pellet or insoluble phase was diluted in deionized water 1:10 (w/v) prior to the particle size measurement. So prepared cream and pellet phases were suspected to be in the micro scale and therefore analyzed using a Malvern Mastersizer.

## 5.3 Results and Discussion

### 5.3.1 Data processing

Data was processed using the “normalmixEM” algorithm within the R programming language. The algorithm is used for finite mixture models, a detailed description is given by the programmers of the algorithm under Derek et al. (2020). Since the distributions of the particle volumes did not show a monomodal distribution, a multiple component model was fitted with either k=2, k=3 or k=4. Three and four component models had a lower logarithmic likelihood than the two component model throughout all tested samples during this trial, which is not surprising, since the particle distributions in the different phases showed a bimodal distribution over processing. Therefore, the two component model represented the best fit in the analyzed phases and was used for further distribution analysis.

### 5.3.2 Particle size distribution in cream phase

Fig.42 gives a summary for the measured particle size distribution in the analyzed cream phases. In general a shift from larger to smaller particles over the course of processing becomes apparent, however it appears to be not very pronounced. As it was stated above a definitive conclusion cannot be drawn by viewing the distributions, therefore the distributions were modeled.

Over the course of the creaming reaction in model processed cheeses, the cream phase of the centrifugally separated matrix shows smaller particle sizes, indicated by the lighter colours being in the range of smaller particles. In general, the particle sizes varied only little in range. To check this observation, the modelled particle sizes (of small and large components) were plotted over the processing time.

Fig.43 indicates that small and large fat particles detectable in the cream phase of the model processed cheese follow the same trend: first, the fat particles grow in size during the first exponential phase of structure formation. The premixing process seems to create smaller fatglobules, than the system can maintain during the first stage of the creaming reaction. After reaching a maximum in size at the end of the first exponential phase of structure formation at 45 minutes, the fat particles become smaller. This leads to the conclusion, that the first stage of structure formation is not defined by the formation of a fine emulsion with small fat particles, but rather by the formation of a continuous network in the bulk phase. This is also indicated by Fig.31 in chapter 4, a strong adsorption of proteins to the interphase could only be detected during the second exponential phase of structure formation. Regarding the development of the fat particle sizes during this phase,

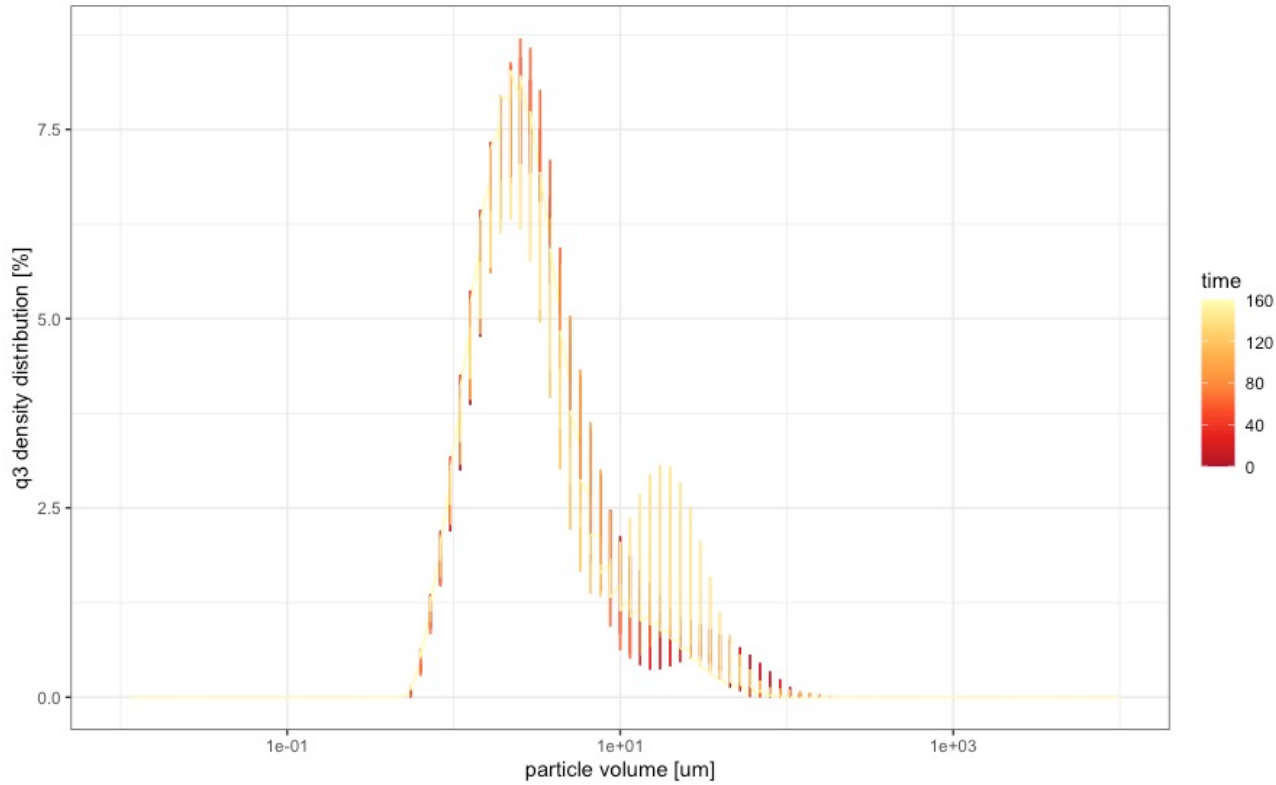


**Fig. 42.** q3 density distribution of measured particle sizes of centrifugationally separated cream phases: darker colours indicate shorter processing time, lighter colours indicate longer processing times.

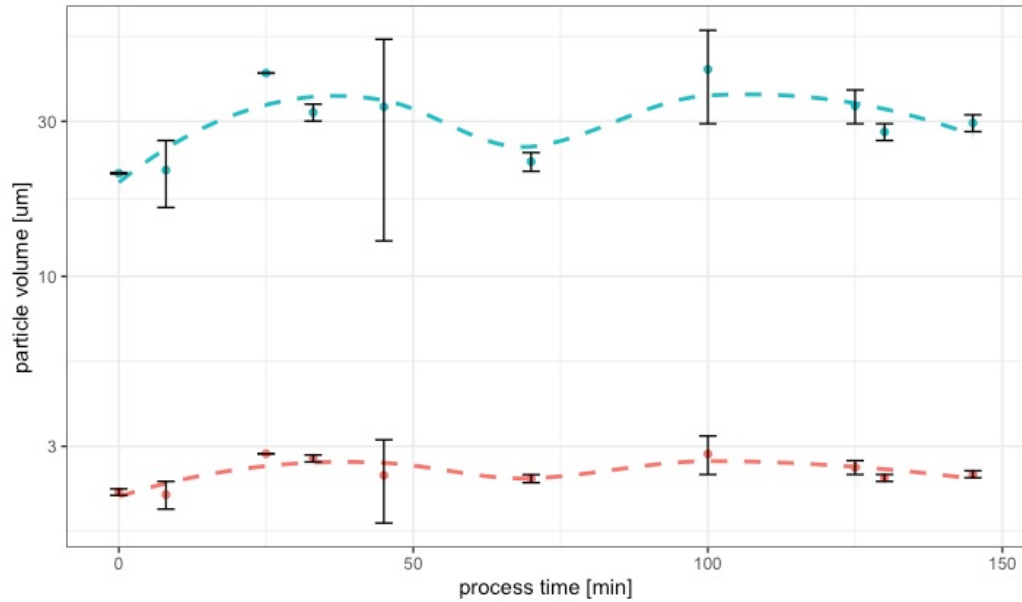


**Fig. 43.** Development of Particle Volume of small (red) and large (blue) fat particles over processing time

the data seems also conclusive, since, after growing in size again towards the beginning of the second exponential or log phase (100 minutes of processing), the fat globules shrink and a fine emulsion is

formed up to the end of the investigated process. The detectable changes are however minimal, which can also lead to the conclusion, that the changes of fat binding in the matrix is not a structure defining step, since there seems to be no progressive change in fat particle sizes. Since it is known from previous investigations in this work, that the hydration properties of the proteins, at the interphase and in the pellet increase during structure formation, it can be assumed, that the actual fat globule size at late stages of processing are smaller than the displayed values, since the protein shell, which was shown to grow in size is part of the particle. Vollmer, Kieferle, Youssef, et al. (2021) and Vollmer, Kieferle, Pusl, et al. (2021), as well as Lenze et al. (2019), N. Noronha, Duggan, Ziegler, O'Riordan, et al. (2008) and El-Bakry et al. (2011) all reported the formation of a fine emulsion during processing, so the general trend to bind the fatglobules stronger during processing can be seen in this work as well. It has to be considered however, that in this study, no other surfactants were used. So the abundance of smaller fatglobules or the significant shrinkage of the fat globules might be an effect that is not induced (primarily) by casein. It can be assumed that the displayed emulsification processes in the cited works are mainly due to whey proteins, which are commonly present by the use of milk powders or by the use of dairy cream or butter as the fat phase, which are per se emulsions. In the upscaling event already described previously, differently homogenized casein emulsions, by homogenization of a 5% casein emulsion at different pressure rates were added to 15% protein after homogenization and processed continuously. The samples during processing revealed, what was already seen in Lenze et al. (2019) and elsewhere; smaller initial fatglobules lead to faster structure formation. The decrease of the fat particle size was stronger in the upscaled system, however it can be concluded, that the trend displayed here are in accordance with the literature.

Looking at the density distribution of the fat particles, meaning the amount of small and large particles in the system, the same conclusions can be derived (Fig.44).

It shows that the distribution of small and large components in the investigated cream phase over the course of processing. The density distribution of the small components has the same trend than the development of the particle sizes in general, which leads to the assumption that the system in general puts work into the formation of smaller fatglobules. The amount of large components has a maximum at 70 minutes of processing, also the large particles display their smallest size during processing at this point. Both effects are also in conclusion with the findings of Lenze et al. (2019), where the formation of a small interconnected network of fat particles is hypothesized, described by microscopic techniques, as well as particle size measurements. It seems likely, that the system is only able to bind a lesser amount of fat into small fat globules or particles over the course of processing, since a further emulsifying agent is missing. In Röck (2010) it was shown, that the addition of

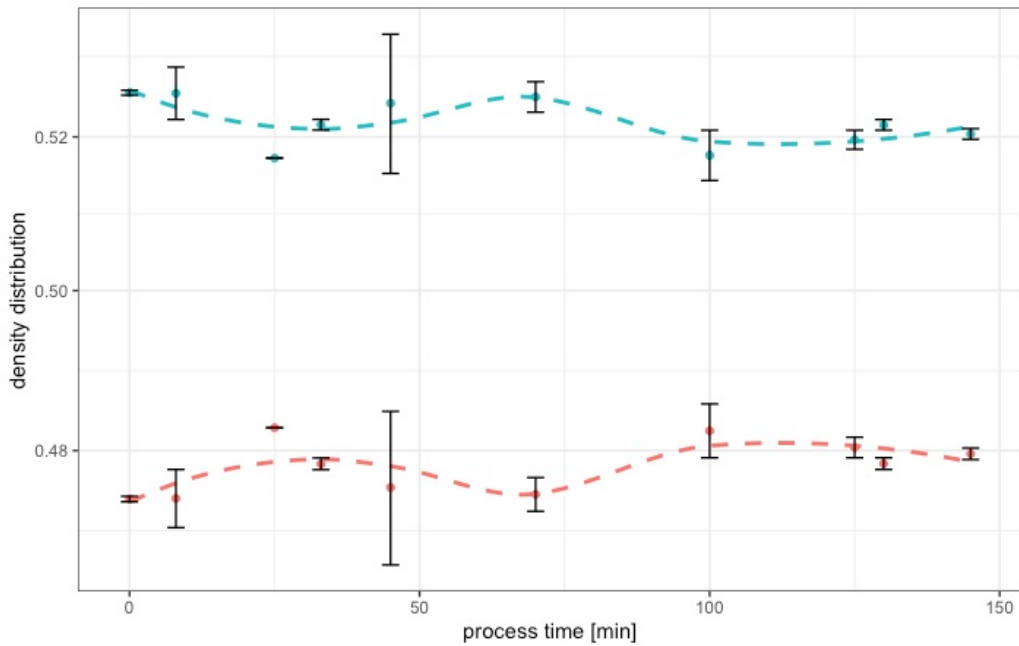


**Fig. 44.** Development of density distribution of small (red) and large (blue) fat particles over processing time

small-level surfatants led to a vast increase of the structure formation processes, up to a point where no plateau phase was detectable anymore. This was also seen in the samples prepared during upscaling that were homogenized to an initial fat globule size of 1 um. The structure formation process in those samples was ~50% shorter than the controls (data not shown).

In all samples with a surfactant or pre-emulsified fat, also in this study, the initial increase Indications that caseins at higher concentrations can bind ever smaller amounts of fat was already described by Brunner (1991). This seems also be the case in the model processed cheese analyzed herein, however with the difference that the amount of “free casein” increases *in-situ* during processing.

Vollmer, Kieferle, Youssef, et al. (2021) investigated a matrix similar in composition, but processed at lower speed at six different processing times. These processing times were also represented in this study, however with smaller values for the respective processing times. The formation, elongation, and alignment of fibrillar structures was reported as well as their detailed function within the structure formation reaction. In principle, a shell like structure made out of fibrillar building blocks was reported to surround the fatglobule, enclosing it at later processing stages.

### 5.3.3 Particle size distribution in insoluble or pellet phase

Fig.45 gives a summary for the measured particle size distribution in the analyzed pellet phases. In general, a shift form medium sized particles into smaller and larger particles over the course of processing becomes apparent:

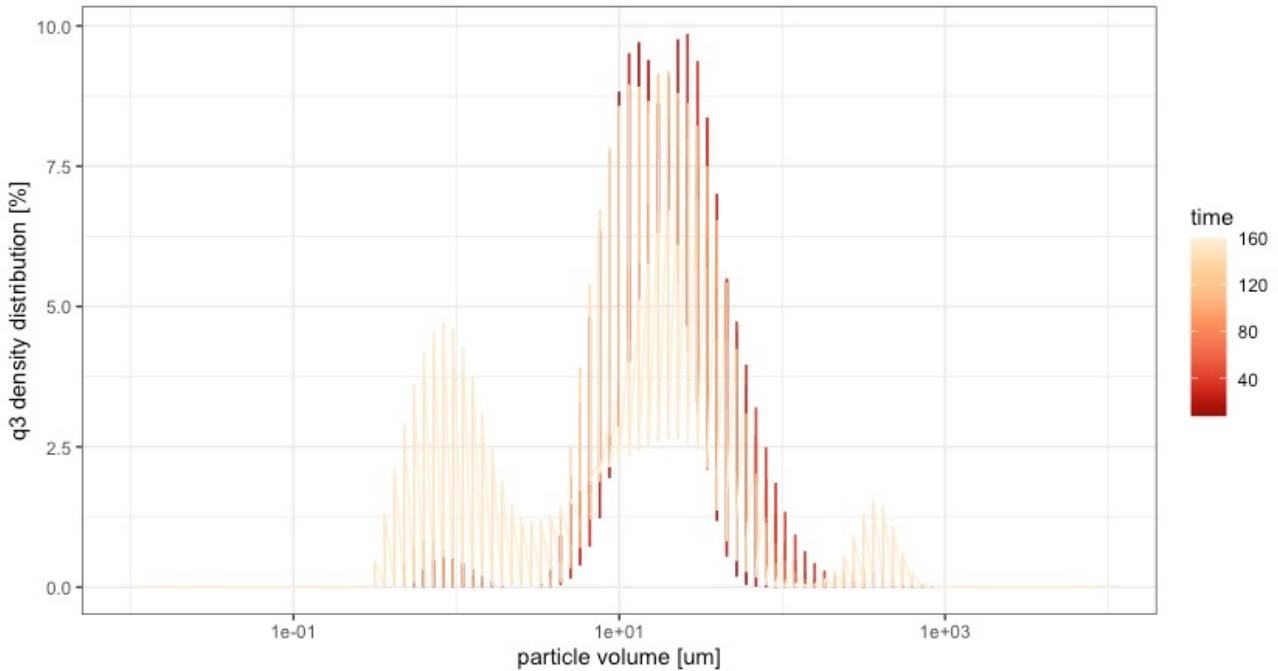


**Fig. 45.** q3 density distribution of measured particle sizes of centrifugally separated insoluble or pellet phases: darker colours indicate shorter processing time, lighter colours indicate longer processing times.

Even though three distributions are apparent in general, the two component model still had the best fit, since the single measurements showed a bimodal distribution throughout. A separation of the bulk phase into two different types of aggregates or aggregate scales is indicated. To check this observation, the modelled particle sizes are shown in Fig.46. It indeed shows, that at later processing stages, smaller aggregates become apparent, because the small components decreased from 10 microns to around 3 microns between 120 and 150 minutes of processing. The larger aggregate increased during this processing stage, from 70 microns to 10 microns. It can be theorized, that the larger network is constructed by the smaller entities, a conclusion that was also drawn in Vollmer, Kieferle, Youssef, et al. (2021).

The effect of the melting salts can be seen at a process time of 25 minutes, showing the lowest size in the pellet for large and small components. During the first exponential phase of structure formation (75 minutes), a larger insoluble network is formed, where small and large particles are interconnected.

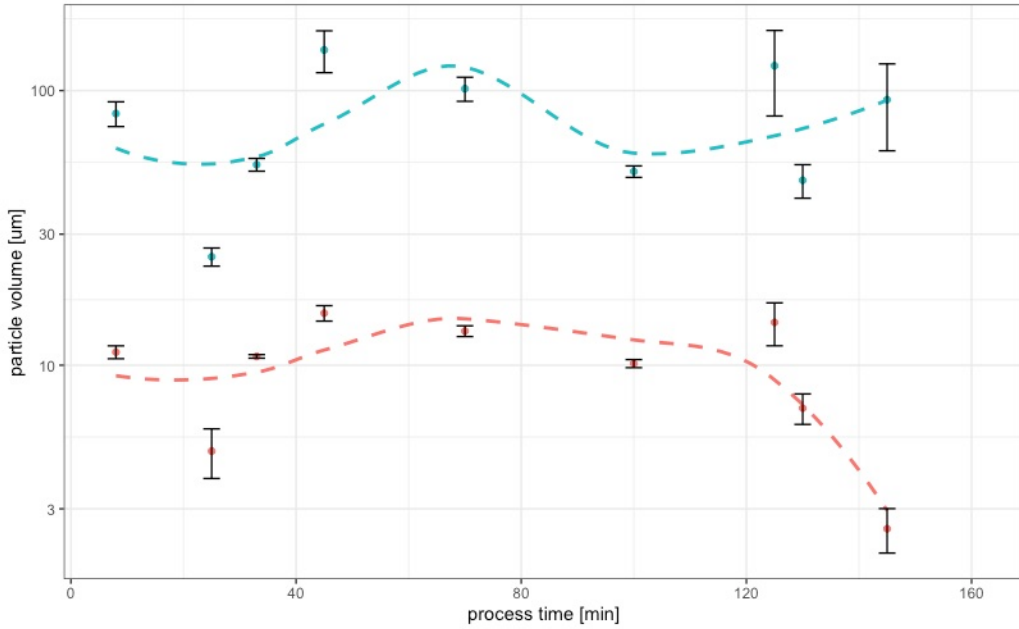


**Fig. 46.** Development of Particle Volume of small (red) and large (blue) insoluble particles over processing time

Additionally, since the decrease in particle size at the end of processing in the pellet is a gradual process, it can also be assumed that the fragmentation of the hydrophobic aggregate with beginning pase separation is displayed here.

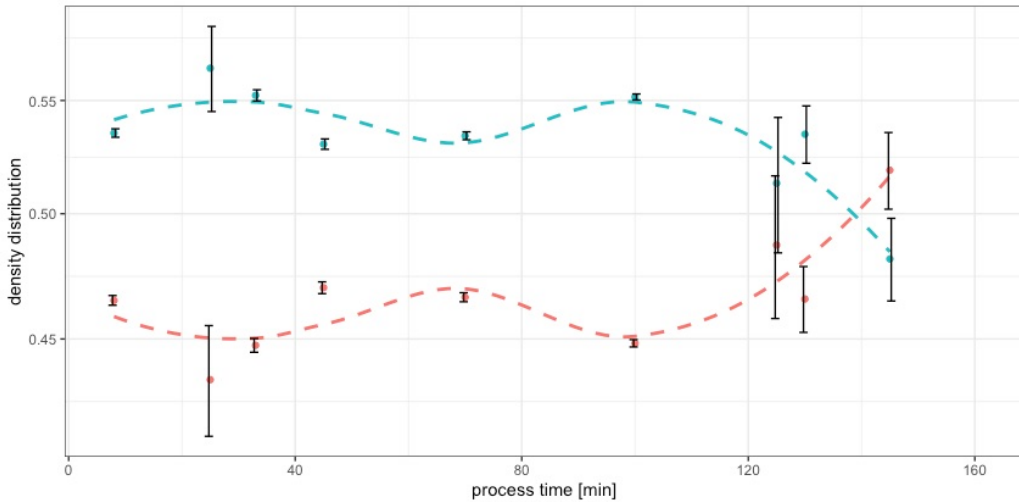


**Fig. 47.** Development of Density Distribution of small (red) and large (blue) insoluble particles over processing time

The density distribution of the insolubly aggregated particles as indicated in Fig.47 changes significantly in the last exponential phase of structure formation. Up to this point, the smaller components have also a smaller proportion of particles in the matrix. During the end of the investigated process, the smaller components form the larger domain of the network, which is also

indicated by a larger swelling volume of the investigated pellet Fig.47.

Kees de Kruif et al. (2015) determined the water holding capacity of casein gels by comparison of the swelling and de-swelling behaviour under different process conditions (like temperature) and salt concentrations. Gels that were linked with transglutaminase were also investigated. It was found, that enzymatically linked gels swell to a lesser extend than physically linked casein gels. Also the water binding and water release behaviour of highly concentrated renneted casein gels were the same as in casein micelles. The network formed in the pellet shrinks overall in particle size, however the volume of the pellet after dilution and centrifugational separation increased. Below is an image of the increasing swollen pellet volume from model processed cheese after various processing times (Fig.48).

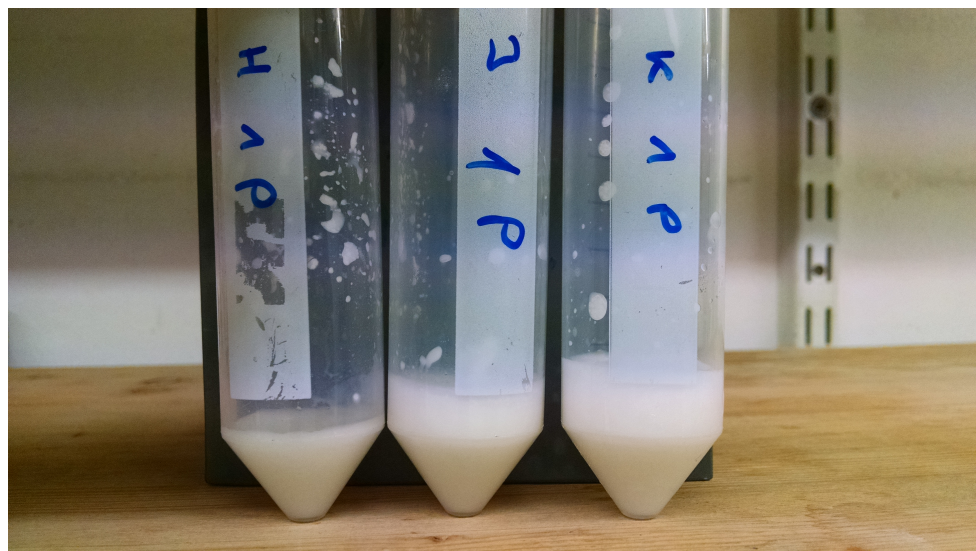


**Fig. 48.** Volume of a diluted and centrifugationally separated aliquot of model processed cheese: left to right: increase of apparent water binding capacity of insoluble aggregates after 125, 135 and 145 minutes of processing.

In contrast to Kees de Kruif et al. (2015), the casein particles that are formed during the structure formation of model processed cheeses investigated herein didn't dissolve completely after dilution. This leads to the conclusion, that the emulsifying salt mixture used herein leads to a formation of a more hydrophobic network, that can't be easily dissolved by water.

The results of the particle size analysis in the pellet as well as the findings of Vollmer, Kieferle, Youssef, et al. (2021) indicate, that the model processed cheese system undergoes a process of higher order structuring shortly before and during the second stage of structure formation. Taking into account that the small fat particles grow smaller during the last stage of structure formation, it can be derived that the components in the pellet phase and the fat globules are interconnected and form a particulate network made out of smaller substructures, as it was described in Dickinson (2012).

The results however don't suggest a de-emulsification process. Rather it seems, that a shell of proteins is built around the fat globules, which becomes more rigid during processing and can therefore also rupture at late processing stages and release the enclosed fat.

#### 5.3.4 Particle size distribution in the soluble or serum phase

The serum phase was analyzed using DLS, since the expected sizes after ultracentrifugation of the serum phase were estimated to be in the nano-scale. An overview of the measured particle size distributions is shown in Fig.49.

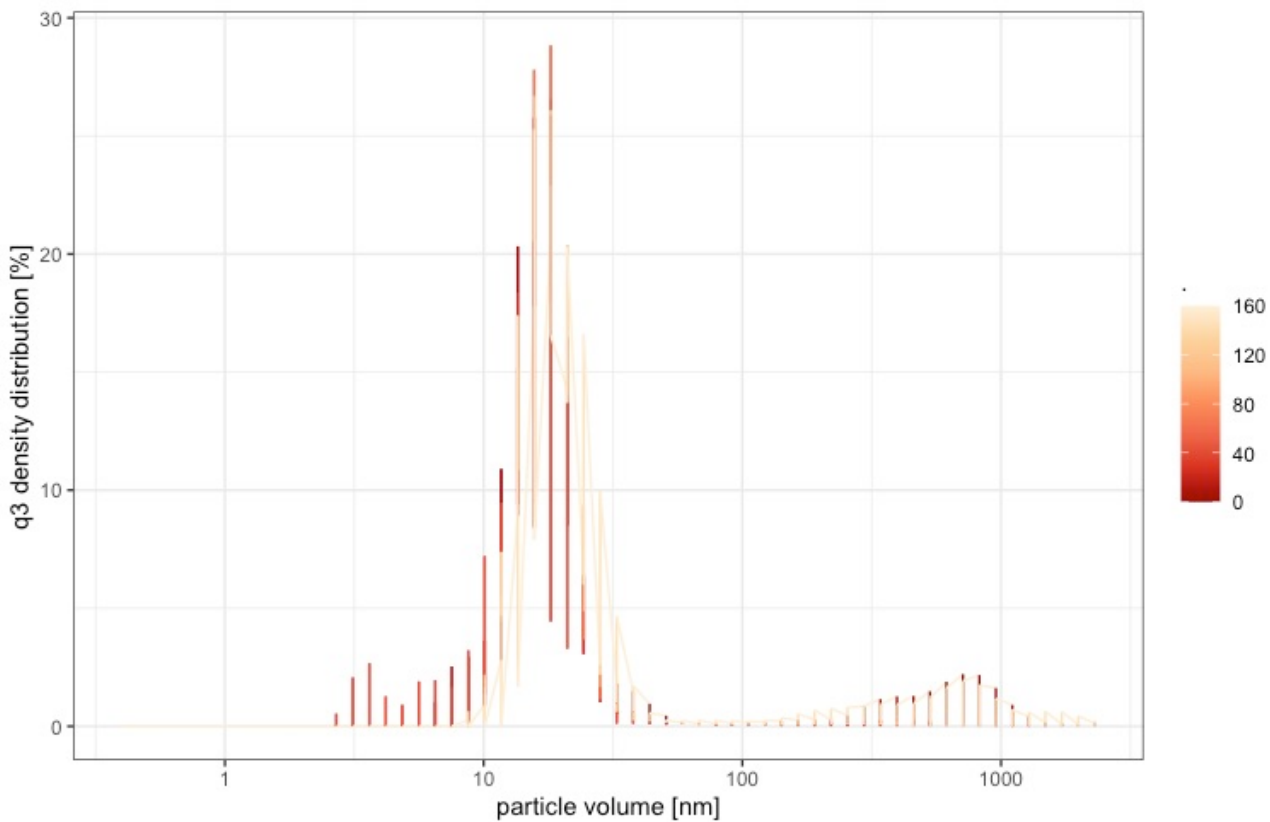


**Fig. 49.** q3 density distribution of measured particle sizes of centrifugationally separated (70.000g) soluble or serum phases: darker colours indicate shorter processing time, lighter colours indicate longer processing times.

It shows a more dynamic course for the development in the particle sizes which remain soluble, during the course of processing. The darker colours at 5-10 nm indicate free caseins before processing next to intact casein micelles at ~500 nm. Over the course of processing, medium sized (10-70 nm) structures develop next to larger structures around 700 nm. However, to get a detailed picture of the processes happening in the serum phase, the modeled particle size or volume distribution in the serum phase is shown below.

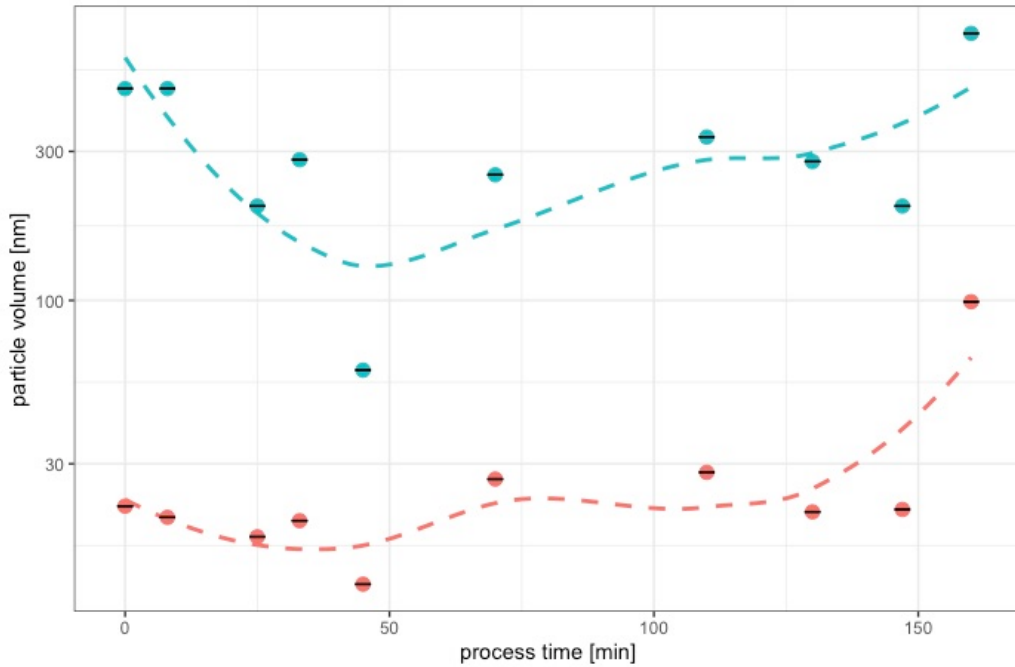


**Fig. 50.** Development of Particle Volume of small (red) and large (blue) soluble particles over processing time after ultra centrifugation (70.000g)

Fig.50 indicates shrinking soluble particles up to the end of the first exponential phase of structure formation. After that, a step-wise increase in particle sizes, in the small as well as in the large fractions was observed. The decrease in particle sizes in the serum phase up to process times of 50 minutes to a minimum value of ~50 nm for the large component and ~10 nm for the small component. This process time marks the end of the first exponential phase, it can be assumed, that small hydrophilic or amphoteric aggregates or even protein monomers are present that emulsify the fat into an emulsion filled gel. Subsequently the soluble aggregates increase in size, to a plateau of 30 nm for the small component and 300 nm for the large component, respectively. During the second stage of structure formation, between 140 and 160 minutes of processing, the small components triple in size to a value of 100 nm, the large components increase in their size to a value of 750 nm.

During this stage of processing, the small insoluble aggregates decrease, while the large components increase. This indicates a phase separation. It shows that a hydrophobic network, that binds only little amounts of water in the dense system is present next to a large hydrophilic network, that stores the water and potentially also the ions. This is also indicated by the LM-images obtained by Vollmer, Kieferle, Youssef, et al. (2021), shown in section 2 of this work. Areas of lower protein density next to areas with high protein density became present. In a follow up study (Vollmer, Kieferle, Pusl, et al. (2021)), the phase separation could not be seen, however the samples lacked a first exponential increase in apparent viscosity. The samples were processed with 25% more mass so it is thinkable that

the samples did not reach yet a critical number of particle-particle interactions that could initiate the phase separation, since at later stages of processing, the dense protein network, which is suspected to be the hydrophobic network in this work, became apparent. The strong display of phase separation in Vollmer, Kieferle, Youssef, et al. (2021) can be due to the low processing speed and lower mass that was processed. By processing the samples in that way, the growth of particles was not hindered and thus the pressure on the matrix to form aggregates from those aggregates was enhanced. This was done to show the suspected hydrophilic network next to the hydrophobic network, since it was suspected, that higher mixing speed could also lead to higher mixing of the *in-situ* separated phases and therefore to not display the phenomena of overcreaming, as it was discussed in Lee et al. (2003).

#### 5.4 Summary and Outlook

For the investigated particle sizes in the cream phase it can be concluded, that casein doesn't act as a strong emulsifier when used in a model processed cheese system without other surfactants. It binds the fat into smaller units, however not as pronounced as when, for example, whey proteins are present to emulsify the fat phase. This effect has been shown in processed cheese systems, especially by Lenze et al. (2019) and Röck (2010). The stabilization of fat during heat treatment of milk has been studied extensively by Dumpler (2018) and showed various stabilization mechanisms where the interaction of beta-lactoglobulin or whey proteins in general and caseins or the casein micelle, respectively, affected the stability of the systems.

The particle sizes of the cream showed, that the fine emulsion is formed at later processing stages. When considering the flexibility of larger fatglobules compared to the rigidity of smaller fat particles (Dickinson (2012)), the course of the measured apparent viscosity can be explained. At the end and after first log phase, the fat globule sizes increase, as well as the particle sizes in the pellet. This indicates, that the plateau phase is defined by aggregation of the molecules in the bulk to a larger network, whereby the fat size increases which keeps the elasticity in the system, hence no increase in apparent viscosity. During the second exponential phase, these newly formed structures in the bulk bind and emulsify the fat phase, structures that are too large break into smaller subunits by the pressure the system puts on itself. These fragmented aggregates, however are also hydrophobic in nature, hence the fat is also stabilized by the fragments of the hydrophobic aggregates.

This is also supported by the fact, that in the hydrophobic or insoluble phases of the system, the particle sizes shrink, while in the soluble or serum phase, the particle sizes increase during processing. This can be explained by the formation of small hydrophobic particles that form larger networks,

next to hydrophilic aggregates that tend to bind more and more amounts of water and probably also the ions in the system. This process later leads to phase separation of the matrix.

In sum, the particle sizes and distribution are in accordance with the findings of Vollmer, Kieferle, Youssef, et al. (2021), Lenze et al. (2019) and the data presented so far. It can be concluded, that two different phases of structure formation occur during the processing of model processed cheeses. Also, the particle sizes in the investigated pellet indicate the formation of a separated casein network out of larger and smaller substructures. It is further to be determined, if the hydrophobic network is a product of the high protein concentration or the processing condition, i.e agitation ( $v$ ) and high Temperature.

## 6 Colloidal aggregation of rennet casein under the influence of shear, heat and emulsifying salts

### 6.1 Introduction

Caseins are flexible proteinogenic molecules which show a wide range of aggregation behaviour in response to their environment or treatment. Also, they are bioactive molecules which can carry minerals due to post-translational modification of the serine groups with phosphate. Their bioactivity or function as a potential carrier is not limited to ions; since they can perform hydrophilic as well as hydrophobic interactions with itself and other molecules (Casanova et al. (2021)). Therefore the aggregation mechanisms that lead to the formation of the processed cheese structure investigated within this study can be of versatile nature. The aggregation of casein, however, seems to be the reason for the gelation of the model system in cold state.

In food systems like processed cheese, gelation of the matrix occurs due to the heat set gelation of the casein (micelles). Nicolai and Chassenieux (2021) recently reviewed the gelation of caseins by heat and concluded that gelation of casein micelles is hindered under the addition of calcium chelating agents. The structure, stability and reaction properties of the casein micelle is mainly defined by the interaction of the protein moieties in the micelle with the CCP (Gaucheron (2011)). The aggregation phenomena resulting from casein in (partly) native state are also steered by their initial degree of mineralization. It could be shown that demineralization of native micelles promotes the formation of hydrophobic aggregates (Nogueira et al. (2020)). Since the structure formation in processed cheese uses the demineralization of the casein micelle to form new structures, it can be assumed that the protein-protein interactions coming from the free caseins from the demineralized micelle are also interacting to form hydrophobic aggregates.

From the compositional analysis in terms of particle size distribution and protein concentration of the processed cheese matrix alone, a conclusive pathway for the theorized aggregation to occur could not be given. Also, the creaming reaction was investigated so far in this work mainly in presence of a dispersed phase. Since Lee et al. (2003) already showed protein network formation in fat free gels, the threshold value for measureable protein aggregation in a processed cheese system can be measured by processing of a diluted casein solution with melting salts. The aim was to find substructures that might represent the building blocks or a representative model of such structures, that initiate a structure formation as seen in the TEM images of Vollmer, Kieferle, Youssef, et al. (2021). To achieve this, solutions of low concentrations (1% and 3% casein) were processed with a

respective aliquot of emulsifying salts, in order to model the special environment in the bulk phase at a molecular or nano scale.

Also, as it was concluded in the previous section, this part of the study should determine, if the aggregation phenomena seen in the model matrix so far are occurring due to the high concentration of the proteins in the system or the agitation ( $v$ ) which forces collision of the particles.

## 6.2 Material and Methods

For further analysis of the swelling behaviour, casein solutions of specific concentrations, with and without melting salts, were investigated. The solutions were prepared with rennet casein. Protein contents of 1% and 3% were investigated. For this purpose, the protein powder was dissolved in the required concentration in deionised water and then stored at 4°C Under constant stirring for at least 12 hours. Depending on the test, the melting salts listed above were added in quantities adapted to the protein quantity of the model cheese samples. After 12-hours of swelling, 35 grams of the casein solution were measured in a Rheometer (Anton Paar,MCR 302, Austria) using a rotating vane and cup geometry and a shear rate of 50/s, to simulate the processes in the custom made processing cup. The process was started and stopped at the desired process time. Afterwards, the samples were transferred into a 50ml purification tube and stored in the 4°C refrigeration until further analysis. For every process time that was analyzed (0, 20, 40, 60, 80, 100, 120, 140, 160 and 180 minutes) a new casein solution was processed, so as to have the same amount of reacting mass in every process (analogue to the sampling of the processed cheese as in section 3 and 4 of this work). Samples were processed in duplicate and measured as a duplicate of a duplicate ( $N=4$ ).

### Particle Size Analysis

The expected particle sizes were expected to be at nano-scale. Therefore, ultra centrifugation at 70.000g was applied to samples. The supernatants of the samples were then filtered at a cutoff of 2500 nm using a MERCK syringe filter. A one time use polymeric measuring cuvette for a Malvern Zetasizer was cleared from any dust using pressured air. The processed samples were filtered directly into the measuring cuvette to avoid contamination of the samples with dust particles. The particles were then measured at a Malvern Zetasizer, each sample was measured ten times over several minutes. The so obtained data was processed using the R programming environment. Component analysis for multimodal distribution was performed, using the “nomalmixEM” algorithm as described in the previous section.

### HPLC measurements

The supernatants of the processed samples after ultra centrifugation at 70.000g were analyzed using the HPLC procedure as described in section 4. To obtain a suitable concentration, the samples were first diluted 1:1 (v/v) with deionised water. Afterwards, 200 microl of sample was mixed with 800 microl of guanidine buffer (see chapter 4), filtered into a vial and measured with RP-HPLC according to the method displayed in Dumpler (2018).

### 6.3 Results and Discussion

Fitting of the particle sizes was performed as it was described in section 5 of this work. First, an overview plot for the measured particle sizes was prepared, with a colour scale representing the processing times. Afterwards, the particle sizes were modeled to obtain size and distribution for the single components.

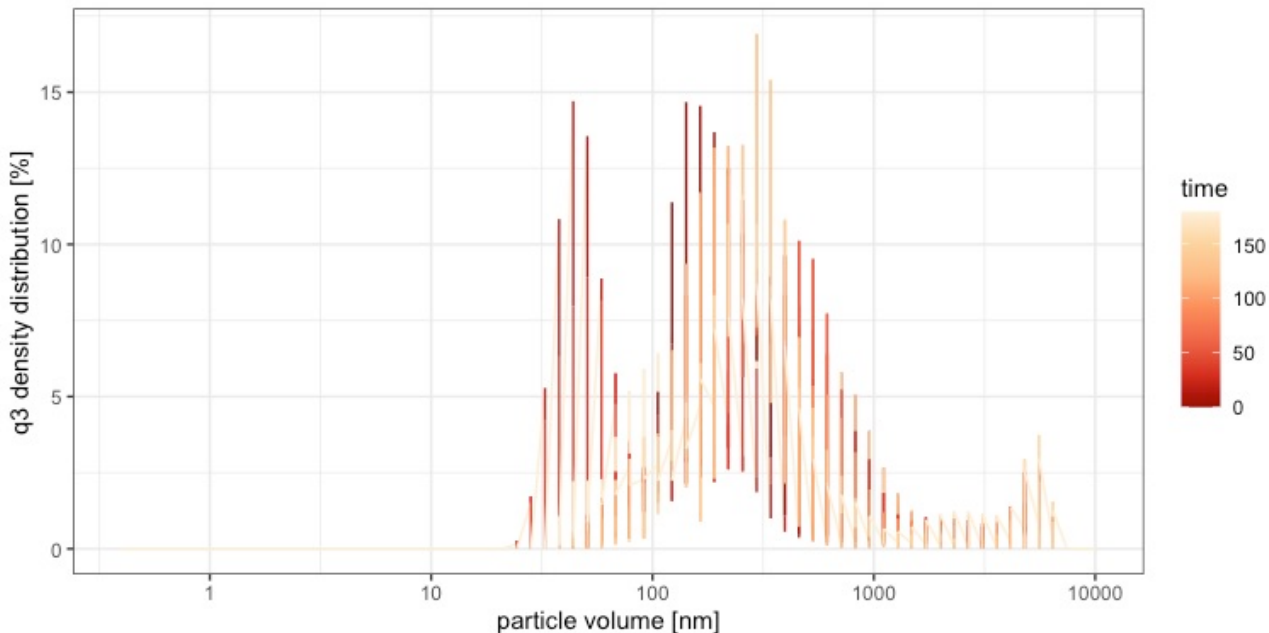


**Fig. 51.** Overview of measured particle size distribution in solutions made from 1% c(TP) casein, processed with melting salts, after ultracentrifugation (70.000g) and subsequent filtration (2500 nm): darker areas indicate shorter, lighter areas longer processing times. In-situ reaggregation after filtration at 4000 nm

Fig.51 displays no indication for seed formation apparent, even distribution throughout. Tendency for larger aggregates at later processing times indicates a tendency to reaggregate, since the samples have undergone filtration before measurement. A conclusion therefrom is, that at later processing times, highly active or ‘reactive monomers’ are present, that tend to aggregate, especially in the ionically charged environment present here. The high tendency for demineralized caseins to show hydrophobic aggregation was also shown in Nogueira et al. (2020).

The findings of Vollmer, Kieferle, Youssef, et al. (2021) and Vollmer, Kieferle, Pusl, et al. (2021) indicate hydrophobic aggregation as well. However in an environment with a total protein concentration TP of 1% casein, the monomers might not reach a certain number to form singular, potentially small structures, that could be identified as seeds. In an environment with a protein concentration of 3% casein, however, such small structures are visible (Fig.52).

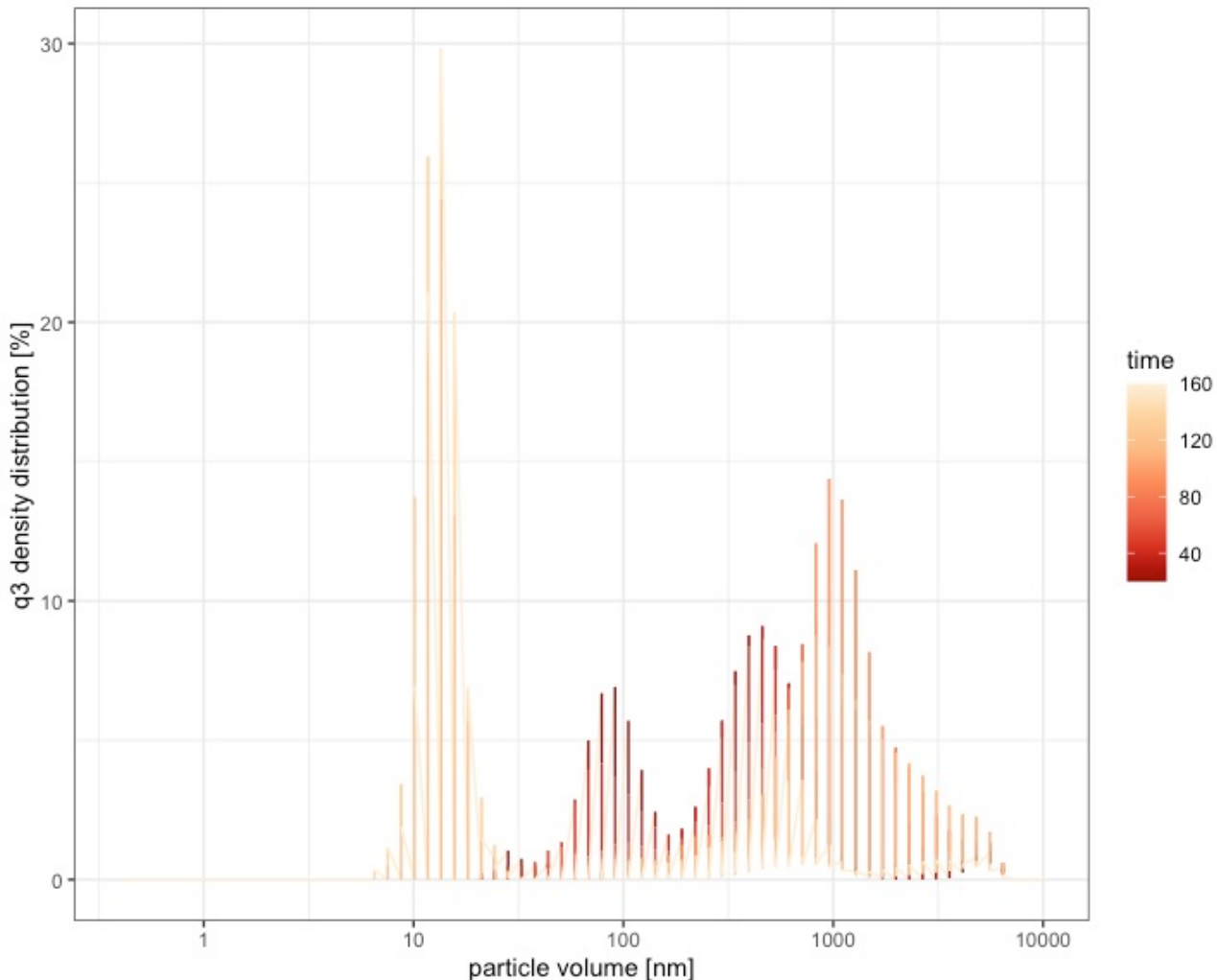


**Fig. 52.** Overview of measured particle size distribution in solutions made from 3% c(TP) casein, processed with melting salts, after ultracentrifugation (70.000g) and subsequent filtration (2500 nm): darker areas indicate shorter, lighter areas longer processing times. Strong indication for seed development at later processing stages visible at 10 nm

As already seen in 1% TP solutions, the 3% TP solutions also showed reaggregation phenomena after longer processing times. Even more so, a critical concentration seems to be reached, to form a substructure on their own. Also, a certain incubation time seems to be needed to “kick-start” the aggregation by reaching a critical concentration of primary aggregates. The critical concentration can also be seen in terms of a critical fractal dimension, that was reported elsewhere (Lazzari et al.

(2016)) for colloidal aggregation. It has to be considered that a polydisperse matrix is present. Hence, hydrophobic particles with a small radius of gyration might appear next to large molecules that are hydrated.

Vollmer, Kieferle, Youssef, et al. (2021) reported the formation of dense aggregates next to amorphous structures that later were again separated into smaller subunits. At the final processing stage of 415 minutes, one of these subunits are characterized as needles, displaying roughly the same length ( $\sim 14$  nm) as the small component found after 140 minutes of processing in the casein solution. The nature of the detected fibrils was discussed, but no conclusive answer could be given.

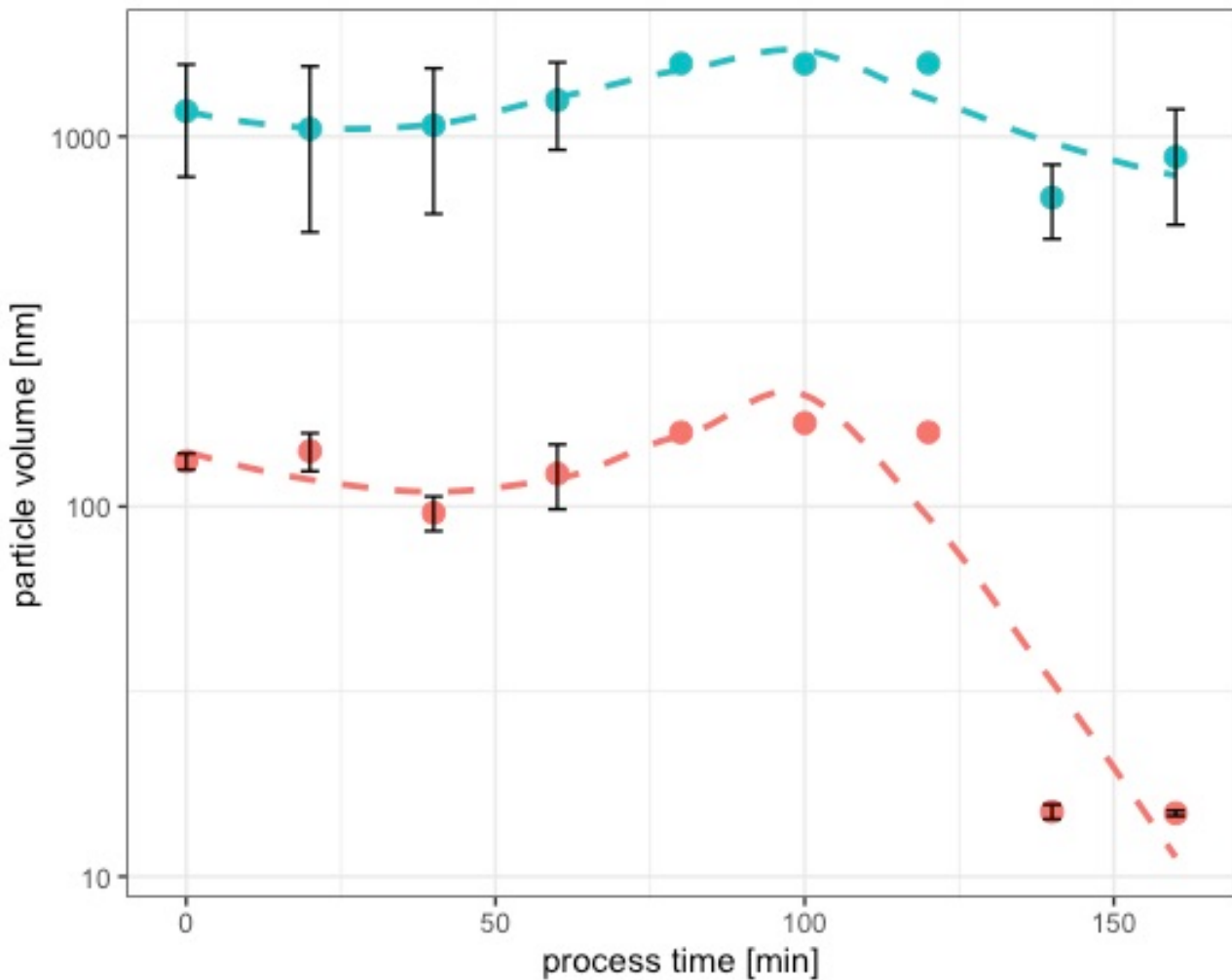


**Fig. 53.** Development of modelled particle volume, plotted over processing time; small particles indicated by red sphere, large particles indicated by blue sphere with an applied 'loess fit' (y x, dashed line). Data shows formation of a very small aggregate of 14nm after 140 min of incubation

The modeled distribution (Fix.53) represents the experimental data well. A two component model ( $k=2$ ) seems sufficient and prevents over-fitting, in particular when the medium sized aggregates at  $\sim 150$  nm seem to disappear after the formation of the small aggregates. In addition, the large

particles seem to decrease as well, while the small particles in between 140 and 160 minutes of processing don't decrease in size any further. The modelled density distributions revealed that up to 80 - 100 minutes of processing, the distribution of small to large components was about 50:50 (%). At late processing times, this distribution changes to 30:70 small to large components. This suggests, that the small components are removed from the soluble phase, by participating in hydrophobic aggregation, since the samples were treated with ultracentrifugation. What also applies here, is the theory, that up to 120 minutes of processing, we see hydrated particles, and the measured particle volume of ~100 nm shows their radius of gyration, i.e. the hydrate shell. The strong decrease to a tenth of the initial particle size suggests the loss of the hydrate shell from the measured particle, which speaks again for hydrophobic aggregation, as well as for a reformation of the system, since apparently, the charged parts of the small particles are turned inward as to not bind large amounts of water.

It can be hypothesized, especially in combination with the measured protein concentration in the supernatent after ultra centrifugation (Fig.55), that the aggregates of > 100 nm are soluble, strongly hydrated dimers of alphaS1 and beta casein. The formation of the kappa casein seed, which is hydrophobic and therefore very small in size, happens simultaneously. In fact, the modellation of a three component model (data not shown) suggested this, since the density distribution of the smallest component (~14 nm in size) rose at the end of the process from 13% to 36%.

The density of the small component increases at the end, which is probably due to reaggregation of the reactive seed into larger structures, hypothetically similar or comparable to the small structures identified as needles in Vollmer, Kieferle, Youssef, et al. (2021).

This theory can be supported by the additional data obtained from the system of 3% TP processed with emulsifying salts. The flow-curve obtained by the set-up in the processing in a rheometer shows a gradual increase, beginning at 75 minutes, followed by a steep increase with a maximum at ~135 minutes and a decrease after 140 minutes with the tendency to remain at higher plateau level after 160 minutes of processing (Fig.54. The flow curve displayed here resembles the flow curve of a fat-free model processed cheese system as in Lee et al. (2003). It was theorized, that the proteins form a network, which leads to a peak in viscosity, before the network fragmentizes or collapses. This seems to be displayed here as well.

Fig.55 shows the composition of the suspected aggregates. Between 100 and 120 minutes of processing, kappa casein decreases to its final value. Also, an increase in beta casein as well as a decrease in alphaS1 casein is visible in the supernatant at this stage of processing. Up to this stage of

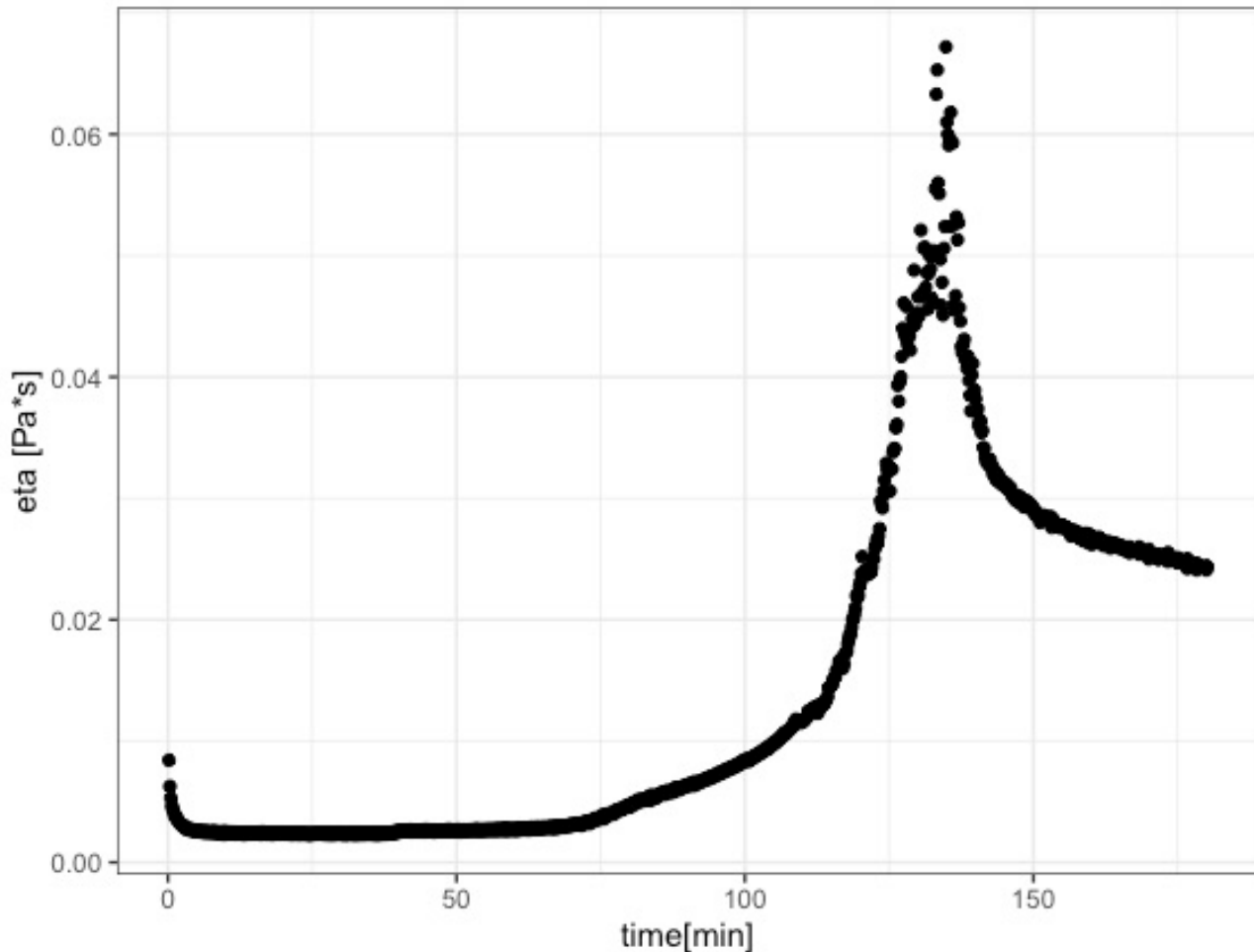


**Fig. 54.** Flow curve of a 3 TP casein solution processed with a vane blade geometry

processing, respectively between 50 and 100 minutes, alphaS1 and beta casein increased in the supernatant in the same fashion, suggesting the formation of a hydrophilic aggregate of  $\sim 140$  nm in size (of gyration). After 120 minutes beta casein also decreases significantly up to the end of the process. Also, alphaS1 casein decreases further. No change in concentration of the alphaS2 casein in the supernatant was detected, which suggests, that alphaS2 casein is not participating in the formation of a hydrophobic network, at least not in the same degree as the other caseins.

In accordance with the appearance of insoluble visibly large aggregates at the stirrer of the rheometer (Fig.56) after 140 minutes of processing it can be stated, that a large insoluble aggregate was formed out of kappa casein, alphaS1 casein and beta casein. The slight increase in beta casein prior to the decrease at the end might be due to a release from an hydrophilic aggregate, which those two caseins readily form (Lucey and Horne (2018)).

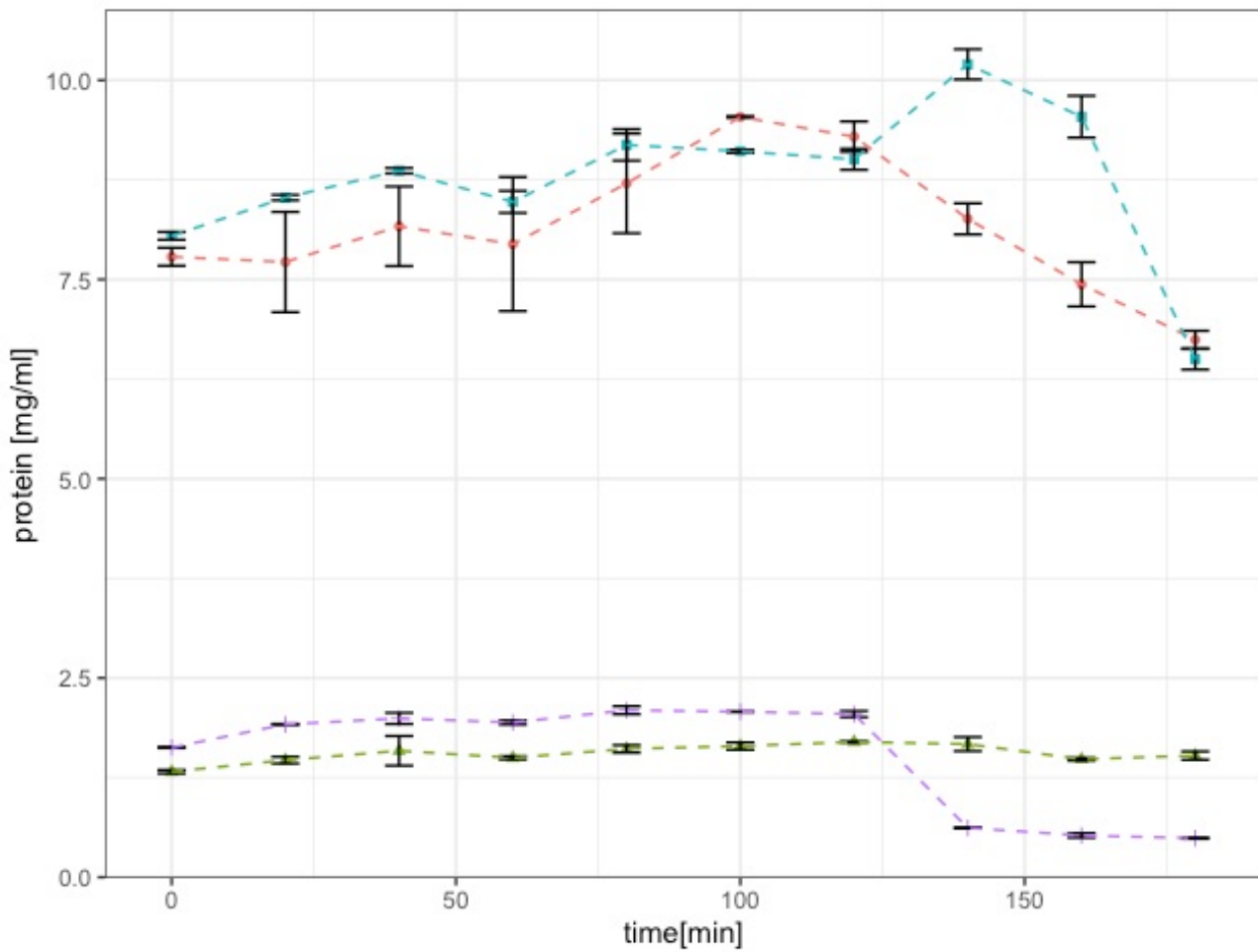


**Fig. 55.** Development of measured particle concentration in supernatant of samples made from 3% TP, processed with emulsifying salts; beta casein (blue), alphaS1 casein (red), kappa casein (violet) and alphaS2 casein (green)

#### 6.4 Summary and Outlook

One aim of this study was to explore the theory, of aggregation phenomena on a colloidal level could reveal structures that are also present in the dense matrix, due to the same ionic environment and strength.

It could be seen by compositional analysis with RP-HPLC, that the soluble structures in the colloidal solution first increase in concentration and are made up of a chimera of alphaS1 and beta casein. This increase only lasts until a processing time of 120 minutes: after, a decrease in alphaS1 and kappa casein can be seen, after 140 minutes of processing, beta casein also decreases. This suggests an insoluble (i.e. hydrophobic) aggregation of those three caseins in a step wise manner.

In order to form hydrophobic aggregates without any degree of covalent interaction, one must consider the possible connection points for this type of interactions in the respective casein. In



**Fig. 56.** Visible large flocculated aggregate at the stirrer of the vane geometry after 140 minutes of processing

section 1 of this work, a computed hydrophobic cluster analysis plot as it was also shown in Lucey and Horne (2018), was performed. Under the use of this, a possible alignment of beta and alphaS1 casein might become possible, when the two centers of phosphorylation as marked specifically in Fig.7 in section 1 of this work, are screened or reduced in charge in way that they can allow close range between the particles. Another possibility is, that alphaS1 and beta casein are associated at only specific hydrophobic binding points via hydrophobic interaction into for example circular structures. Fibrils from other molecules like *beta-lactoglobulin* are known to have translucent properties in solution. The aggregates detected in this study were opaque. Due to the turbidity of the aggregate but its ordered particulate structure it might be theorized, that the initial kappa casein fibrils and the amorphous or linear aggregate from alphaS2 and beta casein are hydrophobically associated in a turbular way, therefor the lacking translucence.

This suggests a mechanism for the hydrophobic aggregation occurring here. The mechanism takes into account, that kappa casein will be the first to get released from its CCP, since it sits on the outside of the micelle. Hence, the formation of the primary aggregate, so to say a kappa casein seed that might

also be seen in the needles in Vollmer, Kieferle, Youssef, et al. (2021) after 415 minutes of processing (which then become visible due to fragmentation of the network), becomes plausible. Nogueira et al. (2020) showed the aggregation mechanisms of demineralized casein micelles next to native micelles upon rehydration. It could be shown that the partly demineralized casein micelles had a higher resistance to stirring than native micelles. It was found that this was due to exposition of reactive groups and increase in the tryptophan hydrophobicity, which then led to hydrophobic aggregation. In addition it was found that removing 15% of the CCP led to a larger pore size of the casein micelle.

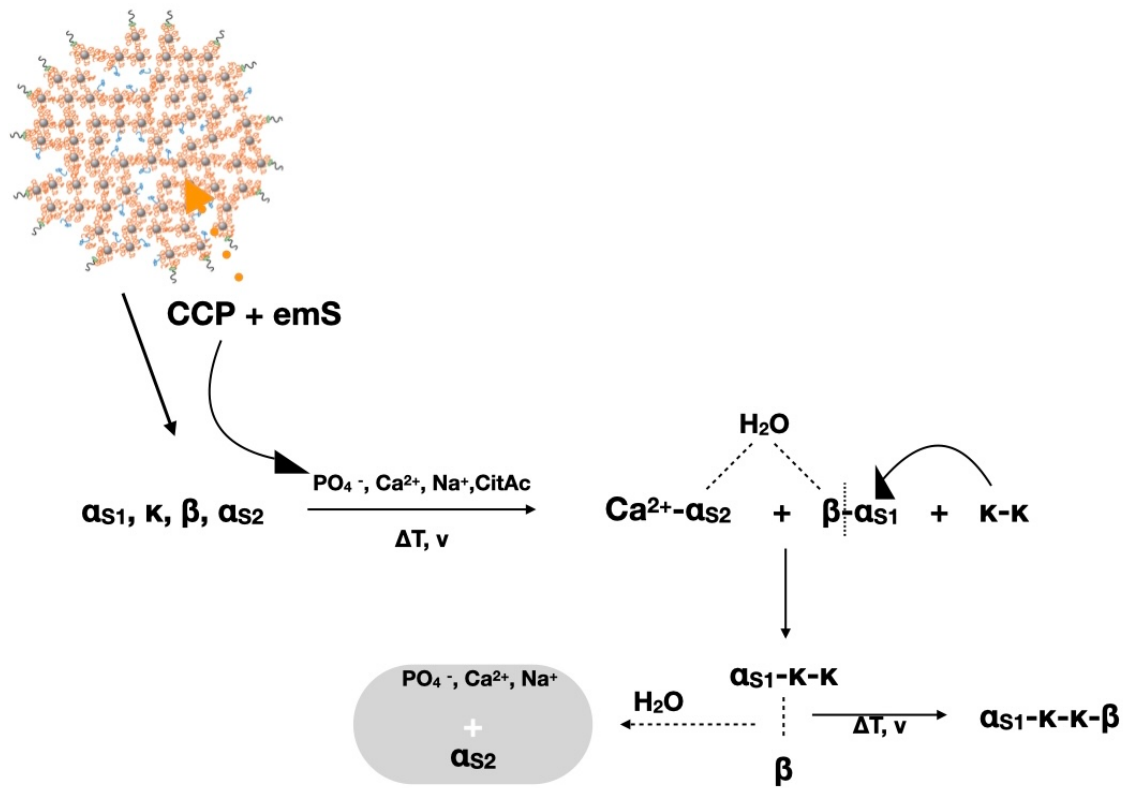


**Fig. 57.** Proposed reaction mechanism for hydrophobic aggregation and consequential phase separation: full lines are insoluble aggregation or ionic-bond, dashed lines indicate association. Grey box indicates phase separation.

The reaction mechanism presented in Fig.57 shows the primary formation of a (possibly irreversible) kappa casein hydrophobic seed next to a hydrophilic (and reversible) aggregate out of alphaS1 and beta casein. In the next step of the reaction (at 100 minutes of processing), the hydrophilic aggregate dissociates due to a suggested “hydrophobic pull,” maybe comparable to a dipole inducing +I or -I effect that occurs in organic molecules on a substituted carbon atom. Also this pull could be depletion from co solvent (i.e. the ions) exclusion from one aggregate. An intermediate hydrophobic aggregate is formed out of the already aggregated kappa casein and the newly released alphaS1 casein. This intermediate further aggregates with beta casein (after 140 minutes of processing) to

form the growing hydrophobic network. It is suggested, that the network growth is limited in the dense processed cheese system, due to the shear pressure the dense matrix applies on itself, which then leads to probably irreversible fragmentation of the hydrophobic aggregate made out of kappa, alphaS1 and beta casein.

Comparing the abundance of visible aggregates in the 1% casein solutions, as well as the small component of ~14 nm, it is possible that either a fractal dimension of aggregates is not (yet) reached, to initiate this aggregation mechanism. Since the solutions are constantly stirred during heating, it can also be the case that the incubation time for visible aggregation to occur in a 1% TP casein solution must be longer than the tested times (maximum of 180 minutes) within this study.

The phenomena seen in this study can be attributed to the aggregation phenomena seen in processed cheese. The measured protein concentrations of the pellet and cream phase in section 4 of this work showed an increase in those protein moieties, that decreased in the supernatant of this study. In combination with the imaging data obtained by Vollmer, Kieferle, Youssef, et al. (2021) and Vollmer, Kieferle, Pusl, et al. (2021) it can be concluded that the formation of the fine casein network is primarily formed by initially sized or aggregated seeds that further promote a hydrophobic aggregation process that is irreversible and happens due to a seeding effect that was induced by reaching a critical concentration of a primary aggregate. In conclusion with these works where a casein fibrilization in the equal model processed cheese matrix was detected, it can be theorized, that in this study the primary aggregate, or “seed” for fibrilazation is displayed, as well as the amorphous large aggregate that was found within TEM analysis. A final clarification could be done by TEM imaging of the colloidal aggregate and comparison to the already obtained images.

Regarding the rework effect as described in detail by Lenze et al. (2019) and others, it can be theorized, that the formation of a hydrophobic aggregate, mainly comprising of alphaS1 and beta casein is formed at late processing stages. Adding such material to a “fresh” matrix then includes the primary aggregate. Since the emulsification of the fat into fine particles is enhanced during these stages of processing as well, it can be stated, that those structures are also better at emulsifying fat, than otherwise aggregated casein particles or monomers therein. This is also in conclusion with the theory of a hydrophobic particle.

## 7 Upscaling and NMR relaxometry of model process cheese

### 7.1 Introduction

The basis of nuclear magnetic resonance spectroscopy (NMR) is the fact that atoms have magnetic fields characteristics. Subatomic particles, such as neutrons, electrons, and protons, revolve around their axis, which in particle physics is called spin. Atomic nuclei with an odd number of protons, e.g.,  $^1\text{H}$ , have a total spin ( $I$ ). Atoms with an even number of protons, e.g.,  $\text{C}$ , have no total spin due to the pairing of the protons. A parallel orientation of the magnetic moment results in the energetically preferred orientation of it. The difference in occupation that occurs creates a magnetisation vector which is the basis of a successful NMR measurement (Schuh and Chan (1982)).

The NMR measurements were used to investigate the mobile water phase of the processed cheese system at different process times. The interpretation of the relaxation times can determine the chemical and physical, bound or unbound state of  $^1\text{H}$  protons and thus of water.  $^1\text{H}$  nuclei from immobilised water have considerably shorter relaxation times than nuclei from the mobile water phase. This can be attributed to the interactions of the immobile protons with their environment, which are much more frequent than those of the mobile phase of the system. By measuring the decaying signal intensity over the relaxation time, a spectrum of the different water phases in the melted cheese system was obtained (Hinrichs, Goetz, et al. (2004)). Studies on the water-binding capacity of protein microparticles using time-domain nuclear magnetic resonance were performed also by Peters et al. (2016). Water immobilization by whey protein concentrate was investigated by NMR in Hinrichs, Götz, et al. (2004).

NMR measurements on food and model systems thereof, especially low-resolution experiments on cheese, are a common practice (Gotz et al. (2004)). Chen and Liu (2012) investigated the effect of different types and amounts of emulsifying salts on the chemical and physical properties of processed cheese samples. Furthermore, signal components were also attributed to the fat protons. N. Noronha, Duggan, Ziegler, O'Riordan, et al. (2008) identified four stages of hydration and/or matrix development in the preparation of imitation cheese made from casein. Two stages could be attributed to hydrophilic interactions of caseins with the bulk as well as two later stages, where the interactions of proteins with fat dominated the matrix formation. Hinrichs, Bulca, and Kulozik (2007) investigated changes in water mobility during renneting or acidification of solutions from casein micelles, using low resolution NMR. Here, a method was presented to fit the signal to relaxation times of differently bound fractions of water - immobile, weakly mobile, mobile and very mobile

protons from water were detected. In Khanal et al. (2018), different low fat cheddar cheeses were investigated during ripening. Using low-field NMR, different stages of water mobility could be identified in samples containing alginate as additive. El-Bakry et al. (2011) investigated a processed cheese matrix at multiple subsequent steps of preparation, besides other methods, using a T2 relaxation NMR protocol. The different sample stages showed a multi staged structure formation from a liquid dispersion to a cohesive mass.

Further use of time-domain or low-resolution NMR measurements can be found as well in composite science. Besghini, Mauri, and Simonutti (2019) present NMR measurements for the investigation of polymerization or crystallization kinetics in rubber. Gelation and sol-gel phase transition phenomena in non-biogenic, organic materials like Poloxamers are investigated via T2 relaxation by Shaikhullina et al. (2020). Testamanti and Rezaee (2019) gives use of low-field or low-resolution magnetic resonance for the evaluation of reservoirs for the petroleum industry and is especially focussed on the provision of a regularization algorithm for the determination of T2 relaxation spectra from shells. Determination of the T2 distribution from the decaying signal can be obtained by the CONTIN Computer Program, where an inverse Laplace transformation of the signal is performed, in order to find the T2 distribution (Moody and Xia (2004), Kenneth P. Whittall (1996), Borgia, Brown, and Fantazzini (1998)). Another possibility to obtain the relaxation and diffusion distributions in two dimensions is the use of the Fredholm integral equation of the first kind (Mitchell, Chandrasekera, and Gladden (2012)). However, this can lead to a regularization bias, since the inverse Laplace transform represents an ill-posed problem (Berman et al. (2013), Giovannelli and Idier (2015)), especially for a multi-component environment as it is the case in processed-cheese samples. Fitting the envelope curve of the exponential decay with discrete parameters as in Hinrichs, Bulca, and Kulozik (2007) leads to unbiased T2 distributions, however only for the discrete parameters. Least-squares and linear programming algorithms can help to reduce the non-uniqueness of the fitted solution, meaning that the fit is not constrained by initially given discrete parameters and can therefore represent the spectrum in a more accurate way (Kenneth P. Whittall and MacKay (1989)). Therefore a fitting function, using a non-linear least squares algorithm was programmed within the R programming language. First a parameter estimate for the fraction  $f$  of the polyexponential decay was applied, with a subsequent fit using the nls of the measured decay over the timespan, to determine the T2 relaxation also outside the given range as displayed in the starting values, as seen in the code snippet in section 5.2.3.

## 7.2 Material and Methods

### 7.2.1 Preparation of cheese samples

Composition of the cheese premix can be found in Chapter 3. Only samples from rennet casein were produced for the NMR measurements, since they appeared to deliver the most homogenous product samples. In order to speed up the analysis time, the model process cheese was processed in a 500g batch, the matrix was processed in a Vorwerk Thermomix processing machine. Samples were taken every five minutes and cooled at 4 C.

### 7.2.2 NMR measurement

The measurement was carried out in the sample tubes provided. The processed cheese sample was punched out with the open end of the sample tube and slightly compacted with a plastic rod to avoid air inclusions. The initial analysis was performed at 10°C using the NMR analyser mq20 minispec (Bruker Corporation , Billerica, USA). Each sample was measured in duplicate for different process times (0- 225 min, in 2.5 to 5 min steps), resulting in a total of 132 measurements. Measurement parameters for the NMR experiment were adapted from Hinrichs, Bulca, and Kulozik (2007), which resulted in 20.000 measurement points per sample. The reason for this high number of sampling points was to ensure inclusion of possibly late relaxing proton fractions.

### 7.2.3 Curve-fitting

The envelope curve obtained by the decaying signal of the nuclear magnetic spins was fitted using the R Programming Environment. The curve was fitted using a non-linear least squares (NLS) algorithm, where the parameters were estimated in a two step fitting protocol (see code snippet and explanation below). Documentation of the mathematical basis for the used R code can be found in Borchers (2021).

## 7.3 Results and Discussion

### 7.3.1 T<sub>2</sub> relaxation in model processed cheese

During the curve fitting process, an envelope curve of three exponential terms in the form of

$$y(k) = f1e^{-1/4k1^2t^2} + f2e^{-t/k2} + f3e^{-t/k3}$$

fitted all the obtained data best. This means that three different fractions of protons, which differ in their T2 relaxation time, could be detected. The amount or fractions  $f$  as fitted with formula xx for the measured relaxation signal for the samples was plotted over the process times of the samples (Fig.58).

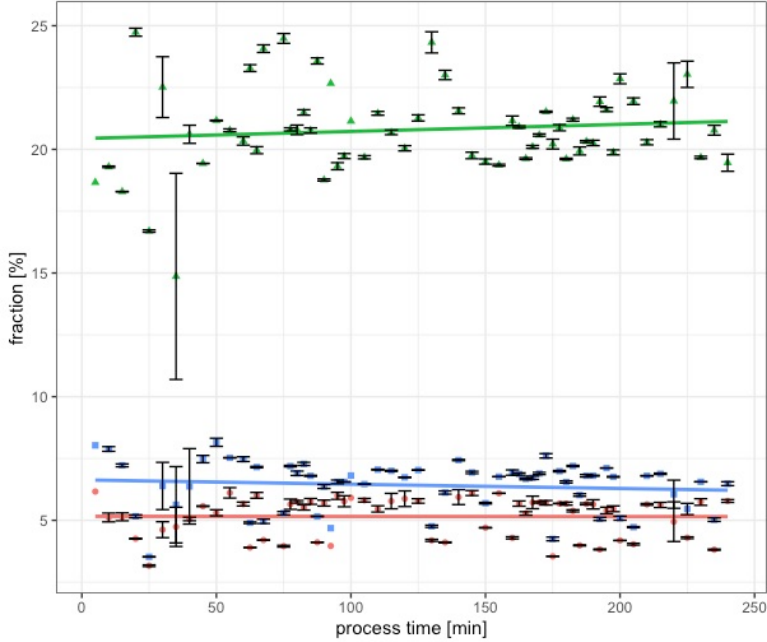


**Fig. 58.** Development of the fractions of T2 relaxation times of fatty phase (red) and mobile water phase (blue) with respective linear model fit: fraction of bound fat increases, while fraction of mobile water decreases.

The fraction of the immobile water phase was in the range as presented in Hinrichs, Bulca, and Kulozik (2007). The fraction of the mobile water phase however is far below the values for the respective phase from the adapted model data in Hinrichs. This seems reasonable, since the amount of mobile water is far lower in the present study, which is by design and due to the high dry matter. A fraction of T2 relaxation components is apparent in Fig.58 as indicated by the green colour, which wasn't detected in fat-free systems.

Fig.59 shows the development of T2 distributions for the detected fatty and mobile water-phase. In N. Noronha, Duggan, Ziegler, O'Riordan, et al. (2008), cheese prepared in a blade cooker was investigated using T2 relaxation. Three proton fractions were found after numeric inversion, with relaxation times of 15-20 ms, 60-80 ms and 350-500 ms. The three fractions were attributed to the protons of immobile water, fat, and moderately bound water, respectively. El-Bakry et al. (2011) analyzed the formation of a processed cheese matrix from a liquid dispersion that was formed to a cohesive mass using a Farinograph. The T2 relaxation times attributed to the protons of fat were between 80 and 120 ms, depending on the process time. An increase in T2 relaxation for the fat

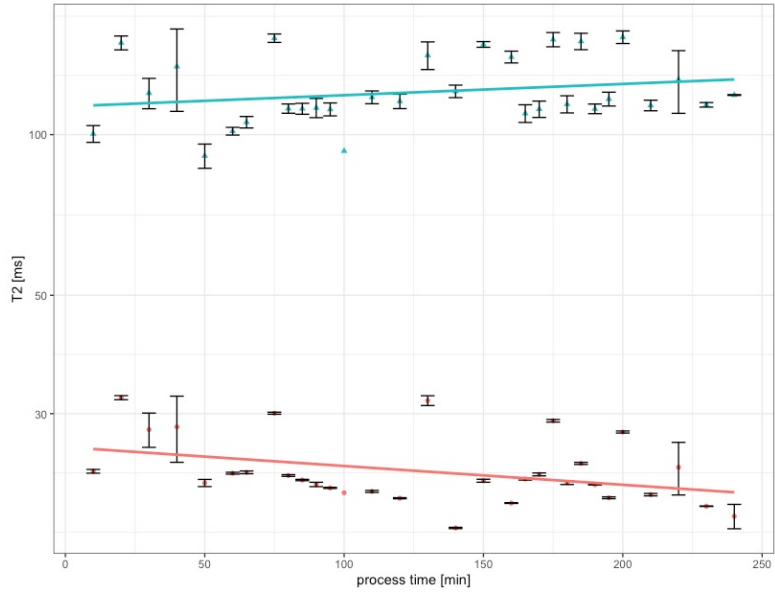


**Fig. 59.** Development of T2 relaxation times of fatty phase (red) and mobile water phase (blue) with respective linear model fit: Increase in water mobility and decrease of mobility of the fatty phase

protons was reported, followed by a decrease of fat T2 relaxation time. Hence a two step emulsification process was reported, next two a two step structure build up indicated by two peaks in the Farinograph. The fraction that can be attributed to the fat phase in this study is the one obtaining between 15 and 25% as indicated in Fig.xx and a T2 relaxation time of ~20 ms. The differing relaxation T2 relaxation times regarding the T2 relaxations displayed in Tablexx are due to differing NMR protocols, which are adapted towards the macro-scaled matrices. Since the matrix in this study was a fine dispersion and a fine emulsion after melting, the long-time measurement protocol of Hinrichs, Bulca, and Kulozik (2007) was chosen to display the changes on the investigated micro-scale.

The biggest fraction of the model cheese matrix is the dispersed phase, as represented by Fig.58. Also the volume fraction of the fatty phase increases, which is consistent with the data obtained by Vollmer, Kieferle, Youssef, et al. (2021) and chapters 4 and 5 of the present study. Also, the amount of mobile water protons decreases, which is also in conclusion with previous findings.

Analogous to the distribution of the relaxation times (Fig.59), the relaxation time for the watery phase shows an overall increase over the process time, whereas the the T2 relaxation time for the fatty phase decreases. A decrease in T2 relaxation time indicates a stronger interaction of the magnetized protons with their environment, here the gel matrix. An increase in T2 relaxation represents a lesser interaction. Hence it can be concluded, that over the course of processing of the model processed cheese matrix, fat gets bound more tightly by the matrix, whereas mobile water is

released. The T2 relaxation time data was analyzed using a linear model, accuracy of the fit was determined by an  $R^2$  of 0.93.

### 7.3.2 Protein concentration in the serum phase

The protein concentration in the serum phase was measured after dilution and centrifugation of the matrix and subsequent centrifugation of the liquid components at 500g. The by RP-HPLC measured protein concentrations were compared to the concentrations of the serum.

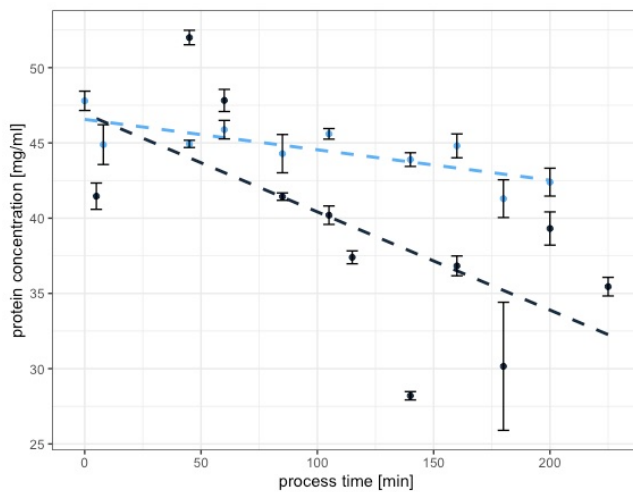


**Fig. 60.** Development of measured protein concentration in the centrifugally separated serum phase (500g) over the course of processing (black), with a linear fit (dashed line), compared to the development of the total protein concentration in the serum phase processed in a batch process in a rheometer (see chapter 3) and centrifugally separated at 6000g (blue, see chapter 4)

Fig.60 shows the development of the total protein concentration of the processed cheese matrix used for the NMR measurements, compared to the total protein concentration in the serum as presented in chapter 3. The difference in the measured samples lies in the centrifugational separation speed (6000g or 500g respectively) as well as in the mode of preparation (batch, or continuous upscaled process). Overall the protein concentrations measured in both preparation modi are in the same range of ~30-50 mg/ml. Also, both measurements show a general trend of a decreasing concentration of soluble protein during processing. The initial increase in the protein concentration can be explained by the dissociation of the casein micelle, induced by the melting salts. After reaching a maximum concentration, the amount of protein detectable in the serum phase decreases up to a processing time of ~145 minutes to a minimum value of ~28mg/ml. The increase in protein concentration towards the end of the continuous process can be explained by the appearance of reactive aggregates which are already associated but are not separable by the relatively low G-Force of 500g.

### 7.3.3 Particle size distribution in the serum phase of the upscaled, continuous process

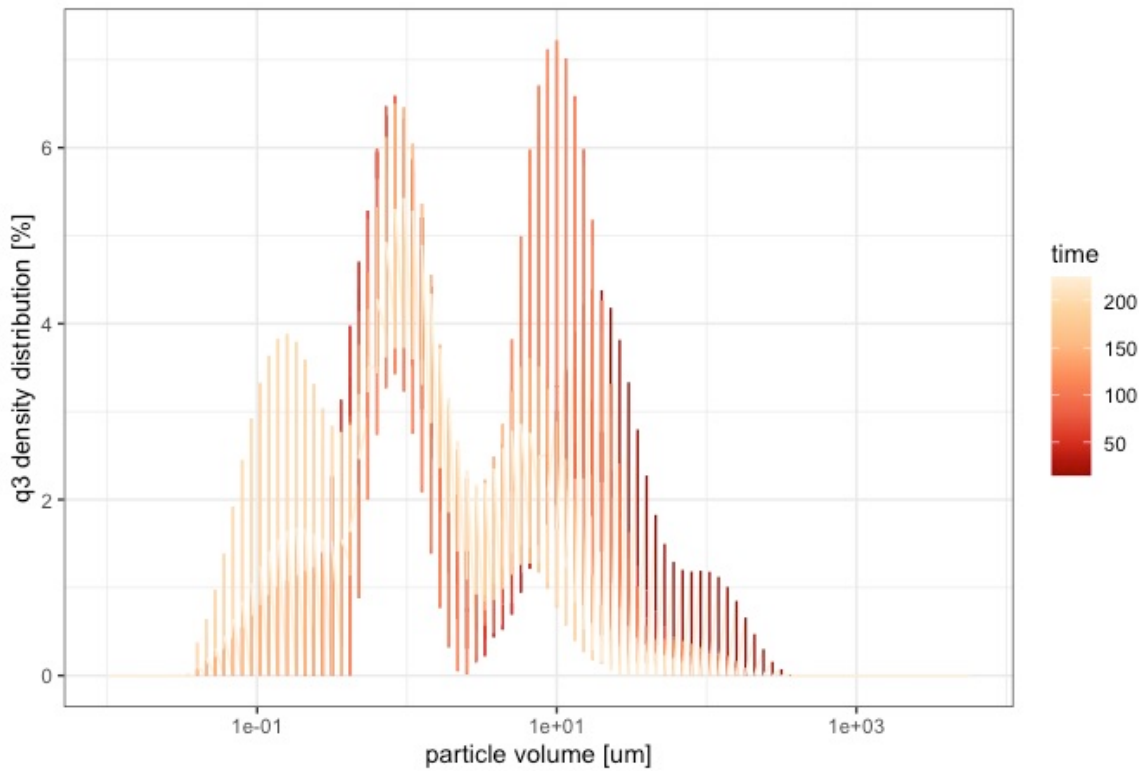


**Fig. 61.** Overview of particle size distribution of centrifugally (500g) separated cream phase, obtained from the continuous, upscaled process; darker colours indicate shorter, lighter colours indicate longer processing times.

Fig.61 gives an overview of the particle size distribution measured in the serum phase as obtained by the protocol first described in section 4 of this work. The general trend was again, that smaller particles were apparent at later processing stages. To get a deeper insight towards the dynamic process, the modellation protocol for bimodal particle size distributions as first described in section 5 was applied towards the raw measurement data.

In Fig.62 the development of the measured and subsequently modeled particle sizes is displayed over the process time. As already found in the pellet of the model processed cheese, and in the 3% TP solutions prepared from rennet casein with the respective aliquot of emulsifying salts as displayed in section 6. The development of particle sizes here differed however with the particle sizes from the serum after ultracentrifugation. This can be explained by the applied G-force: 500g to 70.000g seems a reasonable explanation as to why the development of particle size distribution is reversed in the respective “soluble” phases. It can be theorized, that 70.000g is a strong enough force, to separate the mainly hydrophobic, from the mainly hydrophilic structures.

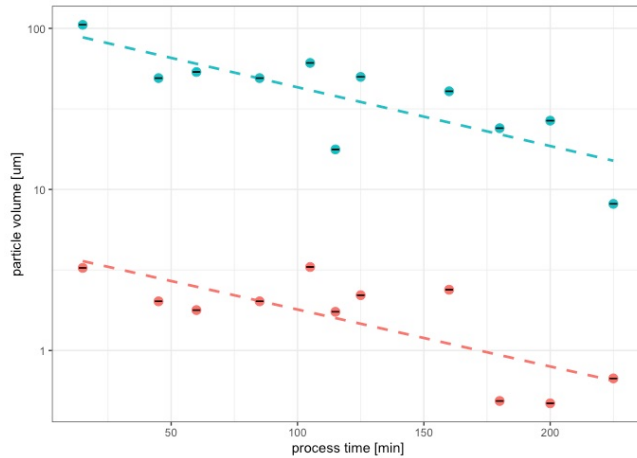


**Fig. 62.** Development of modelled particle volume in the serum phase obtained by the centrifugation protocol described in section 4 from samples prepared for NMR measurements over process time: Decrease in small (red) and large component (blue) detectable, with a steep decrease of the small particles at the end of processing (180 - 200 minutes)

### 7.3.4 "Offline" Rheology of continuous process

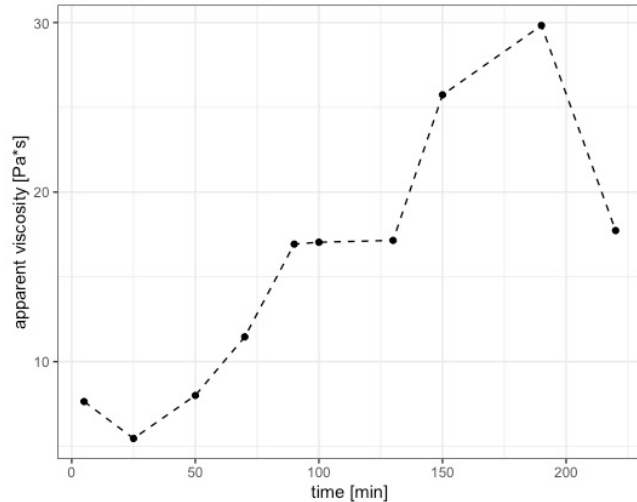


**Fig. 63.** Rheological profile of the samples prepared for NMR measurements: measured mean viscosity of the samples processed continuously in the Thermomix, measured with a cone-plate geometry. Data from single measurements of the samples was mean centered before plotting.

The measured apparent viscosity  $\eta$  as displayed in Fig.63 was measured after sampling an aliquot from the continuous process and measuring it with a cone-plate geometry at a shear rate of  $50 \text{ s}^{-1}$  and  $85^\circ\text{C}$ . Comparing the viscosity of the upscaled process, the viscosity is higher in range but follows a step-wise structure build-up, as reported before here and elsewhere. The decrease in the last measurement point at 225 min can be attributed to high fluctuations in the measurement and indicate an adherent, string forming or particulate, but however more dense matrix and not a

liquidation or any of the such, as discussed extensively in section 3 and elsewhere in this work.

## 7.4 Conclusion and Outlook

The relative comparison of T2 relaxation times for different proton fractions in model processed cheese systems during manufacture or processing showed to be a good protocol for measuring the different stages of formation in macroscopic scaled systems as displayed in N. Noronha, Duggan, Ziegler, O’Riordan, et al. (2008) and El-Bakry et al. (2011). This study showed, that with an adapted NMR protocol, the changes in microstructure could be detected following the detailed processing of a model processed cheese matrix, that was targeted to investigate casein interactions. In analogy with the studies mentioned above, a multi-step structure formation was detectable, comprising a restructuring of the mobile water phase, as well as a two step emulsification phase of the fat. The obtained T2 relaxation times from the model processed cheeses were compared to their particle sizes in their soluble fraction, the protein concentration in the same fraction and the viscosity at specific processing times as measured with a cone-plate geometry using a Rheometer.

The detected step-wise rise in viscosity corresponded with a shrinking particle size in the serum as well as a decreasing protein concentration measured in the serum. The T2 relation time of mobile protons from mobile water fractions increased, while the respective fraction  $f$  decreased. This is in conclusion with the measurement data from the serum phase, since less soluble protein correspond with less bound water molecules , hence the increase in T2 relaxation time and the general evaporation of water from the system, as indicated by a slightly decreasing water fraction  $f$ . T2 relaxation times for the protons corresponding to fat [T2f] were conclusive in a similar way. The viscosity increase corresponded with an overall decrease of T2f, which indicates a stronger interaction of the protons with the matrix, i.e. a stronger interaction of fat particles with the matrix. In a similar way, the fraction of protons relaxing from the fat phase increased, which leads to the conclusion that the fatglobules grow in number and shrink in size. A matrix comprising of ripened mozzarella, corresponding to peptidized rennet casein, butter and whey protein concentrate was analyzed, varying in amount and type of emulsification in Chen and Liu (2012). The obtained NMR data was fitted to a Gaussian distribution using a numeric inversion program. Four components were fitted, T2 relaxation times were numerically in the range of this study. However, the two middle T2 relaxation times were attributed to immobile protons from water. No explanation was given, as to why the immobile water phase should display two signals. It is indicated, that the fraction of this large component in the relaxing signal is due to the immobile phase interacting with the protons in and adsorbed to the fat phase.

It can be concluded, that T2 relaxation time determination can lead to specific insight towards the compositional changes during the processing of composite materials. However, signal processing and signal identification is a crucial and admittedly somewhat arbitrary process, that relies mainly on empiric observations of previous works. Hence, especially changes in T2 relaxation during manufacture and processing can't give absolute results but comparable results for the individual investigated systems. Larger insight on composition can be gained by the use of other, special types of NMR measurements. The aggregation phenomena of soft-solids like processed or cream cheese could be obtained via pulsed field gradient-nuclear magnetic resonance (PFG-NMR). Le Feunteun, Ouehrani, and Mariette (2012) distinguished dissolved casein monomers besides casein particles during the rennet coagulation of highly concentrated casein suspensions. The concentration of monomers increased during the experiments, while the amount of casein particles decreased. Salami et al. (2013) also performed PFG-NMR measurements to measure the diffusion of non-micellar phosphocaseinate and sodium caseinate preparations in environments with different Polyethylene glycols. However, the T2 relaxation time experiments of this study gave conclusive results in combination with the other experimental data throughout this work.

## 8 Correlation Analysis of Experimental Data using the R programming language

Correlation analysis is a powerful statistical tool, that can lead to further insight into closed datasets. Some trends or even applied fits during this study empirically suggested multiple correlations in the experimental data. One example of such an empirically suggested correlation is the development of especially alphaS1 and beta caseins to the interphase, as described in section 4 of this study, with the apparent viscosity obtained by means of rheological processing. The fit for the increase in the total protein measured at the interphase after a centrifugational washing procedure already revealed an  $R^2 = 0.98$  for the correlation with the viscosity increase (data not shown). To elucidate possibly more of such structures a correlation analysis was performed on the compositional data alone, and as a cross correlation analysis.

Do to so, data preparation, also known as data-wrangling is crucial and takes a lot of time in numeric analysis in general. Only a structured set of data is useful in numeric analysis, best prepared in the way that every observation is a row and every variable is a column (Wehrens (2011AD)). Data, that is reshaped in that way is called “tidy” data, accordingly, many programs used in R for that matter include the prefix tidy. In this study, the CRAN “tidyverse” package was used for data wrangling. The “tidyverse” is a bundle of self supporting packages (due to the same API key) that helps reshape calculate or clear imported data sets. Especially when dealing with large data sets as in NMR analysis or DLS, a programmed data pre preparation gives better oversight over the data, than the graphical displays usually used. Documentation of the “tidyverse” can be found under <https://cran.r-project.org/web/packages/tidyverse/index.html>. Correlation analysis was performed using base R functions as well as the CRAN “lares” package (documentation under <https://cran.r-project.org/web/packages/lares/index.html>). The R programming environment has additional powerful built-in tools and add-on packages for graphical correlation analysis. When working with large datasets, it is important to analyze the data in logical clusters. The experimentally obtained data of protein concentration in various centrifugationally separated phases were analyzed, the results are displayed in the next section.

### 8.1 Results

The function “scatterplotMatrix” plots a given set of data against itself and gives a graphical display (correlation plot) of possible correlations within the measurement data. The diagonal of this

graphical display is the density distribution of the data. The goal here was to find similarities in the concentration or desorption behavior of caseins in the investigated, centrifugationally separated (and respectively washed) phases. The full correlation plot for the compositional analysis in cream, pellet and serum phase as well as for the wash-phases can be found in Appendix B of the Supplementary Material.

This analysis should besides other purposes serve to validate the observations driven from the experimental data. One observation was, that the single concentrations of the caseins in the purified cream phase and the pellet phase developed in a similar fashion. To check this observation, a correlation plot for the caseins measured in the cream and interphase was created (Fig.64)

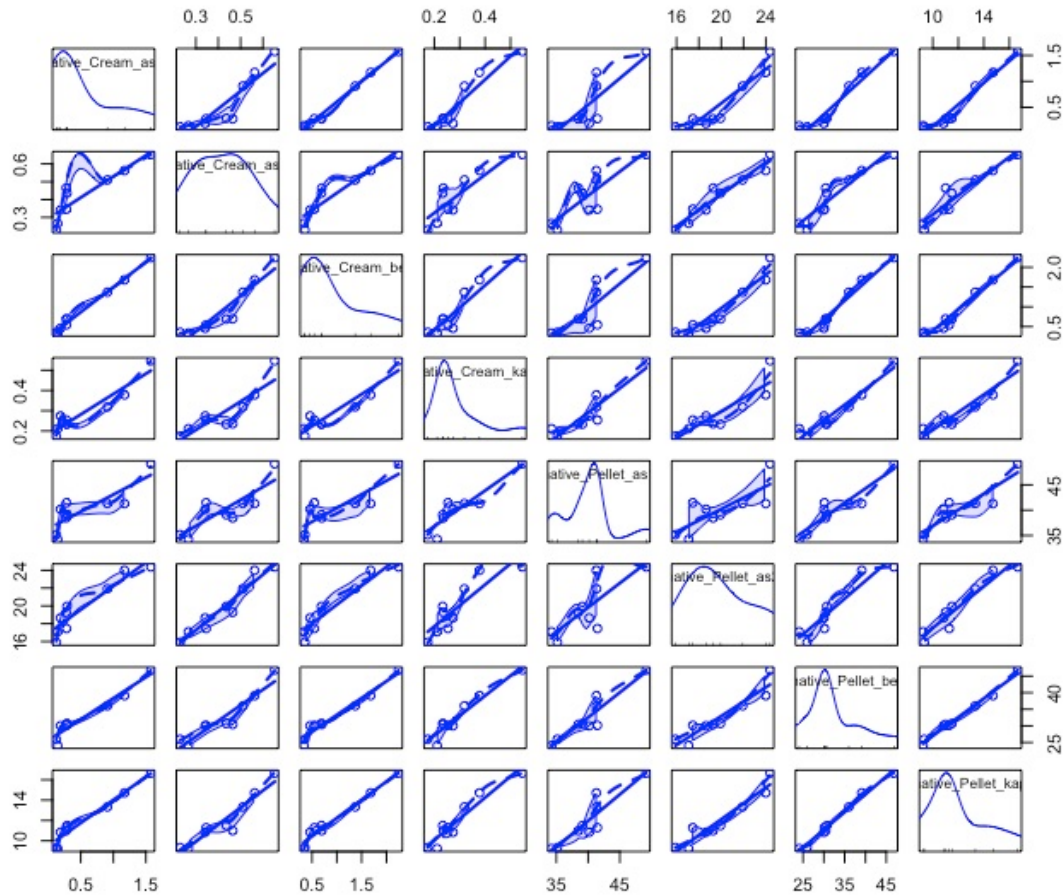


**Fig. 64.** Correlation plot of the protein concentrations measured in the cream 1:4 and pellet 5:8 phase. Protein concentrations are displayed in the order alphaS1, alphaS2, beta and kappa casein.

Strong correlations can be assumed between the development of kappa casein and beta casein in the pellet, as well as alphas1 casein and beta casein in the cream. However useful for an overview, getting concrete insight towards which measured species in this set correlates the most, more specific

correlation plots were obtained. The function “cross\_cor()” gives an output of the correlations found in a data set, ranked by their level of significance (either positive or negative values). By analyzing, for example, the compositional data from chapter 3 in that manner, an estimation for protein interaction can be made. This is due to the fact, that the phases were measured at the same apparent processing point. If the interactions of two associated or aggregated proteins increase or decrease simultaneously at per- or proceeding processing points (i.e. the respective processing times or the arbitrary values A:K), it can be concluded, that they are interacting or aggregating and therefore decrease or increase in a similar manner in the respective phases. Thus, a correlation of the measured concentrations of such caseins over the course of processing should be detected.

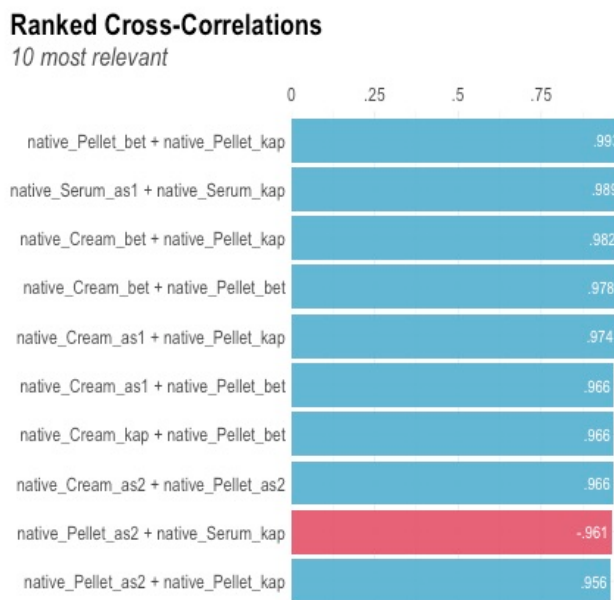
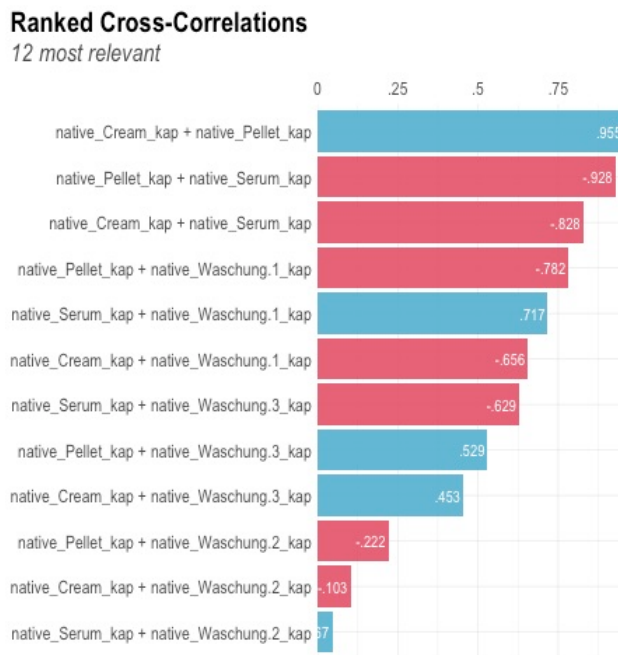


**Fig. 65.** Most significant correlations of the concentrations of single caseins in the investigated phases during processing: red colour indicates negative, blue colour positive correlations.

In Fig.65 the 10 most highly ranked correlations between the development of the casein concentrations in the investigated phases over the course of processing are displayed. It can be seen that proteins in the pellet and the proteins in the cream develop in a similar manner as it was already visible in the scatterplot, as displayed in the previous figure. Especially the development of kappa casein and beta casein concentration in cream and pellet, as well as the development of concentrations of kappa with alphaS1 casein in both phases and the interaction of beta and alphaS1 casein in pellet and cream phase during processing showed high correlations. The highest correlation between the development of measured protein concentrations of alphaS2 casein is with itself in the respective cream and pellet phase. Following the logic above, this would mean, that this casein species mainly tends to interact with itself. This would be in conclusion with the findings of Vollmer,

Kieferle, Youssef, et al. (2021), where an in-situ separation of the model processed cheese into protein rich and protein depleted areas could be shown. Hence the protein rich structures appear due to a high interactions of caseins, namely kappa, beta and alphaS1 casein, to hydrophobic clusters or even fibrils, depleted from alphaS2 casein, that then mainly interacts with itself.

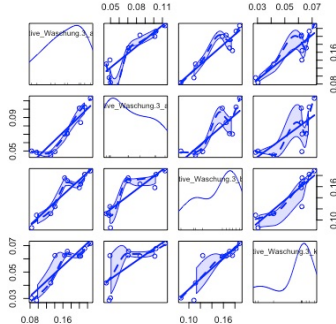
Another hypothesis, if the casein fibrils, mainly comprising kappa casein, as it was described extensively in Vollmer, Kieferle, Youssef, et al. (2021) and Vollmer, Kieferle, Pusl, et al. (2021), could potentially be found in the analysis of the casein population in the intermediate spaces of the fatglobules. In theory, these spaces were analyzed by compositional analysis of the wash phases. In Fig.66 it is apparent that the kappa casein is not directly bound to the cream phase.



**Fig. 66.** Cross-correlation for the measured kappa casein concentrations in the different phases; blue indicates positive, red negative correlations.

The top correlation of measured kappa casein in the investigated phases is inbetween kappa casein in the cream phase and kappa casein at the interphase. In chapter 4, it was theorized, that the structures around the fat particle are fed by the structures from the pellet, since they occur entangled in the non-diluted system. Vollmer, Kieferle, Youssef, et al. (2021) showed, that fibrils that were later confirmed to consist mainly of kappa casein, connected the fat-globules in the model processed cheese matrix to a fine stranded network. The fibrils were suspected to be found in the pellet after compositional analysis. Hence it can be said, that during this study, potentially aggregated kappa casein can be found especially in the hydrophobic phases of the model cheese matrix. Potentially loosely bound kappa casein fibrils might be found in the data of the third

washing step, since a significance of ~0.5 is displayed for kappa casein from the third washing experiment and the kappa casein in the pellet. Fig.67 shows the correlation plot for washing step 3.



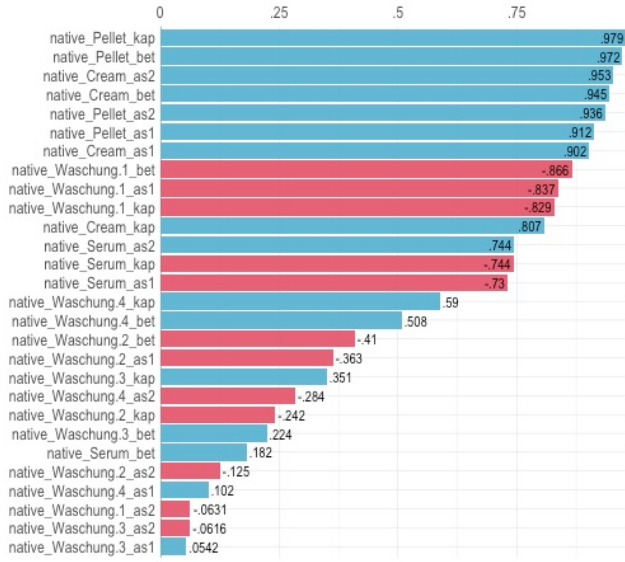
**Fig. 67.** Correlation plot for the third washing step; proteins are displayed in their measured concentration in the order alphaS1, alphaS2, beta and kappa casein.

Fig.67 shows that the density of kappa casein (bottom right square) is normal distributed around a value at the end of the series, i.e. the end of processing. Hence the correlation from the concentrations of kappa casein measured in the wash phase 3 with the kappa casein in the pellet phase comes most likely from the adsorption processes during the second phase of structure formation.

What can be also done is to look for correlations of a dataset with a specific corresponding data vector. The implemented setup “corr\_var()” seems ideally suited to check for the correlation of the measured apparent viscosity as interpreted as structure formation throughout this trial and in previous works, and the measured particle concentrations in the respective phases. Since we assume, that a hydrophobically linked network was formed, a step-wise increase in potentially hydrophobically interacting proteins in the pellet and in the cream phase is expected. Fig.68 gives results following this expectation.

Almost every protein fraction in the investigated hydrophobic phases corresponded to a positive structure formation. Almost, as so to that kappa casein is missing in this top rank. This can be interpreted as that the suspected kappa casein fibrils don't interact in the structure build up in the cream, but stabilize it by interconnection. It is interesting, that they seem to help forming hydrophobic bonds to large networks, since their basic function in milk is to prevent this type of aggregation from happening (Holt et al. (2013)). Interesting from this analysis is as well, that the biggest negative correlation was given by three proteins in the wash phase, beta, alphaS1 and kappa casein. It can be concluded, that the desorption of these proteins from the intermediate spaces of the fatglobules doesn't further promote the structure formation, since less and less of these species can be found in the first washing phase of the centrifugationally separated cream. The fourth protein species

**Correlations of app.visc**



**Fig. 68.** Correlation of the measured apparent viscosity with the data from the compositional analysis. Displayed are the top 10 correlations as indicated by significance level. A positive correlation is indicated by the blue colour, a negative correlation by the colour red.

alphaS2, of the first wash phase can be found almost at the bottom of the list of correlation values. This indicated, that the adsorption or desorption of alphaS2 casein to or from the intermediate spaces of the fat globules is not related to the viscosity increase.

## 9 General Discussion and Outlook

The main aim of this study was to elucidate the structure formation processes occurring in protein rich, dispersed on a molecular level. The driving force that lead to structure formation of the investigated model process cheese systems, as well as to phase separation, was hydrophobic interaction in a special ionic environment, containing melting salts. Concerning the plots of the hydrophobic cluster analysis as shown in chapter 1 and the fact that the emulsifying salts enable especially kappa, alphaS1 and beta caseins to interact on a larger hydrophobic surface, the formation of insoluble structures during the processing of casein matrices is conclusive with the data presented within this work.

It has to be sated that the viscosity measurement is not representative for the “art” that is rheology. What can be obtained by the set-up is the follow-up of the structure-formation process and a relative comparison of the structure development therein, which was sufficient for this study. Rheological characterization with oscillatory shear has been performed vastly elsewhere, for example in Lenze et al. (2019).

The differences in the apparent viscosity seen in the aluminum and steel are most likely to be due to a promoted autocatalytic reaction as it was presented for example in Lenze et al. (2019) and Černíková et al. (2018), also referred to as the addition of rework. Rework addition is a term describing the process of adding pre-processed material to a non-processed matrix, in order to accelerate the structure formation. The samples processed in the aluminum cup showed faster processing times and lower values of viscosity in general. The latter is probably due to the increased heat transfer in the aluminum cup. The first effect however could be due to the far more porous surface of the aluminum cup, where special pre aggregated protein seeds are formed in the cracks of the cup, which then promote the autocatalytic reaction. This would also explain the remaining variance (29%) in the process times that led to the model fit. The modellation of a flow-curve or an overall rheological profile for the model processed cheese was performed. A set of sample was used for this process, that were processed in an aluminum processing cup as in Lenze et al. (2019). The measured apparent viscosities were calculated and fitted into a gam (general additive model), which displayed a good representation of all the obtained flow-curves that displayed a two-step structure formation. The modeled flow-curve appeared to display the shape of the curve seen in Vollmer, Kieferle, Youssef, et al. (2021).

This model flow-curve might be specific for a system that contained solely casein as the structuring and emulsifying agent. A step wise structure formation could be detected, however the steps seemed

to display underlying aggregation processes that were specific of caseins alone. In principle, the observed exponential phases of this study were opposite in their relative length, as compared to the preceding work. Samples processed in a steel cup showed a longer process time, at lower stirring speeds as in the samples analyzed in Vollmer, Kieferle, Youssef, et al. (2021) as well as in samples that were processed at double the stirring speed (see chapter 3 model testing). In some models, where rennet casein was the source material, a pronounced second plateau phase during the second exponential phase was observable. The formation of the casein fibrils and the amorphous aggregates as seen in Vollmer, Kieferle, Pusl, et al. (2021) and Vollmer, Kieferle, Youssef, et al. (2021) could be further characterized in this study. Samples made from sodium caseinate without melting salts but an acidulant showed a distinct structure formation up to the first plateau. It was discussed, that since this model had no calcium, the only structure forming component was kappa casein, which adsorbed to the interphase which led to the viscosity increase. The method for the purification of a cream phase obtained from processed cheese and subsequent RP-HPLC analysis presented herein can be used in the future to further clarify this effect, since it can also the adsorption of beta casein to the interphase that led to the structure increase.

This shows the necessity of a purification protocol of dispersed phases from soft solid composite materials. A protocol for caseins was presented in this study. By that, the functional properties of the caseins were investigated by compositional analysis with RP-HPLC. Model processed cheese was separated into three different phases, using centrifugation at moderate (6.000g) speeds. An insoluble pellet phase, a serum phase with soluble protein and a cream phase with adsorbed protein to the interphase could be obtained. The separation into three phases showed reproducible results in upscaling.

Comparing the measured concentrations in the cream and pellet phases, it could be seen that they develop in a similar manner. In Vollmer, Kieferle, Pusl, et al. (2021) it was theorized, that the fibrils from kappa casein are not the sole contributor to structure formation, which seems reasonable, since the kappa casein poses the smallest fraction of protein in the casein micelle. It was suggested that other proteins aggregate with kappa casein to form a fibrillar structure that has not been described in literature. The samples analyzed in the cited work however were processed without TSC as emulsifying salts. It has been reported, that the ratio of DSP and TSC can be used to tune functional properties and that both salts are necessary for processed cheese functionality in general (El-Bakry et al. (2011)). It can be theorized, that the occurrence of fibrillar structures in the cheese mass is dependent on the calcium chelation properties of the salt mixture, and the incubation time. The presence of TSC might lead to a faster chelation of calcium ions. Since it is not known, how the

differing emulsifying salts work on a molecular level in the casein micelle, it can be also theorized, that TSC chelates calcium ions from the casein micelle, that furthers more initially “reactive” protein and thus an earlier occurrence of fibrils is observable. This would also explain the strong differences in viscoelastic properties of the model processed cheeses cited in the literature, when different mixtures or amounts of emulsifying salts are used.

A particle size analysis on the centrifugationally separated phases was performed. The particle sizes in the insoluble pellet phase showed a decrease in small components at a simultaneous increase of large components during the second half of structure formation. The soluble particles were investigated after ultracentrifugation using DLS instead of light scattering, therefore their radius of gyration was measured. It could be seen, that the hydrophilic parts of the system first shrink during the first exponential phase of structure formation, while they increase in size during the second exponential phase of structure formation. Since the matrix was diluted, the displayed particle sizes are of course not the de-facto particle sizes in the processed cheese. However, it was possible to identify potential building-blocks that shape the properties of the model. These were large soluble aggregates next to small aggregates that were hydrophobic in nature and were further connected to a larger network that also emulsified the fat.

It became apparent from the particle size measurements of the cream phase that the emulsification of the system was rather a ‘by-product’ of hydrophobic network formation, coming from the proteins. It can be concluded that a pronounced first exponential phase was especially found in other models not investigated in detail during this study, namely models that also contained other surface active protein moieties. 69 can explain this in more detail. Lenze et al. (2019) investigated the effect of replacing 2% milk powder (containing the more surface active whey proteins) in a ‘real-type’ processed cheese matrix coming from natural cheese and butter, with different protein entities. The replacement of 2% of the surface active proteins, i.e. the milkpowder, with dissociated (i.e. non micellar) casein, already leads to a complete disappearance of a first exponential increase in apparent viscosity. Native casein and rennet casein don’t seem to alter the structure formation process. The first exponential phase of structure formation displayed in this study showed only minor adsorption of caseins to the interphase, with the developed method for purification and subsequent analysis of the protein concentration and composition in the cream phase, the adsorption of whey proteins next to caseins can be studied in the future.

The compositional analysis revealed, that the secondary aggregates besides the suspected kappa casein are made up out of beta and alphaS1 casein. The alphaS2 casein proved to play a secondary role in the formation of large insoluble aggregates, however the correlation analysis performed in the

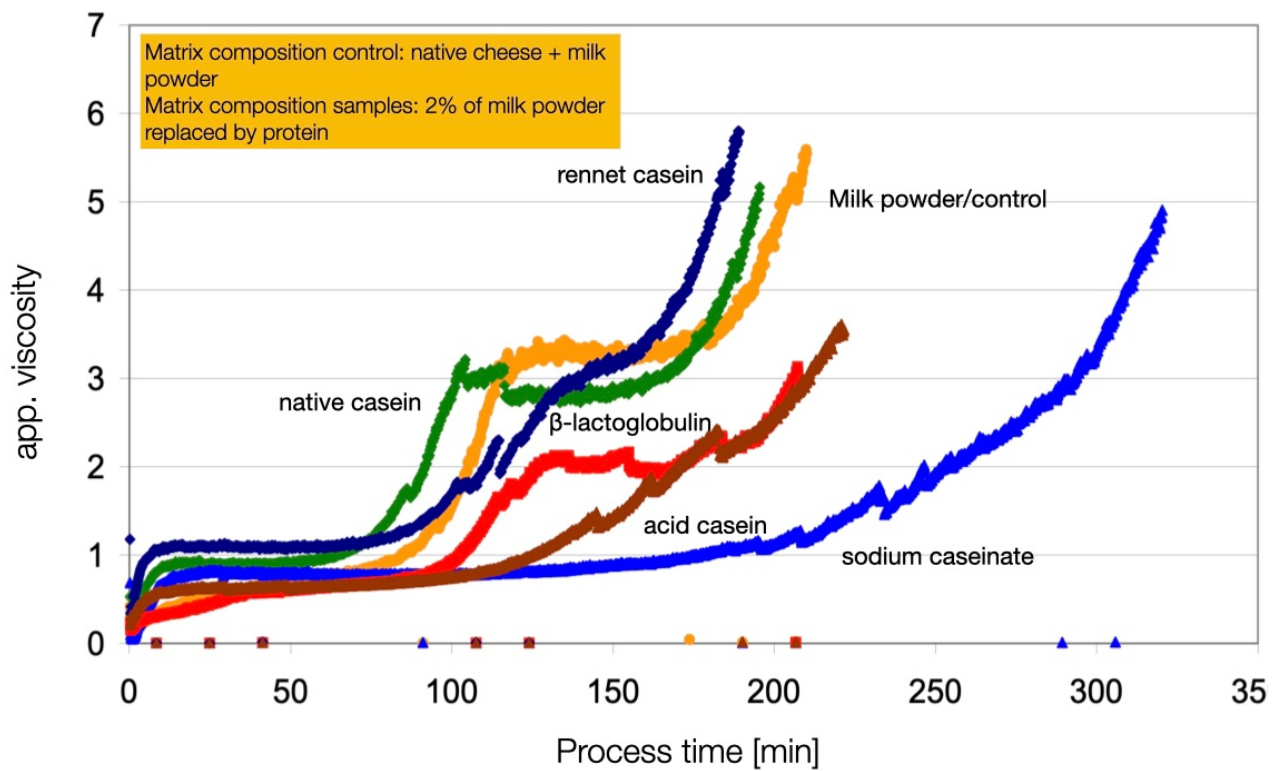


**Fig. 69.** apparent viscosities in model processed cheeses cited in the literature, in dependence of replacement of small amounts of milk powder with the displayed protein source. Distinct first exponential phase cannot be seen in samples, when dissociated casein was added

last section of this work gave insight towards alphaS2 residing mainly in the soluble fractions of the matrix. It can be concluded, that the protein-rich structures found during TEM imaging in Vollmer, Kieferle, Youssef, et al. (2021) are amorphous aggregates from alphaS1 and beta casein, possibly connected by kappa casein fibrils or seeds therefrom. The areas that had a lesser protein density are supposedly populated by the alphaS2 casein. Further, it was hypothesized that the calcium (and possibly other ions) as well as large amounts of water were stored with the alphaS2 casein, due to the depletion forces coming from the hydrophobic network formation, excluding water and ions. This results in a structure that is not completely solvable in water and thus hydrophobically aggregated. Sapir and Harries (2015) showed two different types of depletion: entropic and enthalpic depletion. Entropic depletion occurs under the formation of a hard repulsive core of interacting molecules that co-solutes cannot penetrate. Enthalpic depletion was considered to display the ‘hard-core’ repulsion, next to repulsive ‘soft-shell,’ which is defined by steric interactions. Since the described effects (adsorption to fat, concentration in pellet of selected caseins, step-wise increase in viscosity) are not observable in a model system of sodium caseinate and emulsifying salts, it can be theorized, that the matrix segregation, is a part of structure formation. The depletion force occurs at short distances

and is a strong local force (Semenova et al. (2010)). It is widely studied for liquid casein emulsions (see for example Radford and Dickinson (2004), Dickinson and Golding (1997), Dickinson (2012)) but to the author's knowledge has not yet been presented for dense casein matrices like processed cheese. In emulsions, or in liquid systems in general, depletion is happening either at random or during heating due to Brownian movement. Often, it is described as depletion flocculation in dense or gelled systems, meaning an enhanced aggregation of particles due to the depletion of co-solvates from the aggregate. In the model samples the depletion is induced by the forced collision of the particles coming from the constant stirring of the matrix thus inducing a shear force by the matrix on itself, as well as by heating. This theory could be supported by experimental data, when investigating a colloidal system containing 3% total protein (w/w) of casein and an aliquot of melting salts. After 140 minutes of processing, large aggregates were visible. Beforehand, an increase in viscosity during heating as well as the appearance of a ~14 nm sized particle, next to larger aggregates became apparent. At later processing stages, the samples showed a high tendency to reaggregate, which hints to a favored aggregated state of caseins. This is in conclusion with the report of "sticky" fibrillar structures in the matrix as cited in the literature. The "stickiness" is herein interpreted as reactivity, or tendency to aggregate. The HPLC analysis of the supernatants of the colloid samples revealed an initial decrease in kappa casein after 100 min of processing (heat and stir), with a subsequent decrease of beta and alphaS1 casein. Hence the primary seed, that led to hydrophobic aggregation that was looked for in this study was revealed to be a kappa casein fibril or primary aggregate (as seen in the needles after 415 minutes of processing as in Vollmer, Kieferle, Youssef, et al. (2021)), on to which alphaS1 and beta caseins aggregate.

Vollmer, Kieferle, Youssef, et al. (2021) reported such a matrix separation in a model processed cheese system, that was processed using high heat (90 C) and approximately half the amount of stirring speed (~8 rpm) in a small processing unit with a sample weight of ~40 g. The matrix separated into areas of high electron density, where the appearance of fibrillar or tubular aggregated casein was detected and areas of lower protein density, where amorphous aggregates were displayed. This fits the results obtained in this study well and could further target investigations on the power of depletion or molecular exclusion in general in the formation of dense matrices. To further explore the theory, that the hydrophobic aggregate is not only formed in the dense matrix but also in diluted form, it is highly suggested to investigate the aggregate that is formed in the colloidal solution by TEM. Also, a variation in salt composition in these easy to prepare systems is highly suggested. Since the fibrillar structures only appeared at late processing stages in samples cited in the literature that were prepared without TSC, the preparation of the colloid samples without TSC should reveal,

if the matrix separation is in its overall degree dependent on process or chemical (i.e. compositional) conditions.

The exclusion of alphaS2 casein from the hydrophobic network must be due to electrostatic reasons, if this theory is applied. It is possible that the calcium is indeed present in chelated form. If this would be the case it can be theorized, that alphaS2 casein has a specific affinity for complexed calcium that the other caseins lack, which could further elucidate the binding of the casein micelle. If the calcium is in ionic form, the same applies, since then a special sensitivity or a binding modulus to ionic calcium of alphaS2 over the other caseins can be theorized. In the ranking of calcium sensitivity, alphaS2 caseins rank the highest, their high solubility in water is dependent on their centers of phosphorylation (Aoki, Toyooka, and Kako (1985)). From the results obtained during this trial, it can be theorized that the alphaS2 casein poses as the “definitive connector” to the ionic calcium or the CCP, whereas alphaS1 and beta casein can interact with each other, ionic calcium or CCP, or the alphaS2 casein. Kappa casein is believed to be genetically designed to sit on the outside of the micelle to carry the negative charge of CMP into the milk serum (Dagleish and Corredig (2012), Holt et al. (2013)). Further exploring the concept of genetic design, it can be theorized that kappa casein was not designed to interact in close range, therefore it aggregates to seeds or fibrils, that leads to further hydrophobic aggregation of beta and alphaS1 casein. This theory can also be supported by the fact that the melting salts are entering the casein micelle from the outside in, therefore, the outer lying kappa caseins are one of the first caseins to be released from the micelle and therefore start to aggregate early and selectively with each other during processing.

Diffusing wave spectrometry (DWS) poses as another tool to follow aggregation processes, as in Alexander, Corredig, and Dagleish (2006), but also destabilization phenomena, as in Hemar and Horne (1999) and Vogt et al. (2015). The latter used DWS and small amplitude oscillation rheology, on heated cheeses (Mozzarella, medium Cheddar, aged Cheddar) and determined a progressive increase of free water in the system as cheese is heated. This effect is also seen in the T2 relaxation data obtained in this study. Over the course of processing, a progressive increase in the mobile fraction of water ( $T_2 \sim 120$  ms) was apparent, whereas the T2 relaxation of the detected fat-phase decreased. Considering the effects of matrix separation, it can be concluded from Vogt et al. (2015) that a matrix separation in heated cheeses is also indicated by a redistribution of water. Since the progressive loss of mobile water is detectable without apparent (or forced, as in Dang, Wolfschoon Pombo, and Kulozik (2019)) syneresis or water evaporation as indicated by a strongly increasing dry matter, this must mean that there are areas in the aggregated casein structure, that fulfill the function to hold the water in the system, whereas the other caseins participate in hydrophobic

network formation.

When over-processing the cheese matrix, i.e. excessing the amount of energy and forced collision from agitation that is needed to perform the ‘creaming-reaction,’ a particulated, almost crystalline structure of the cheese becomes apparent. It has to be noted, however, that these samples were by design strongly overprocessed, in order to find an apparent “end” point of the creaming reaction, or a maximal aggregated product. This overprocessing also lead to a notable increase in dry matter of >10%, however, what could be seen were lighter and darker areas in the protein structure (Fig.70).



**Fig. 70.** Over-processed ‘end-point’ of the creaming reaction, appearance of the product. Incorporation of lighter globular areas (circle) into a darker matrix, containing fat (asterix)

Applying the general concept of imaging techniques that darker areas indicate areas of higher protein density, it can be readily concluded from the appearance of the samples at the “end point” of the creaming reaction, that a phase separation has taken place. From the investigation of the centrifugationally separated phases it was apparent, that the structures that were defined herein as ‘hydrophobic-aggregates’ were insoluble in water, but did show a stronger tendency to swell. The swelling behaviour was displayed in the pellet as well as in the cream phase (chapter 4 of this work). This shows, that the hydrophobic structures are formed under the exclusion of water at their core, but with hydrophilic structures, that are probably high in charge, at their surface. This also means, that the hydrophobic network formation might occur *in-situ* under the exclusion of water, without the necessity of water to leave the system, since it can be, in a way, compartmentalized in the system. This behavior of proteins is commonly known and one of the main reasons, why many proteins, such

as whey proteins, appear in globular form. This is supported by the fact that the samples investigated in Vollmer, Kieferle, Youssef, et al. (2021) were not processed to the particulate “end-point” of the creaming reaction as described earlier, but were still elastic, probably due to the remaining water in the system.

The particle sizes measured in the pellet and in the differently centrifuged serum phases were in conclusion with the obtained TEM images of the model cheese mass, cited in the literature. From particle size analysis in the pellet, it could be seen that a large network develops during medium to late processing stages, that further is fragmented into smaller sub-units at late processing stages.

Fig. 71 shows the TEM image of the beginning matrix fragmentation.

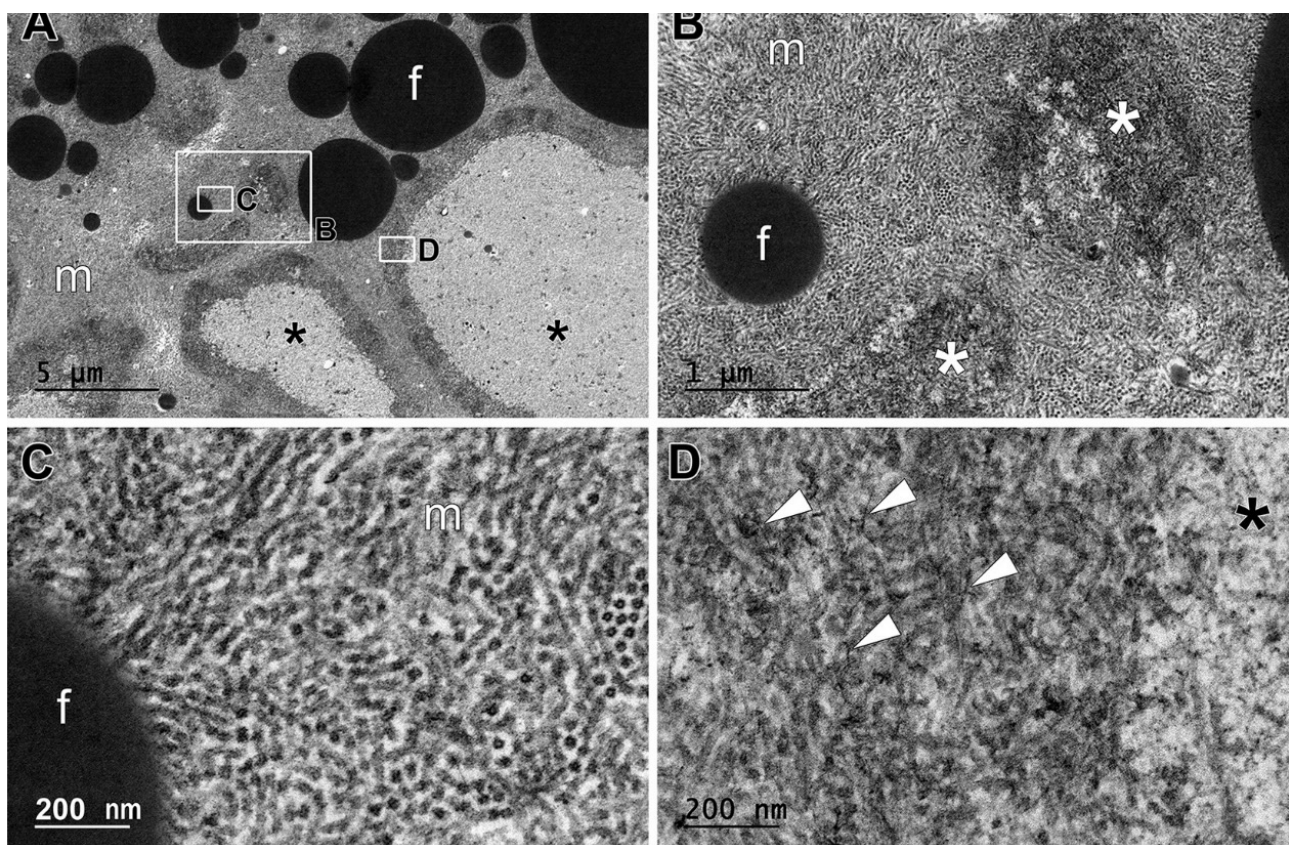


**Fig. 71.** TEM imaging of model processed cheese prepared at low stirring speeds after 415 minutes of processing; lighter areas display areas with low protein density (asterisk), these are surrounded by a dens band of a protein network that showed breakage of fibrils into needelels (arrowheads) and amorphous structures, the surrounding matrix (m) displayed convoluted and fragmented fibrillar structures, that emulsify the fat.

In chapter 6 of this work, a reaction meachanism for the protein aggregation occuring in the model processed cheese system was shown. This mechanism consists of a two step aggregation process that leads to phase separation. As it was discussed earlier, for phase separation to occur in this environment, alphaS2 casein is supposed to be in a state, that either still has calcium bound to it, or

binds calcium more readily than the remaining caseins. Hindmarsh and Watkinson (2017) showed the presence of previously unclassified calcium structures in the casein micelle. New immobile phosphorus bodies were found, that were suggested to reside from phosphoserine-to-phosphoserine linkages that can be inter- or intra-proteinogenic. Looking at the HCA plots Fig.7, alphaS2 has a serine free, hydrophobic planar area between residues 80 and 140, neighbored by large serine containing areas. In a dense environment, where caseins cannot swell or (all) carry large hydrate shells, they might conform into a structure as suggested in Fig.7. An intramolecular calcium binding of alphaS2 casein could be the reason, why no (exponential) structure formation was seen in the sodium casein models, since the alphaS2 casein in sodium caseinate either lacks the intramolecular bond to begin with or cannot form it due to a minimal concentration of calcium ions. Since sodium caseinate is readily used in combination with calcium in processed cheese production, and since calcium is long known to prevent sodium caseinate emulsions from depletion flocculation (Dickinson and Golding (1998)), it is thinkable from the results obtained in this study, that the formation of an intramolecular phosphoserine - calcium - phosphoserine bridge in alphaS2 casein is the reason why it is not participating in the hydrophobic aggregation. The structure formation as well as the subsequent phase separation is suggested to occur due to depletion.

Sapir and Harries (2015) made vast investigations on the depletion force. Depletion occurs from the exclusion of co-solutes from macromolecules, which creates an attractive force between the macromolecules that exclude the co-solute. Therefore it promotes self-association of the macromolecules. Also attractive depletion forces induced by heat were shown to occur. Considering the findings in this study, entropic depletion of the co-solutes (i.e. ions) from an hydrophobic aggregate seems thinkable. In addition, enthalpic or steric depletion of alphaS2 casein due to its hypothesized non-planar conformation from an intramolecular calcium bond is also contributing to the aggregation processes observed throughout this study.

Therefore, the reaction mechanism shown in section 6 of this work (Fig.57)can be supplemented and a conclusive mechanistic explanation for the phenomena observed and measured within this study on a molecular and macroscopic level, can be given (Fig.72).

The fragmentation of the aggregates at late stages of processing can be considered to be irreversible. Indications for fragmentation were also found during the measurements of the different cream phases: at later processing stages, peptide fragments were apparent. This also includes that by fragmentation, the process becomes fully irreversible. It cannot be estimated, if the formed aggregates are stable at changing milieu conditions. It is expected, that for example ethanolization might reverse the hydrophobic aggregation to some degree.

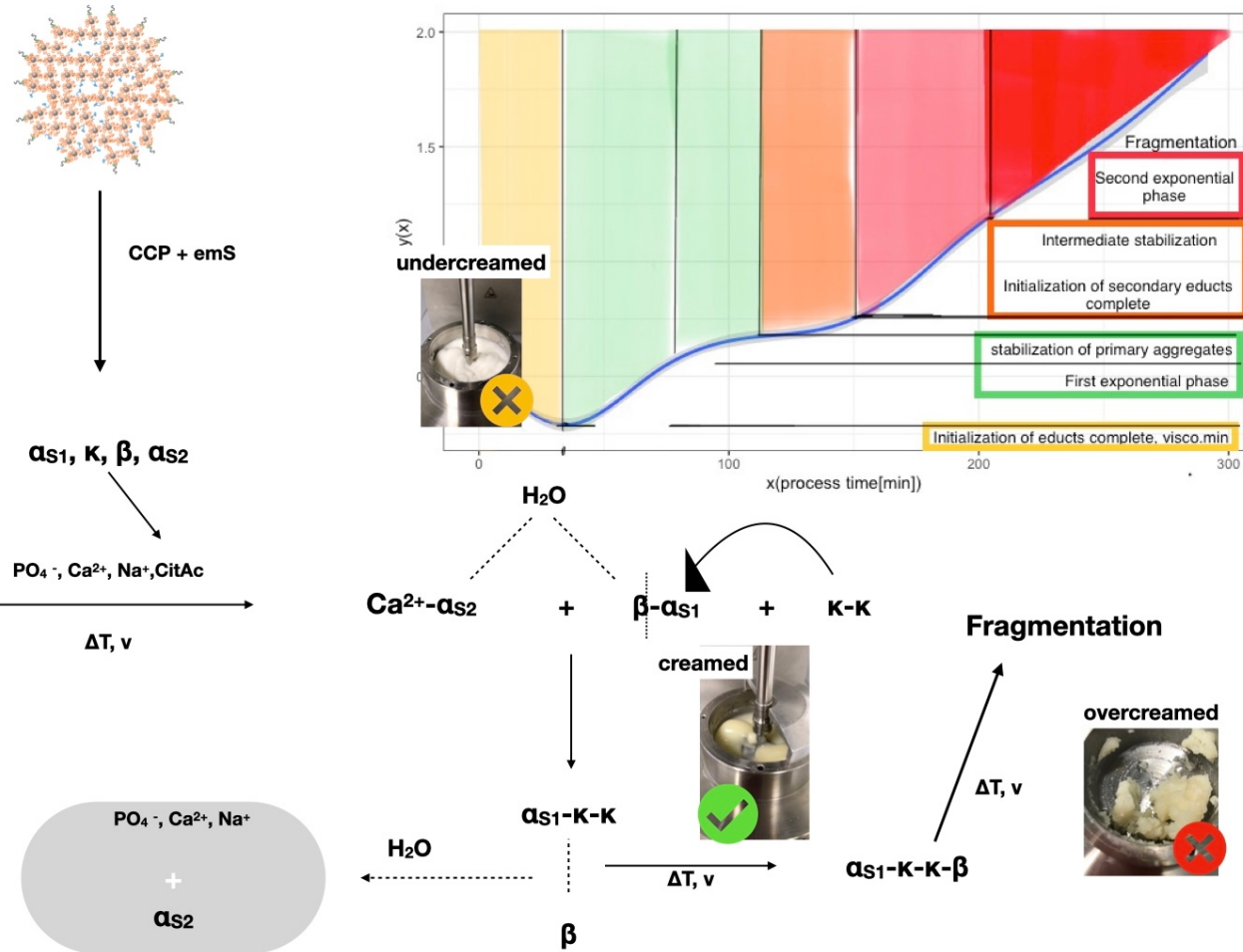


**Fig. 72.** Structural changes that lead to an increase in viscosity in model processed cheese.

Another effect that became apparent from the comparison with previous works, the casein aggregates are not brittle aggregates, but can be aligned during processing which makes them shapeable. This is not new for casein, since pasta filata cheeses use this as a key production step. It is thinkable, to use these now newly identified hydrophobic casein structures in a targeted manner. Since it is a heat set process that seems to allow shear to shape the structure, 3D printing is a possible application for the hydrophobic casein aggregate.

## 10 Bibliography

- Alexander, Marcela, Milena Corredig, and Douglas G. Dalgleish. 2006. “Diffusing wave spectroscopy of gelling food systems: The importance of the photon transport mean free path ( $l^*$ ) parameter.” *Food Hydrocolloids* 20 (2-3 SPEC. ISS.): 325–31. <https://doi.org/10.1016/j.foodhyd.2005.02.021>.
- Aoki, Takayoshi, Kazuhiro Toyooka, and Yoshitaka Kako. 1985. “Role of Phosphate Groups in the Calcium Sensitivity of s2-Casein.” *Journal of Dairy Science* 68 (7): 1624–29. [https://doi.org/https://doi.org/10.3168/jds.S0022-0302\(85\)81005-5](https://doi.org/https://doi.org/10.3168/jds.S0022-0302(85)81005-5).
- Awad, R. A., L. B. Abdel-Hamid, S. A. El-Shabrawy, and R. K. Singh. 2002. “Texture and microstructure of block type processed cheese with formulated emulsifying salt mixtures.” *LWT - Food Science and Technology* 35 (1): 54–61. <https://doi.org/10.1006/fstl.2001.0828>.
- Barth, A P, C F Tormena, and W H Viotto. 2017. “pH influences hydrolysis of sodium polyphosphate in dairy matrices and the structure of processed cheese.” *Journal of Dairy Science* 100 (11): 8735–43. <https://doi.org/https://doi.org/10.3168/jds.2017-12764>.
- Berman, Paula, Ofer Levi, Yisrael Parmet, Michael Saunders, and Zeev Wiesman. 2013. “Laplace inversion of low-resolution NMR relaxometry data using sparse representation methods.” *Concepts in Magnetic Resonance Part A: Bridging Education and Research* 42 (3): 72–88. <https://doi.org/10.1002/cmr.a.21263>.
- Berta, Marco, Erwin Muskens, Erich Schuster, and Mats Stading. 2016. “Rheology of natural and imitation mozzarella cheese at conditions relevant to pizza baking.” *International Dairy Journal* 57: 34–38. <https://doi.org/https://doi.org/10.1016/j.idairyj.2016.02.038>.
- Besghini, Denise, Michele Mauri, and Roberto Simonutti. 2019. “Time domain NMR in polymer science: From the laboratory to the industry.” *Applied Sciences (Switzerland)* 9 (9). <https://doi.org/10.3390/app9091801>.
- Bonfatti, Valentina, Luca Grigoletto, Alessio Cecchinato, Luigi Gallo, and Paolo Carnier. 2008. “Validation of a new reversed-phase high-performance liquid chromatography method for separation and quantification of bovine milk protein genetic variants.” *Journal of Chromatography A* 1195 (1-2): 101–6. <https://doi.org/10.1016/j.chroma.2008.04.075>.
- Bonizzi, Ivan, Joanna Natalia Buffoni, and Maria Feligini. 2009. “Quantification of Bovine Casein Fractions by Direct Chromatographic Analysis of Milk. Approaching the Application to a Real Production Context.” *Journal of Chromatography A* 1216 (1): 165–68. <https://doi.org/https://doi.org/10.1016/j.chroma.2008.11.045>.

- Borchers, Hans W. 2021. “<i>pracma</i>. R package version 2.3.3.”
- Borgia, G. C., R. J. S. Brown, and P. Fantazzini. 1998. “Uniform-Penalty Inversion of Multiexponential Decay Data.” *Journal of Magnetic Resonance* 132 (1): 65–77.  
<https://doi.org/10.1006/jmre.1998.1387>.
- Brickley, C. A., S. Govindasamy-Lucey, J. J. Jaeggi, M. E. Johnson, P. L. H. McSweeney, and J. A. Lucey. 2008. “Influence of emulsifying salts on the textural properties of nonfat process cheese made from direct acid cheese bases.” *Journal of Dairy Science* 91 (1): 39–48.  
<https://doi.org/10.3168/jds.2007-0393>.
- Brighenti, M, S Govindasamy-Lucey, J J Jaeggi, M E Johnson, and J A Lucey. 2018. “Effects of processing conditions on the texture and rheological properties of model acid gels and cream cheese.” *Journal of Dairy Science* 101 (8): 6762–75.  
<https://doi.org/https://doi.org/10.3168/jds.2018-14391>.
- Brunner, A. 1991. “Untersuchungen Zur Struktur in Caseinatgelen Und Caseinat-Lipid-Emulsionen.” *Dissertation, Technische Universität München, Fakultät für Brauwesen, Lebensmitteltechnologie Und Milchwissenschaft, Hieronymus Buchreproduktions GmbH, München*.
- Casanova, Federico, Luis Gustavo Lima Nascimento, Naaman F. N. Silva, Antonio F. de Carvalho, and Frédéric Gaucheron. 2021. “Interactions Between Caseins and Food-Derived Bioactive Molecules: A Review.” *Food Chemistry* 359: 129820.  
<https://doi.org/https://doi.org/10.1016/j.foodchem.2021.129820>.
- Chen, L., and H. Liu. 2012. “Effect of emulsifying salts on the physicochemical properties of processed cheese made from Mozzarella.” *Journal of Dairy Science* 95 (9): 4823–30.  
<https://doi.org/10.3168/jds.2012-5480>.
- Clare, D. A., and H. E. Swaisgood. 2000. “Bioactive Milk Peptides: A Prospectus1.” *Journal of Dairy Science* 83 (6): 1187–95.  
[https://doi.org/https://doi.org/10.3168/jds.S0022-0302\(00\)74983-6](https://doi.org/https://doi.org/10.3168/jds.S0022-0302(00)74983-6).
- Cunha, Clarissa R., Renato Grimaldi, Maria Regina Alcatara, and Walkiria H. Viotto. 2013. “Effect of the type of fat on rheology, functional properties and sensory acceptance of spreadable cheese analogue.” *International Journal of Dairy Technology* 66 (1): 54–62.  
<https://doi.org/10.1111/j.1471-0307.2012.00876.x>.
- Černíková, Michaela, Jana Nebesářová, Richardos Nikolaos Salek, Romana Popková, and František Buňka. 2018. “The effect of rework content addition on the microstructure and viscoelastic

- properties of processed cheese.” *Journal of Dairy Science* 101 (4): 2956–62.  
<https://doi.org/https://doi.org/10.3168/jds.2017-13742>.
- Dalgleish, Douglas G., and Milena Corredig. 2012. “The structure of the casein micelle of milk and its changes during processing.” *Annual Review of Food Science and Technology* 3 (1): 449–67.  
<https://doi.org/10.1146/annurev-food-022811-101214>.
- Dang, Bich Phuong, Alan F Wolfschoon Pombo, and Ulrich Kulozik. 2019. “Physicochemical Changes During the Creaming Reaction in Acid Curd Fresh Cheese: Water Mobility and Forced Synaeresis.” *International Journal of Dairy Technology* 72 (2): 295–302.  
<https://doi.org/https://doi.org/10.1111/1471-0307.12585>.
- Derek, Author, David Hunter, Ryan Elmore, Thomas Hettmansperger, and Hoben Thomas. 2020. *Package ‘mixtools’*.
- Dickinson, Eric. 2006. “Structure formation in casein-based gels, foams, and emulsions.” *Colloids and Surfaces A: Physicochemical and Engineering Aspects* 288 (1): 3–11.  
<https://doi.org/10.1016/j.colsurfa.2006.01.012>.
- . 2012. “Emulsion gels: The structuring of soft solids with protein-stabilized oil droplets.” *Food Hydrocolloids* 28 (1): 224–41. <https://doi.org/10.1016/j.foodhyd.2011.12.017>.
- Dickinson, Eric, and Matt Golding. 1997. “Depletion flocculation of emulsions containing unadsorbed sodium caseinate.” *Food Hydrocolloids* 11 (1): 13–18.  
[https://doi.org/10.1016/S0268-005X\(97\)80005-7](https://doi.org/10.1016/S0268-005X(97)80005-7).
- . 1998. “Influence of calcium ions on creaming and rheology of emulsions containing sodium caseinate.” *Colloids and Surfaces A: Physicochemical and Engineering Aspects* 144 (1-3): 167–77.  
[https://doi.org/10.1016/S0927-7757\(98\)00573-1](https://doi.org/10.1016/S0927-7757(98)00573-1).
- Dumpler, Joseph. 2018. “Heat Stability of Concentrated Milk Systems,” January.  
<https://doi.org/10.1007/978-3-658-19696-7>.
- Dumpler, Joseph, Heidi Wohlschläger, Ulrich Kulozik, and Joseph Dumpler josephdumpler. 2017. “Dissociation and coagulation of caseins and whey proteins in concentrated skim milk heated by direct steam injection.” *Dairy Sci. & Technol* 96: 807–26.  
<https://doi.org/10.1007/s13594-016-0304-3>.
- El-Bakry, M., E. Duggan, E. D. O’Riordan, and M. O’Sullivan. 2011. “Casein hydration and fat emulsification during manufacture of imitation cheese, and effects of emulsifying salts reduction.” *Journal of Food Engineering* 103 (2): 179–87. <https://doi.org/10.1016/j.jfoodeng.2010.10.014>.

- Fox, P F. 2009. *Dairy Chemistry And Biochemistry*. <https://doi.org/10.1201/9781420046359-p1>.
- Fox, Patrick F., Timothy P. Guinee, Timothy M. Cogan, and Paul L. H. McSweeney. 2016. *Fundamentals of cheese science, second edition*. <https://doi.org/10.1007/978-1-4899-7681-9>.
- Fu, Wei, Yurika Watanabe, Keita Inoue, Natsumi Moriguchi, Kazunao Fusa, Yuya Yanagisawa, Takaaki Mutoh, and Takashi Nakamura. 2018. “Effects of pre-cooked cheeses of different emulsifying conditions on mechanical properties and microstructure of processed cheese.” *Food Chemistry* 245 (4): 47–52. <https://doi.org/10.1016/j.foodchem.2017.10.075>.
- Fu, Wei, Yurika Watanabe, Hayaka Satoh, Keita Inoue, Natsumi Moriguchi, Kazunao Fusa, Yuya Yanagisawa, Takaaki Mutoh, and Takashi Nakamura. 2018. “Effects of emulsifying conditions on creaming effect, mechanical properties and microstructure of processed cheese using a rapid visco-analyzer.” *Bioscience, Biotechnology and Biochemistry* 82 (3): 476–83. <https://doi.org/10.1080/09168451.2018.1431106>.
- Gaucheron, Frédéric. 2011. “MILK SALTS | Distribution and Analysis.” In *Encyclopedia of Dairy Sciences*, 908–16. <https://doi.org/10.1016/B978-0-12-374407-4.00355-1>.
- Giovannelli, Jean Francois, and Jerome Idier. 2015. *Regularization and Bayesian Methods for inverse problems in signal and image processing*. <https://doi.org/10.1002/9781118827253>.
- Gogaev, K. A., G. Ya Kalutskii, and V. S. Voropaev. 2009. “Asymmetric rolling of metal powders. III. Forward slip in asymmetric rolling of metal powders.” *Powder Metallurgy and Metal Ceramics* 48 (7-8): 384–87. <https://doi.org/10.1016/j.idairyj.2015.06.001>.
- Gotz, J, Prof Dr Horst Weisser, Joachim Götz, J Gotz, and Prof Dr Horst Weisser. 2004. “Applications of NMR to food and model systems in process engineering.” *Lehrstuhl für Brauereianlagen Und Lebensmittel-Verpackungstechnik* Habilitati: 126. <http://tumb1.biblio.tu-muenchen.de/publ/diss/ww/2004/goetz.pdf%7B/%%7D0Ahttp://tumb1.biblio.tu-muenchen.de/publ/diss/ww/2004/goetz.html%7B/%%7D0Ahttp://deposit.ddb.de/cgi-bin/dokserv?idn=970777841>.
- Guinee, T. P., M. Carić, and M. Kaláb. 2004. *Pasteurized processed cheese and substitute/imitation cheese products*. Vol. 2. C. [https://doi.org/10.1016/S1874-558X\(04\)80052-6](https://doi.org/10.1016/S1874-558X(04)80052-6).
- Hemar, Yacine, and David S. Horne. 1999. “A diffusing wave spectroscopy study of the kinetics of Ostwald ripening in protein-stabilised oil/water emulsions.” *Colloids and Surfaces B: Biointerfaces* 12 (3-6): 239–46. [https://doi.org/10.1016/S0927-7765\(98\)00079-4](https://doi.org/10.1016/S0927-7765(98)00079-4).
- Hindmarsh, JP, and P Watkinson. 2017. “Experimental evidence for previously unclassified calcium

- phosphate structures in the casein micelle.” *Journal of Dairy Science* 100. <https://doi.org/10.3168/jds.2017-12623>.
- Hinrichs, Ruth, Selda Bulca, and Ulrich Kulozik. 2007. “Water mobility during renneting and acid coagulation of casein solutions: A differentiated low-resolution nuclear magnetic resonance analysis.” *International Journal of Dairy Technology* 60 (1): 37–43. <https://doi.org/10.1111/j.1471-0307.2007.00290.x>.
- Hinrichs, Ruth, Joachim Goetz, Michael Noll, Alan Wolfschoon, Hermann Eibel, and Horst Weisser. 2004. “Characterisation of the water-holding capacity of fresh cheese samples by means of low resolution nuclear magnetic resonance.” *Food Research International* 37 (7): 667–76. <https://doi.org/10.1016/j.foodres.2004.02.005>.
- Hinrichs, Ruth, Joachim Götz, Michael Noll, Alan Wolfschoon, Hermann Eibel, and Horst Weisser. 2004. “Characterisation of different treated whey protein concentrates by means of low-resolution nuclear magnetic resonance.” *International Dairy Journal* 14 (9): 817–27. <https://doi.org/10.1016/j.idairyj.2004.02.003>.
- Holt, C., Ja J. A. Carver, H. Ecroyd, and D. C. DC Thorn. 2013. “Invited review: Caseins and the casein micelle: Their biological functions, structures, and behavior in foods1” 96 (10): 6127–46. <https://doi.org/10.3168/jds.2013-6831>.
- Horne, D., and J. A. Lucey. 2017. “Letter to the Editor: Hydrophobic interactions in the caseins: Challenging their dismissal by Holt et al. (2013).” *Journal of Dairy Science* 100 (7): 5119–20. <https://doi.org/10.3168/jds.2017-12668>.
- Horne, David S. 2017. “A balanced view of casein interactions.” *Current Opinion in Colloid and Interface Science* 28 (March): 74–86. <https://doi.org/10.1016/j.cocis.2017.03.009>.
- Hougaard, Anni B., Anna G. Sijbrandij, Camilla Varming, Richard Ipsen, and Ylva Ardo. 2015. “Emulsifying salt increase stability of cheese emulsions during holding.” *LWT - Food Science and Technology* 62 (1): 362–65. <https://doi.org/10.1016/j.lwt.2015.01.006>.
- Hubbard, Arthur. 2003. *Food Colloids, Biopolymers and Materials*. Vol. 265. 1. [https://doi.org/10.1016/s0021-9797\(03\)00514-9](https://doi.org/10.1016/s0021-9797(03)00514-9).
- Huppertz, T., P. F. Fox, and A. L. Kelly. 2018. “The caseins: Structure, stability, and functionality.” In *Proteins in Food Processing*, 49–92. Elsevier. <https://doi.org/10.1016/B978-0-08-100722-8.00004-8>.
- Huppertz, Thom, Inge Gazi, Hannemieke Luyten, Hans Nieuwenhuijse, Arno Alting, and Erix

- Schokker. 2017. "Hydration of casein micelles and caseinates: Implications for casein micelle structure." <https://doi.org/10.1016/j.idairyj.2017.03.006>.
- Kang, Dong-Hee, Fiona Louis, Hao Liu, Hiroshi Shimoda, Yasutaka Nishiyama, Hajime Nozawa, Makoto Kakitani, et al. 2021. "Engineered whole cut meat-like tissue by the assembly of cell fibers using tendon-gel integrated bioprinting." *Nature Communications* 12 (1). <https://doi.org/10.1038/s41467-021-25236-9>.
- Kees de Kruif, C. G., Skelte G. Anema, Changjun Zhu, Palatasa Havea, and Christina Coker. 2015. "Water holding capacity and swelling of casein hydrogels." *Food Hydrocolloids* 44: 372–79. <https://doi.org/10.1016/j.foodhyd.2014.10.007>.
- Khanal, Bal Kumari Sharma, Bhesh Bhandari, Sangeeta Prakash, Dasong Liu, Peng Zhou, and Nidhi Bansal. 2018. "Modifying textural and microstructural properties of low fat Cheddar cheese using sodium alginate." *Food Hydrocolloids* 83: 97–108. <https://doi.org/https://doi.org/10.1016/j.foodhyd.2018.03.015>.
- Knudsen, Jes C., and Leif H. Skibsted. 2010. "High pressure effects on the structure of casein micelles in milk as studied by cryo-transmission electron microscopy." *Food Chemistry* 119 (1): 202–8. <https://doi.org/10.1016/j.foodchem.2009.06.017>.
- Lamichhane, Prabin, Alan L. Kelly, and Jeremiah J. Sheehan. 2018. "Symposium review: Structure-function relationships in cheese." *Journal of Dairy Science* 101 (3): 2692–2709. <https://doi.org/https://doi.org/10.3168/jds.2017-13386>.
- Lazzari, S., L. Nicoud, B. Jaquet, M. Lattuada, and M. Morbidelli. 2016. "Fractal-like structures in colloid science." *Advances in Colloid and Interface Science* 235: 1–13. <https://doi.org/10.1016/j.cis.2016.05.002>.
- Le Feunteun, Steven, Minale Ouethrani, and Francois Mariette. 2012. "The rennet coagulation mechanisms of a concentrated casein suspension as observed by PFG-NMR diffusion measurements." *Food Hydrocolloids* 27 (2): 456–63. <https://doi.org/10.1016/j.foodhyd.2011.09.008>.
- Lee, S. K K., R. J J. Buwalda, S. R R. Euston, E. A A. Foegeding, and A. B B. McKenna. 2003. "Changes in the rheology and microstructure of processed cheese during cooking." *LWT - Food Science and Technology* 36 (3): 339–45. [https://doi.org/10.1016/S0023-6438\(03\)00012-4](https://doi.org/10.1016/S0023-6438(03)00012-4).
- Lenze, Sonja, Alan Wolfschoon-Pombo, Katrin Schrader, and Ulrich Kulozik. 2019. "Effect of the Compositional Factors and Processing Conditions on the Creaming Reaction During Process

- Cheese Manufacturing.” *Food and Bioprocess Technology* 12 (4): 575–86.  
<https://doi.org/10.1007/s11947-019-2234-6>.
- Liang, Yichao, Graeme Gillies, Lara Matia-Merino, Aiqian Ye, Hasmukh Patel, and Matt Golding. 2017. “Structure and stability of sodium-caseinate-stabilized oil-in-water emulsions as influenced by heat treatment.” *Food Hydrocolloids* 66: 307–17.  
<https://doi.org/10.1016/j.foodhyd.2016.11.041>.
- Liang, Yichao, Hasmukh Patel, Lara Matia-Merino, Aiqian Ye, and Matt Golding. 2013. “Structure and stability of heat-treated concentrated dairy-protein-stabilised oil-in-water emulsions: A stability map characterisation approach.” *Food Hydrocolloids* 33: 297–308.  
<https://doi.org/10.1016/j.foodhyd.2013.03.012>.
- Lucey, John A., and David S. Horne. 2018. “Perspectives on casein interactions.” *International Dairy Journal* 85: 56–65. <https://doi.org/10.1016/j.idairyj.2018.04.010>.
- Matsumura, Yasuki, Il Jun Kang, Hiroko Sakamoto, Masao Motoki, and Tomohiko Mori. 1993. “Filler effects of oil droplets on the viscoelastic properties of emulsion gels.” *Topics in Catalysis* 7 (3): 227–40. [https://doi.org/10.1016/S0268-005X\(09\)80174-4](https://doi.org/10.1016/S0268-005X(09)80174-4).
- McClements, DJ. n.d. “Understanding and controlling the microstructure of complex foods.”
- Mezzenga, Raffaele, and Peter Fischer. 2013. “The self-assembly, aggregation and phase transitions of food protein systems in one, two and three dimensions.” *Rep Prog Phys* 76 (4): 46601.  
<https://doi.org/10.1088/0034-4885/76/4/046601>.
- Mitchell, J., T. C. Chandrasekera, and L. F. Gladden. 2012. “Numerical estimation of relaxation and diffusion distributions in two dimensions.” *Progress in Nuclear Magnetic Resonance Spectroscopy* 62: 34–50. <https://doi.org/10.1016/j.pnmrs.2011.07.002>.
- Mizuno, R., and J. A. Lucey. 2005. “Effects of emulsifying salts on the turbidity and calcium-phosphate-protein interactions in casein micelles.” *Journal of Dairy Science* 88 (9): 3070–78. [https://doi.org/10.3168/jds.S0022-0302\(05\)72988-X](https://doi.org/10.3168/jds.S0022-0302(05)72988-X).
- Moody, Jonathan B., and Yang Xia. 2004. “Analysis of multi-exponential relaxation data with very short components using linear regularization.” *Journal of Magnetic Resonance* 167 (1): 36–41.  
<https://doi.org/10.1016/j.jmr.2003.11.004>.
- Nagyova, G., F. Bunka, R. N. Salek, and file = :Users/catinspace/Library/Application Support/Mendeley Desktop/Downloaded/Nagyová et al. - 2014 - Use of sodium polyphosphates

- with different linear lengths in the production of spreadable processed cheese.pdf:pdf Cernikova, M. and Mancik, P. and Gruber, T. and Kuchar, D. doi = 10.3168/jds.2013-7210. n.d.
- Nicolai, Taco, and Christophe Chassenieux. 2021. "Heat-Induced Gelation of Casein Micelles." *Food Hydrocolloids* 118: 106755. <https://doi.org/https://doi.org/10.1016/j.foodhyd.2021.106755>.
- Nogueira, Marcio H., Salma Ben-Harb, Marc Schmutz, Bertrand Doumert, Sarah Nasser, Antoine Derenzy, Romdhane Karoui, Guillaume Delaplace, and Paulo P. S. Peixoto. 2020. "Multiscale Quantitative Characterization of Demineralized Casein Micelles: How the Partial Excision of Nano-Clusters Leads to the Aggregation During Rehydration." *Food Hydrocolloids* 105: 105778. <https://doi.org/https://doi.org/10.1016/j.foodhyd.2020.105778>.
- Noronha, N., E. Duggan, G. R. Ziegler, E. D. O'Riordan, and M. O'Sullivan. 2008. "Investigation of imitation cheese matrix development using light microscopy and NMR relaxometry." *International Dairy Journal* 18 (6): 641–48. <https://doi.org/10.1016/j.idairyj.2007.12.004>.
- Noronha, N., E. Duggan, G. R. Ziegler, J. J. Stapleton, E. D. O'Riordan, and M. O'Sullivan. 2008. "Comparison of microscopy techniques for the examination of the microstructure of starch-containing imitation cheeses." *Food Research International* 41 (5): 472–79. <https://doi.org/10.1016/j.foodres.2008.02.008>.
- Noronha, Nessa, E. Dolores O'Riordan, and Michael O'Sullivan. 2008. "Influence of processing parameters on the texture and microstructure of imitation cheese." *European Food Research and Technology* 226 (3): 385–93. <https://doi.org/10.1007/s00217-006-0549-9>.
- Oliver, Laura, Laura Wieck, and Elke Scholten. 2016. "Influence of matrix inhomogeneity on the rheological properties of emulsion-filled gels." *Food Hydrocolloids* 52: 116–25. <https://doi.org/10.1016/j.foodhyd.2015.06.003>.
- Peters, Jorien P. C. M., Frank J. Vergeldt, Henk Van As, Hannemieke Luyten, Remko M. Boom, and Atze Jan van der Goot. 2016. "Time domain nuclear magnetic resonance as a method to determine and characterize the water-binding capacity of whey protein microparticles." *Food Hydrocolloids* 54: 170–78. <https://doi.org/10.1016/j.foodhyd.2015.09.031>.
- Post, A. E., B. Arnold, J. Weiss, and J. Hinrichs. 2012. "Effect of temperature and pH on the solubility of caseins: Environmental influences on the dissociation of  $\alpha$ -S- and  $\beta$ -casein." *Journal of Dairy Science* 95 (4): 1603–16. <https://doi.org/10.3168/jds.2011-4641>.
- Radford, Stewart J., and Eric Dickinson. 2004. "Depletion flocculation of caseinate-stabilised emulsions: What is the optimum size of the non-adsorbed protein nano-particles?" *Colloids and*

- Surfaces A: Physicochemical and Engineering Aspects* 238 (1-3): 71–81.  
<https://doi.org/10.1016/j.colsurfa.2004.02.020>.
- Ramel, Pere R, and Alejandro G Marangoni. 2018. “Processed cheese as a polymer matrix composite: A particle toolkit for the replacement of milk fat with canola oil in processed cheese.” *Food Research International* 107: 110–18.  
<https://doi.org/https://doi.org/10.1016/j.foodres.2018.02.019>.
- Rebehmed, Joseph, Flavien Quintus, Jean Paul Mornon, and Isabelle Callebaut. 2016. “The respective roles of polar/nonpolar binary patterns and amino acid composition in protein regular secondary structures explored exhaustively using hydrophobic cluster analysis.” *Proteins: Structure, Function and Bioinformatics* 84 (5): 624–38. <https://doi.org/10.1002/prot.25012>.
- Röck, Sonja Martina. 2010. “Untersuchung von Strukturbildungsreaktionen in komplexen milchproteinbasierenden Lebensmittelsystemen - dargestellt am Beispiel von Schmelzkäse.”
- Sadlikova, Ivana, Frantisek Buňka, Pavel Budinsky, Voldanova Barbora, Vladimir Pavlinek, and doi = 10.1016/j.lwt.2010.04.012 Hoza Ignac. n.d.
- Salami, Souad, Corinne Rondeau-Mouro, John van Duynhoven, and Francois Mariette. 2013. “PFG-NMR self-diffusion in casein dispersions: Effects of probe size and protein aggregate size.” *Food Hydrocolloids* 31 (2): 248–55. <https://doi.org/10.1016/j.foodhyd.2012.10.020>.
- Salek, Richardos Nikolaos, Michaela Cernikov, Gabriela Nagyova, Dalibor Kuchar, Helena Bacova, Lucie Minarcikova, Franti Sek, and Bu Nka. 2015. “The effect of composition of ternary mixtures containing phosphate and citrate emulsifying salts on selected textural properties of spreadable processed cheese.” *International Dairy Journal* 44. <https://doi.org/10.1016/j.idairyj.2014.12.009>.
- Salek, Richardos Nikolaos, Michaela Cernikova, Pachlova Vendula, Zuzana Bubelova, Veronika Konecna, and doi = <https://doi.org/10.1016/j.lwt.2016.11.019> Bunka Frantisek. n.d.
- Sandhu, Rita, Nishi Singh, Jyotika Dhankhar, Kamal Gandhi, and Rajan Sharma. 2018. “Dynamic Light Scattering (DLS) Technique, Principle, Theoretical Considerations and Applications.” In, 135–37.
- Sapir, Liel, and Daniel Harries. 2015. “Is the depletion force entropic? Molecular crowding beyond steric interactions.” *Current Opinion in Colloid and Interface Science* 20 (1): 3–10.  
<https://doi.org/10.1016/j.cocis.2014.12.003>.
- Schuh, Joseph R., and Sunney I. Chan. 1982. “Nuclear magnetic resonance.” *Methods in Experimental Physics* 20 (C): 1–52. [https://doi.org/10.1016/S0076-695X\(08\)60150-7](https://doi.org/10.1016/S0076-695X(08)60150-7).

- Semenova, Maria G., Eric Dickinson, Elena Burlakova, and Gennady Zaikov. 2010. "Biopolymers in food colloids: Thermodynamics and molecular interactions." *Biopolymers in Food Colloids: Thermodynamics and Molecular Interactions*, 1–353. <https://doi.org/10.1201/b12817>.
- Shaikhullina, Milyausha, Aliya Khaliullina, Rustam Gimatdinov, Anatoly Butakov, Vladimir Chernov, and Andrei Filippov. 2020. "NMR relaxation and self-diffusion in aqueous micellar gels of pluronic F-127." *Journal of Molecular Liquids* 306: 112898. <https://doi.org/10.1016/j.molliq.2020.112898>.
- Sharma, Prateek, Peter A. Munro, Tzvetelin T. Dessev, Peter G. Wiles, and Robert J. Buwalda. 2016. "Effect of shear work input on steady shear rheology and melt functionality of model Mozzarella cheeses." *Food Hydrocolloids* 54: 266–77. <https://doi.org/10.1016/j.foodhyd.2015.10.009>.
- Solowiej, Bartosz, Siemowit Glibowski Paweł and Muszynski, Jerzy Wydrych, Antoni Gawron, Tomasz Jelin'ski, Paweł Glibowski, Siemowit Muszynski, Jerzy Wydrych, Antoni Gawron, and Tomasz Jelin'ski. 2014. "The effect of fat replacement by inulin on the physicochemical properties and microstructure of acid casein processed cheese analogues with added whey protein polymers." *Food Hydrocolloids* 44: 1–11. <https://doi.org/10.1016/j.foodhyd.2014.08.022>.
- Testamanti, M. Nadia, and Reza Rezaee. 2019. "Considerations for the acquisition and inversion of NMR T2 data in shales." *Journal of Petroleum Science and Engineering* 174 (November): 177–88. <https://doi.org/10.1016/j.petrol.2018.10.109>.
- Thorn, David C., Heath Ecroyd, John A. Carver, and Carl Holt. 2015. "Casein structures in the context of unfolded proteins." *International Dairy Journal* 46 (July): 2–11. <https://doi.org/10.1016/j.idairyj.2014.07.008>.
- Urgu, Sevcan AND Koca, Müge AND Unluturk. 2018. "Effects of Fat Reduction on the Stability, Microstructure, Rheological and Color Characteristics of White-Brined Cheese Emulsion with Different Emulsifying Salt Amounts." *Korean Journal for Food Science of Animal Resources* 38 (5): 866–77. <https://doi.org/10.5851/kosfa.2018.e8>.
- Vogt, Sarah J., Jeremy R. Smith, Joseph D. Seymour, Alistair J. Carr, Matt D. Golding, and Sarah L. Codd. 2015. "Assessment of the changes in the structure and component mobility of Mozzarella and Cheddar cheese during heating." *Journal of Food Engineering* 150: 35–43. <https://doi.org/10.1016/j.jfoodeng.2014.10.026>.
- Vollmer, Almut H., Ingrid Kieferle, Alexandra Pusl, and Ulrich Kulozik. 2021. "Effect of

- pentasodium triphosphate concentration on physicochemical properties, microstructure, and formation of casein fibrils in model processed cheese.” *Journal of Dairy Science*. <https://doi.org/10.3168/jds.2021-20628>.
- Vollmer, Almut H., Ingrun Kieferle, Nabil N. Youssef, and Ulrich Kulozik. 2021. “Mechanisms of structure formation underlying the creaming reaction in a processed cheese model system as revealed by light and transmission electron microscopy.” *Journal of Dairy Science* 104 (9): 9505–20. <https://doi.org/10.3168/jds.2020-20080>.
- Walstra, Pieter. 1999. “Casein Sub-Micelles: Do They Exist?” *International Dairy Journal* 9 (3): 189–92. [https://doi.org/https://doi.org/10.1016/S0958-6946\(99\)00059-X](https://doi.org/https://doi.org/10.1016/S0958-6946(99)00059-X).
- Wehrens, Ron. 211AD. *Chenometrics with R*.
- Whittall, Kenneth P. 1996. “Chapter 3 A N A L Y S I S OF N M R R E L A X A T I O N Department of Radiology University of British Columbia.” *Signal Treatment and Signal Analysis in NMR*, no. 1979.
- Whittall, Kenneth P., and Alexander L. MacKay. 1989. “Quantitative interpretation of NMR relaxation data.” *Journal of Magnetic Resonance (1969)* 84 (1): 134–52. [https://doi.org/10.1016/0022-2364\(89\)90011-5](https://doi.org/10.1016/0022-2364(89)90011-5).
- Wong, Benjamin T, Jiali Zhai, Søren V Hoffmann, Marie-Isabel Aguilar, MaryAnn Augustin, Tim J Wooster, and Li Day. 2012. “Conformational changes to deamidated wheat gliadins and  $\beta$ -casein upon adsorption to oil–water emulsion interfaces.” *Food Hydrocolloids* 27 (1): 91–101. <https://doi.org/https://doi.org/10.1016/j.foodhyd.2011.08.012>.